AD_____

Award Number: DAMD17-99-1-9029

TITLE: Chemokine Receptors and Integrin Function in Prostate Cancer

PRINCIPAL INVESTIGATOR: James B. McCarthy, Ph.D.

CONTRACTING ORGANIZATION: University of Minnesota
Minneapolis, Minnesota 55455-2070

REPORT DATE: August 2002

TYPE OF REPORT: Final

PREPARED FOR: U.S. Army Medical Research and Materiel Command
Fort Detrick, Maryland 21702-5012

DISTRIBUTION STATEMENT: Approved for Public Release;
Distribution Unlimited

The views, opinions and/or findings contained in this report are those of the author(s) and should not be construed as an official Department of the Army position, policy or decision unless so designated by other documentation.

REPORT DOCUMENTATION PAGE

Form Approved
OMB No. 074-0188

1. AGENCY USE ONLY (Leave blank)	2. REPORT DATE	3. REPORT TYPE AND DATES COVERED
	August 2002	Final (15 Jan 99 - 14 Jul 02)

4. TITLE AND SUBTITLE
Chemokine Receptors and Integrin Function in Prostate Cancer

5. FUNDING NUMBERS
DAMD17-99-1-9029

6. AUTHOR(S) :
James B. McCarthy, Ph.D.

7. PERFORMING ORGANIZATION NAME(S) AND ADDRESS(ES)
University of Minnesota
Minneapolis, Minnesota 55455-2070

E-MAIL:
mccar001@umn.edu

8. PERFORMING ORGANIZATION REPORT NUMBER

9. SPONSORING / MONITORING AGENCY NAME(S) AND ADDRESS(ES)
U.S. Army Medical Research and Materiel Command
Fort Detrick, Maryland 21702-5012

10. SPONSORING / MONITORING AGENCY REPORT NUMBER

11. SUPPLEMENTARY NOTES
Original contains color plates: All DTIC reproductions will be in black and white.

12a. DISTRIBUTION / AVAILABILITY STATEMENT
Approved for Public Release; Distribution Unlimited

12b. DISTRIBUTION CODE

13. ABSTRACT ***(Maximum 200 Words)***
Changes in prostate tumor cell adhesion are important considerations in the progression, invasion and metastasis of prostate cancer. The originally funded studies focused on evaluating the effects of chemokines, which are chemotactic cytokines, on the activation of prostate carcinoma adhesion and migration. The results demonstrated that a specific chemokine, termed IL-8, stimulated the migration and adhesion of advanced prostate carcinoma cells. The purpose of the proposal was to further define the importance of IL-8 in the activation of integrins, which are major adhesion molecules that mediate prostate carcinoma migration and invasion. During the course of these studies, we attempted to develop a model in which we could evaluate the effects of IL-8 on adhesion of prostate cancer cells to endothelial cells. In these studies, we included both large vessel endothelial cells and bone marrow endothelial cells, in an attempt to determine if IL-8 might stimulate adhesion of prostate tumor cells to substrates other than basement membrane components. The bone marrow endothelial cell line was chosen because of the preferential metastasis of prostate cancer to bone. During the course of these studies, we discovered a novel mechanism by which prostate carcinoma cells could adhere to bone marrow endothelial cells. This mechanism involved the elaboration of a specific glycosaminoglycan termed hyaluronan by prostate tumor cells. These studies were further developed to establish the importance of hyaluronan expression in prostate tumor cell adhesion, growth and vascularization. A summary of these findings is also included in the final report.

14. SUBJECT TERMS	15. NUMBER OF PAGES
prostate cancer	49
	16. PRICE CODE

17. SECURITY CLASSIFICATION OF REPORT	18. SECURITY CLASSIFICATION OF THIS PAGE	19. SECURITY CLASSIFICATION OF ABSTRACT	20. LIMITATION OF ABSTRACT
Unclassified	Unclassified	Unclassified	Unlimited

FOREWORD

Opinions, interpretations, conclusions and recommendations are those of the author and are not necessarily endorsed by the U.S. Army.

___ Where copyrighted material is quoted, permission has been obtained to use such material.

___ Where material from documents designated for limited distribution is quoted, permission has been obtained to use the material.

___ Citations of commercial organizations and trade names in this report do not constitute an official Department of Army endorsement or approval of the products or services of these organizations.

N/A In conducting research using animals, the investigator(s) adhered to the "Guide for the Care and Use of Laboratory Animals," prepared by the Committee on Care and use of Laboratory Animals of the Institute of Laboratory Resources, national Research Council (NIH Publication No. 86-23, Revised 1985).

N/A For the protection of human subjects, the investigator(s) adhered to policies of applicable Federal Law 45 CFR 46.

N/A In conducting research utilizing recombinant DNA technology, the investigator(s) adhered to current guidelines promulgated by the National Institutes of Health.

N/A In the conduct of research utilizing recombinant DNA, the investigator(s) adhered to the NIH Guidelines for Research Involving Recombinant DNA Molecules.

N/A In the conduct of research involving hazardous organisms, the investigator(s) adhered to the CDC-NIH Guide for Biosafety in Microbiological and Biomedical Laboratories.

PI - Signature 11/4/02 Date

Table of Contents

Introduction

The overall purpose of the proposed studies was to further understand the molecular mechanisms that govern prostate carcinoma invasion and metastasis. These studies were based on preliminary data in which we had demonstrated that addition of specific soluble factors termed α-chemokines could stimulate the motility and invasion of metastatic prostate cancer cell lines in vitro. These soluble mediators have been implicated in the invasion and metastasis of different tumor types, and they have been implicated in promoting inflammation and/or tumor neovascularization. Our evidence provided in the initial application also implicated these factors as autocrine mediators of tumor behavior. In the first set of studies, we had proposed to further define the mechanism of action of α-chemokines on prostate tumor invasion. We have since determined that α-chemokine treatment of prostate tumors can modulate integrin-mediated adhesion to the glycoprotein laminin. Modulation of integrin function was biphasic, in the sense that α-chemokine treatment stimulated an initial increase in laminin-mediated adhesion, which then subsided back to baseline. These changes occur in the absence of a change in integrin expression levels. The data suggest that α-chemokines could stimulate motility in part by modulating integrin adhesive function, presumably by stimulating signal transduction pathways that lead to changes in integrin avidity.

We also used RT-PCR to determine the nature of the chemokine receptors that are expressed on metastatic PC3-M human prostate carcinomas. The results demonstrated that both CXCR-1 and CXCR-2 receptors are expressed by these cells, indicating that both receptors may be important in mediating prostate tumor motility and invasion. These results were published in the journal The Prostate in October of 1999 [1]. One complicating factor in this model system is that the PC3-M cells express high levels of endogenous chemokine. Although this suggests that IL-8 related chemokines may serve as autocrine factors in prostate tumor invasion, it did create certain technical challenges associated with chronic activation of this receptor/ligand pathway in vitro. A copy of the article describing these results is appended to the annual report.

During the final year of funding, we had proposed to a.) Use antisense approaches to inhibit chemokine receptor expression b.) Initiate studies to define which rho-family GTPases are important for α-chemokine mediated tumor cell motility and invasion. Because of technical issues (described below) we were not able to complete some of the assigned tasks. However, in the course of performing these studies, we did publish several observations documenting the importance of a novel and specific glycosaminoglycan dependent adhesion mechanism. We also related this mechanism to the growth, vascularization and bone metastasis of prostate tumor cells. These results are described below and articles funded by this proposal are included as an appendix with the final report.

Body

STATEMENT OF WORK

Specific Aim #1: To evaluate the ability of the α- chemokines IL-8 and Gro-α to stimulate integrin mediated adhesion, migration and invasion of human prostate carcinoma cell lines with different invasive or metastatic potential.

Months 1-4: Complete analysis of integrin expression, α- chemokine receptor expression on prostate cancer cell line

Completed

Months 2-9: Complete analysis of effects of chemokines on prostate carcinoma cell adhesion, spreading, migration and invasion

Partially completed. During these studies, we evaluated the adhesion of prostate tumor cells to bone marrow endothelial cells and these studies generated a new line of investigation that proved fruitful. The description of these studies is described below and this line of investigation replaced what was described in aim 2 since those studies proved technically challenging.

Months 4-12: Complete analysis of chemokine effect on integrin mediated affinity and avidity

Completed

Month 12: Prepare annual progress report

Most of the studies in Specific Aim #1 of the Statement of Work were completed and published in the journal 'The Prostate'. The manuscript has been appended in the final report that describes these findings. Major conclusions/findings of the manuscript are included in the "conclusions" section, below.

Specific Aim #2: To determine if the α-chemokine induced increase in integrin mediated adhesion is brought about by the action of the rho family of GTPases, we will use a gene transfer approach. This will be done by transfecting dominant negative constructs of rho, rac or cdc-42 GTPases and measuring the effects of α-chemokines on integrin function in invasive and metastatic prostate carcinoma cells

Months 13-24: Transfection of selected prostate carcinoma cell lines with dominant negative constructs of rho, rac and cdc-42 expressing dominant negative or constitutively active versions of these proteins.

Not done for technical reasons (see below)

Months 13-16: Complete characterization of transfectants for integrin and chemokine receptor expression.

Not done for technical reasons (see below)

Months 22-30: Analyze dominant transfectants for inhibition of α-chemokine enhanced integrin mediated adhesion, ligand binding, motility and invasion

Not done for technical reasons (see below)

Month 24: Prepare second annual report and submit competitive renewal application

The studies in the second specific aim were not completed. Because of the endogenous expression of high levels of IL-8 by these cells, we first attempted to use an anti-sense approach to inhibit endogenous receptor expression to determine if this would cause a corresponding decrease in the baseline invasion of these cells. This was supported in part on our observations that CXC antibodies inhibit baseline invasion of these cells (described in accompanying manuscript). The problem we encountered was that we were not able to stably inhibit IL-8 expression in our cells using anti-sense. We attempted to obtain cells that had been derived by another laboratory ([2]Dr. Colin Dinney, MD Andersen) and were to be provided by a collaborator of ours in these studies (Dr. Joel Slaton). However, the original anti-sense cells had to be regenerated by that laboratory, in so doing, they were unable to generate vector control transfectants that were poorly invasive (Dr. Slaton, personal communication). The high endogenous levels of IL-8 in our system made signal transduction studies very difficult to design and execute.

The focus of the signal transduction studies was to be on the rho-family GTPases and their relative importance in facilitating IL-8 mediated adhesion, migration and invasion. The strategy for these studies included a.) Transfecting constructs encoding dominant negative constructs of GTPases and b.) Using cells in which endogenous IL-8 expression had been inhibited for the purpose of studying the effect of exogenous IL-8 on activation of the GTPases. These cells were then to be used to study the effect of IL-8/GTPases on integrin activation. The lack of a suitable cell system in which IL-8 expression had been stably inhibited prevented our successful completion of these studies. We could have completed part of these studies by expressing dominant negative constructs of GTPases, however in the absence of the appropriate cell models, it would not have been possible to discern the specificity of the relationship (if any) between IL-8, specific GTPase activation, and the activation of specific integrins. As a result of our abandoning these studies, a portion of the funds awarded for this grant have been returned to the funding agency (see final budget report).

Additional work performed as part of the original work statement did generate important new findings regarding the adhesive properties of advance prostate tumors and prostate tumor growth, vascularization and bone metastasis. Our original work statement focused on understanding the importance chemokine mediated changes in cell adhesion to prostate tumor invasion and metastasis. The original proposal was based on our observations that IL-8 could stimulate adhesion/migration of prostate tumor cells to the basement membrane protein laminin. During the course of our studies, we also evaluated other adhesive substrates that might be important for prostate tumor metastasis. As part of these studies, we chose to evaluate prostate tumor cell adhesion to bone marrow endothelial cells, because we reasoned that interaction with this population of cells might be important for mediating entry (homing?) into bone, which is a preferential site for metastasis of prostate tumors. Our goal was to evaluate the potential importance of IL-8 in mediating this adhesion. As controls, we utilized endothelial cells from other sources (i.e. human umbilical vein endothelial cells).

Our results demonstrated that androgen independent prostate tumor cells adhered in a very rapid and highly avid fashion [3]. While we could not specifically address the importance of IL-8 due to the reasons described above, we did succeed in identifying a novel adhesion mechanism that may explain bone specific homing of prostate tumors. Our studies indicated that numerous antibodies against well defined adhesion receptors such as integrins, selectins and cadherins had little or no effect on the highly avid adhesion of prostate tumors to bone marrow endothelial cells. However, we did succeed at inhibiting the adhesion of these cells by adding the enzyme hyaluronidase to these adhesion assays. Hyaluronidase degrades the glycosaminoglycan hyaluronan (HA), which is a large negatively charged linear carbohydrate important for both normal and transformed cell adhesion, migration and growth[4, 5]. Additional studies demonstrated that a.) Prostate tumors, rather than bone marrow endothelial cells synthesize and retain the HA in a loosely organized matrix b.) Elevated HA synthesis by prostate tumor cells correlated to elevated expression of two enzymes that synthesize HA (so called HA synthases or HAS). In contrast, a pooled library of normal prostate contained only minimal levels of HA synthases [6]. This is a novel mechanism by which prostate tumor cells might selectively home to bone, and so we pursued this mechanism of prostate tumor cell adhesion to further study its potential importance in prostate tumor progression/metastasis.

We next manipulated HAS expression in cells that lack or express HAS. We first expressed HAS in poorly tumorigenic/metastatic tumor cells (LnCaP). Using these cells we demonstrated that HAS expression per se is sufficient to stimulate HA synthesis and it is sufficient to stimulate LnCaP adhesion to bone marrow endothelial cells (which is normally very low). We also used an antisense approach to inhibit HAS expression in more aggressive PC3MLN4 cells. These cells normally express high levels of HA and exhibit high levels of HA in culture. Vectors encoding antisense HAS 2 or HAS 3 (or both) inhibited HA synthesis in PC3MLN4 cells, with the most significant effect observed when both HAS enzymes were both inhibited. Inhibiting HAS expression also inhibited HA mediated adhesion of these cells to bone marrow endothelial cells, suggesting that increased levels of HAS might facilitate homing of metastatic prostate tumor cells to bone.

Finally, we evaluated the effect of HAS synthesis on the growth of tumors in xenograft models of human prostate tumors [7]. We injected PC3MLN4 cells differentially expressing HAS enzymes into immunocompromised mice. After 3 weeks, tumors were measured, harvested and processed for determining weight, volume and histology. The results demonstrate that inhibited HAS expression leads to a highly significant inhibition in prostate tumor growth and vascularization. Importantly, we were also able to completely reverse the inhibition by including HA in the injection mixture with the cells. These results demonstrate that elevated HA levels lead to increased tumor growth and vascularization, and they also show that it is the product of the HAS enzymes (i.e. HA) rather than the enzymes per se that are important for this biological effect. These results are being further pursued under separate funding that has recently been obtained from the DOD (17-02-1-0102) which were used to partially fund the final manuscript.

Key Research Accomplishments (accomplishments below the line represent progress on areas not originally listed in the work statement but do represent studies that developed from the original work statement)

a. Demonstration that α-chemokines can stimulate prostate tumor motility and invasion in vitro
b. Identification of the chemokine receptors CXC R1 and CXC R2 expressed by prostate cancer cells
c. Treatment with α-chemokines can stimulate integrin mediated adhesion in the absence of a change in integrin surface expression, suggesting that chemokines change integrin avidity and prostate tumor motility
d. Anti-chemokine receptor antibodies inhibit stimulated and basal tumor cell motility. This suggests that endogenous chemokine expression by prostate tumors can act as autocrine motility/invasion factors. Interfering with receptor may represent a novel therapy for tumor invasion

---

e. Prostate tumor cells show selective adhesion to bone marrow endothelial cells
f. Prostate/bone marrow cell interactions depend on increased production of hyaluronan by prostate tumor cells. The receptor on bone marrow endothelial cells for prostate tumor associated hyaluronan remains unknown.
g. Increased hyaluronan expression by prostate tumor cells results from increased expression of specific hyaluronan synthases
h. Manipulation of hyaluronan synthase expression correlates to hyaluronan synthesis and adhesion of prostate tumor cells to bone marrow endothelial cells
i. Stable inhibition of hyaluronan synthesis inhibits the growth and vascularization of tumors in xenograft models of human prostate tumor growth.

Reportable Outcomes

a. Manuscript published on above findings directly related to the work statement. Included in Appendix.

Reiland, J, Furcht, L.T. and J.B. McCarthy. 1999. CXC-chemokines stimulate invasion and chemotaxis in prostate carcinoma cells through the CXCR2 receptor. The Prostate. 41:78-88.

Significance: A specific receptor for the chemokine IL-8 mediates prostate carcinoma migration and invasion. Altered response to this chemokine may be an important factor in prostate tumor progression

b. Additional manuscripts published on findings that developed from observations supported by this proposal that are not directly covered by the work statement (Included in Appendix).

Simpson, M.A., et al., *Hyaluronan synthase elevation in metastatic prostate carcinoma cells correlates with hyaluronan surface retention, a prerequisite for rapid adhesion to bone marrow endothelial cells.* J Biol Chem, 2001. **276**(21): p. 17949-57.

Significance: Prostate carcinoma cells adhere via an integrin independent, hyaluronan dependent mechanism to bone marrow endothelial cells. More metastatic tumor cells, which show comparatively high adhesion to bone marrow endothelial cells, exhibit high levels of hyaluronan and corresponding elevations in specific hyaluronan synthetic enzymes (HAS). This implicates upregulation of HAS in prostate tumor cell adhesion and bone metastasis

Simpson, M.A., et al., *Manipulation of hyaluronan synthase expression in prostate adenocarcinoma cells alters pericellular matrix retention and adhesion to bone marrow endothelial cells.* J Biol Chem, 2002. **277**(12): p. 10050-7.

Significance: Manipulation of the levels of hyaluronan synthases using vectors encoding in either the sense or antisense orientation cause corresponding changes in HA synthesis and adhesion of prostate tumor cells to bone marrow endothelial cells. These results suggest a cause and effect relationship between changes in HAS levels and altered adhesivity of prostate tumor cells.

Simpson, M.A., C.M. Wilson, and J.B. McCarthy, *Inhibition of prostate tumor cell hyaluronan synthesis impairs subcutaneous growth and vascularization in immunocompromised mice.* Am J Pathol, 2002. **161**(3): p. 849-57.

Significance: Inhibiting HAS expression in metastatic, androgen independent prostate tumor cells inhibits the growth and vascularization of prostate tumor cells. This result suggests that upregulated HAS expression, and corresponding elevations in levels of HA, are important for the growth of more advanced/metastatic prostate tumors. The results further suggest that tumor associated HA may facilitate vascularization by enhancing the proliferation/survival of endothelial cells in the tumor microenvironment.

Conclusions

The major conclusion of the findings encompassed within the original work statement is that chemokines can stimulate prostate tumor motility and invasion. Autocrine expression of chemokines by tumors could serve as autocrine factors for tumor

invasion. Furthermore, since chemokines are produced by inflammatory cells, it is also possible that tumor associated inflammation could act to facilitate tumor invasion by increasing the local concentration of inflammatory chemokines. The two major α-chemokine receptors, CXCR1 and CXCR2 were identified on these cells, and anti-CXCR2 antibodies inhibited motility associated with chemokine stimulation. These antibodies also inhibited baseline invasion, suggesting interfering with these receptors could inhibit autocrine and paracrine effects of chemokines on tumor invasion. Additional work on the signaling mechanisms engaged by IL-8 was hampered by the lack of suitable cell models.

We did, however, pursue more promising studies that stemmed from the experiments originally described in the statement of work. These studies demonstrated that metastatic tumor cells exhibit highly avid and specific adhesion to bone marrow endothelial cells and this adhesive mechanism is due to an upregulation of enzymes that synthesize HA. Manipulation of these enzymes alters HA synthesis by these cells and also alters adhesion of these cells to bone marrow endothelial cells. Finally, inhibiting HA synthesis by metastatic, androgen independent prostate cells inhibits the ability of these cells to form tumors and become vascularized. These studies have identified a potential new biomarker for prostate tumor progression and they implicate HAS in the biology of prostate tumor growth, vascularization and metastasis.

References

1. Reiland, J., L.T. Furcht, and J.B. McCarthy, *CXC-chemokines stimulate invasion and chemotaxis in prostate carcinoma cells through the CXCR2 receptor.* Prostrate, 1999. **41**(2): p. 78-88.
2. Inoue, K., et al., *Interleukin 8 expression regulates tumorigenicity and metastases in androgen-independent prostate cancer.* Clin Cancer Res, 2000. **6**(5): p. 2104-19.
3. Simpson, M.A., et al., *Hyaluronan synthase elevation in metastatic prostate carcinoma cells correlates with hyaluronan surface retention, a prerequisite for rapid adhesion to bone marrow endothelial cells.* J Biol Chem, 2001. **276**(21): p. 17949-57.
4. Toole, B.P. and V.C. Hascall, *Hyaluronan and tumor growth.* Am J Pathol, 2002. **161**(3): p. 745-7.
5. Toole, B.P., T.N. Wight, and M.I. Tammi, *Hyaluronan-cell interactions in cancer and vascular disease.* J Biol Chem, 2002. **277**(7): p. 4593-6.
6. Simpson, M.A., et al., *Manipulation of hyaluronan synthase expression in prostate adenocarcinoma cells alters pericellular matrix retention and adhesion to bone marrow endothelial cells.* J Biol Chem, 2002. **277**(12): p. 10050-7.
7. Simpson, M.A., C.M. Wilson, and J.B. McCarthy, *Inhibition of prostate tumor cell hyaluronan synthesis impairs subcutaneous growth and vascularization in immunocompromised mice.* Am J Pathol, 2002. **161**(3): p. 849-57.

Appendices

One publication directly related to work statement:

1. Reiland, J, Furcht, L.T. and J.B. McCarthy. 1999. CXC-chemokines stimulate invasion and chemotaxis in prostate carcinoma cells through the CXCR2 receptor. The Prostate. 41:78-88.

Three publications stemming from, but not directly described within, the work statement:

2. Simpson, M.A., et al., *Hyaluronan synthase elevation in metastatic prostate carcinoma cells correlates with hyaluronan surface retention, a prerequisite for rapid adhesion to bone marrow endothelial cells.* J Biol Chem, 2001. **276**(21): p. 17949-57.

3. Simpson, M.A., et al., *Manipulation of hyaluronan synthase expression in prostate adenocarcinoma cells alters pericellular matrix retention and adhesion to bone marrow endothelial cells.* J Biol Chem, 2002. **277**(12): p. 10050-7.

4. Simpson, M.A., C.M. Wilson, and J.B. McCarthy, *Inhibition of prostate tumor cell hyaluronan synthesis impairs subcutaneous growth and vascularization in immunocompromised mice.* Am J Pathol, 2002. **161**(3): p. 849-57.

The Prostate 41:78–88 (1999)

CXC-Chemokines Stimulate Invasion and Chemotaxis in Prostate Carcinoma Cells Through the CXCR2 Receptor

Jane Reiland,[1] Leo T. Furcht,[1,2] and James B. McCarthy[1,2]*

[1]*Department of Laboratory Medicine and Pathology, University of Minnesota, Minneapolis, Minnesota*

[2]*University of Minnesota Cancer Center, University of Minnesota, Minneapolis, Minnesota*

BACKGROUND. Metastasis of prostate carcinoma requires invasion through the basement membrane, a thin extracellular matrix that underlies the epithelial cells, which must be breached by tumor cells invading into surrounding tissue. The CXC-chemokines, which have been shown to promote the migration of neutrophils and carcinoma cells, are candidates to influence prostate carcinoma-cell invasion.

METHODS. CXC-chemokines were examined for the ability to stimulate prostate cell line PC3 invasion in vitro through a reconstituted basement membrane and long-term migration and short-term adhesion to laminin, a major component of the basement membrane.

RESULTS. PC3 cells responded to IL-8 and GROα with a 1.6–2-fold increase in invasion through reconstituted basement membrane. A corresponding 2–3-fold increase in chemotaxis toward IL-8 and GROa was seen on laminin. Anti-CXCR2 antibody inhibited IL-8-stimulated migration. Expression levels of the β_1 integrins were not changed by IL-8, and $\alpha_{6\beta1}$ integrin was used for both stimulated and baseline migration. In addition to the increases in migration and invasion, 2–6-fold transient increases in adhesion on laminin were seen with both IL-8 and GROα.

CONCLUSIONS. These results suggest that the CXC-chemokines stimulate migration and invasion in part by altering the activation state of the β_1 integrins. The CXC-chemokines act on prostate carcinoma cells through the CXCR2 receptor to promote behavior important for metastasis, and as such may be important in prostate carcinoma progression and metastasis. *Prostate 41:78–88, 1999.* © 1999 Wiley-Liss, Inc.

KEY WORDS: **interleukin 8; integrins; laminin; cell adhesion; basement membrane**

INTRODUCTION

IL-8 and GROα are members of a family of CXC-chemokines (CTAP-III, β-TG, NAP-2, PF-4 GROβ, GROγ, IP-10, GCP-2, and ENA-78) defined structurally by four conserved cysteines and functionally by their ability to stimulate chemotaxis of various cells [1,2]. IL-8 and GROα are produced in sites of inflammation by monocytes, macrophages, and nonleukocyte cells such as epithelial and endothelial cells, fibroblasts, and keratinocytes [1]. IL-8 and GROα are

Abbreviations: FACS, fluorescence-activated cell scan; FN, fibronectin; LMN, laminin; mAb, monoclonal antibody; pAb, polyclonal antibody; PBS, phosphate-buffered saline; RT-PCR, reverse transcriptase-polymerase chain reactions; SFM, serum-free medium.

Grant sponsor: National Cancer Institute/National Institutes of Health; Grant number: CA29995; Grant sponsor: DOD; Grant number: PC970519.

*Correspondence to: Dr. James B. McCarthy, Department of Laboratory Medicine and Pathology, University of Minnesota, Box 609 UMHC, 312 Church St. S.E., Minneapolis, MN 55455.
E-mail: mccar001@maroon.tc.umn.edu

Received 27 July 1998; Accepted 19 April 1999

also produced by tumor cells such as prostate, lung, and melanoma [3–6]. IL-8- and GROα-stimulated adhesion and chemotaxis are important for neutrophil activation and infiltration [7]. In addition, IL-8 and GROα stimulate the migration of other cell types such as T lymphocytes, smooth muscle cells, keratinocytes, and endothelial and tumor cells including melanoma and breast carcinoma [8–11].

IL-8 and GROα stimulation of adhesion and migration may be an important factor in tumor progression. CXC-chemokine expression is correlated with tumor progression in melanomas, which exhibit increased expression of IL-8 when compared to normal melanocytes [5]. Overexpression of GROα in melanocytes results in increased tumorigenicity [12]. Increased expression of IL-8 message and protein in tumors also correlates with increased experimental metastatic potential of melanoma cells in nude mice [6]. IL-8 is also implicated in metastasis of lung carcinoma cells, as neutralizing IL-8 antibodies or IL-8 receptor antisense oligonucleotide inhibit growth and metastasis of lung carcinoma cells in vivo [3,13]. These studies suggest that the CXC-chemokines play a critical role in tumor progression.

IL-8 and GROα act through a family of G-protein-coupled receptors designated the "CXCR receptors." CXCR1 (IL-8RA) binds IL-8 with high affinity but binds other members of the CXC-chemokine family with low affinity. In contrast, CXCR2 (IL-8RB) binds IL-8, GROα, NAP-2, ENA 78, and GCP-2 with high affinity [14,15]. Both receptors mediate IL-8-stimulated chemotaxis in CXCR1 or CXCR2 transfected Jurkat cells [16], and neutrophils can use both receptors to promote chemotaxis [17]. Chemokine binding to CXCR1 and CXCR2 stimulates several signal transduction pathways, including release of intercellular stores of calcium and activation of PLC [18–20], ERK [21], Rho [22], and phosphoinositide metabolism [23]. IL-8 binding to either receptor stimulates changes in adhesion receptor expression, including upregulation of CD11b/CD18, and induction of L-selectin shedding from the plasma membrane on neutrophils [24–26]. It also stimulates cytoskeletal rearrangement, pseudopodia formation, and morphological polarization [1].

Since adhesion and migration are important components of invasion into local or distant sites during prostate tumor metastasis, we examined the ability of the CXC-chemokines to stimulate prostate carcinoma adhesion, migration, and invasion. Invasion was examined using a reconstituted basement membrane, while adhesion and migration were examined using substrata coated with laminin, a major component of the basement membrane. We have found that prostate carcinoma cells are able to respond to two members of the CXC-chemokine family, IL-8 and GROα. Both chemokines stimulate adhesion and migration of prostate carcinoma cells on laminin and also increased tumor cell invasion through reconstituted basement membrane. The effects of IL-8 and GROα are mediated through the CXCR2 receptor, as PC3 cells express CXCR2 mRNA, and neutralizing antibodies for CXCR2 inhibit IL-8-stimulated adhesion and migration. The results suggest that CXCR expression in prostate carcinoma may facilitate local invasion and metastasis.

MATERIALS AND METHODS

Cell Culture

Prostate adenocarcinoma cell line PC3 was obtained from the ATCC (Rockville, MD) and maintained in F12 Kaighn's modification with 7% fetal bovine serum. Cells were plated 1–2 days prior to experiments and used at approximately 50% confluence.

Reagents

Mouse EHS laminin [27] and fibronectin [28] were prepared as described. IL-8 and GROα were purchased from R&D Systems (Minneapolis, MN) or Peprotech (Rocky Hill, NJ). Primers for PCR were produced by the University of Minnesota Microchemical Facility (Minneapolis, MN). Commercially available monoclonal antibodies to IL-8 and CXCR2 (R&D Systems) and alpha 6 integrin (Immunotech, Inc., Westbrook, ME) were used. Purified antibody against the beta 1 integrin subunit (P5D2) was produced and characterized as previously described [29].

Detection of IL-8 Receptor RNA

Total RNA was isolated from PC3 cells by guanidinium-phenol-chloroform extraction, using the Totally RNA Kit according to the manufacturer's instructions (Ambion, Austin, TX). First-strand cDNA was synthesized from total RNA using AMV reverse transcriptase (Gibco BRL, Grand Island, NY) according to manufacturer's instructions. Specific cDNAs for CXCR2 were amplified by PCR with primers 5'CCTTTTCTACTAGATGCCGC and 5'GCGGCATCTAGTAGAAAAGG [18]. Specific cDNAs for CXCR1 were amplified by PCR with 5'GAAGAAGAGCCAACAAAG and 5'CTTTGTTGGCTCTTCTTC. Amplification with PCR Master Mix (Gibco BRL) was performed with 30 cycles at 94°C, 58°C, and 70°C (1 min each) for CXCR2, and 94°C, 60°C, and 70°C (1 min each) for CXCR1, followed by 12 min of 72°C in a Perkin Elmer Cetus (Foster City, CA) DNA Thermocycler 480. Am-

plified products were analyzed by agarose gel electrophoresis.

Cell Adhesion Assay

Microtiter plates (Immobilon, Chantilly, VA) were prepared for adhesion by incubating wells with 100 μl laminin in PBS for 18–24 hr at 37°C in a humidified incubator. Solutions were removed and excess sites were blocked with 1 mg/ml bovine serum albumin (BSA) in PBS for 1–2 hr at 37°C [27]. Subconfluent PC3 cells were released with brief treatment of 0.25% trypsin-EDTA. The trypsin was inhibited with 0.5 mg/ml soybean trypsin inhibitor in SFM (F12 Kaighn's modification with 0.1% BSA, 1 mM sodium pyruvate, and 50 μg/ml gentamicin), and the cells were washed with SFM and resuspended in adhesion medium (SFM with 4 mM HEPES). Cells were incubated with the indicated concentration of chemokine for 0–30 min at 37°C in 5% CO_2. Neutralizing antibodies were added prior to the chemokine when appropriate. Calcein-AM (Molecular Probes, Eugene, OR), a fluorescent probe which is internalized and hydrolyzed by intracellular esterases producing a fluorophor which emits at 530 nM, was added to a final concentration of 1 μg/ml. Approximately 1,000 cells/well were then added to adhesion plate and incubated 37°C for 35 min, gently washed 2–3 times, and quantified in a Cytofluor II fluorescent plate-reader (Biosearch, Inc., Bedford, MA). Separate standard curves were performed for each IL-8 treatment; however, no effect was seen on the fluorescent intensity of the dye with the different chemokine treatments.

Cell Migration Assay

Cell motility was assayed in 48-well microchambers (Neuroprobe, Bethesda, MD) utilizing 8-μm pore size polyvinyl pyrrolidone-free polycarbonate filters (Nucleopore, Pleasanton, CA) precoated on both sides with the indicated concentrations of laminin in PBS (10 mM phosphate, 150 mM NaCl, pH 7.4) for 16–20 hr. The lower wells of the microchamber were filled with SFM and the indicated concentration of chemokine. Adherent PC3 cells were released as for the adhesion assay and resuspended at 4×10^5 cells/ml in SFM, and 50 μl of cells were added to the upper compartment. Neutralizing antibodies were added to the cells before addition to the chamber when appropriate. Cells were allowed to migrate for 6 hr at 37°C in a 5% CO_2 incubator, and cells that had migrated to the underside of the filter were stained and counted.

Cell Invasion Assay

Cell invasion chambers were prepared according to the manufacturer's instructions (Collaborative Biomedical Products, Bedford, MA). PC3 cells (200,000 cells/well) in SFM were added to the upper chamber. SFM containing the indicated concentrations on chemokine and 25 μg/ml fibronectin was added to the lower chamber. Invasion to the lower chamber was assayed after 20–30 hr by visual quantification of cells adhering to the underside of the filter. Experiments were performed three times, and representative experiments are shown.

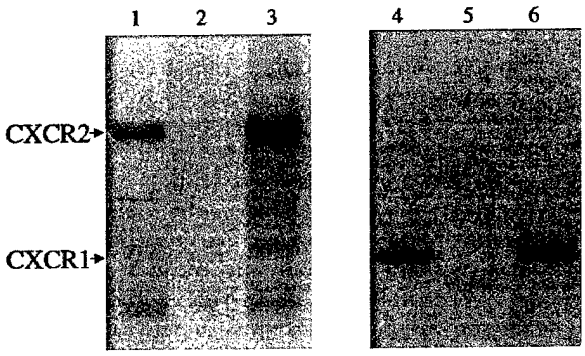

Fig. 1. PC3 cells express CXCR2 mRNA. Total RNA was isolated from PC3 cells (**lanes 1, 2, 4, 5**) or neutrophils (**lanes 3, 6**). cDNA was made using reverse transcriptase and used for RT-PCR with primers for CXCR2 (lanes 1, 3) or CXCR2 (lanes 4, 6). The no-RT control omitted the reverse transcriptase when making the cDNA (lanes 2, 5).

RESULTS

PC3 Cells Express CXCR2 and CXCR1 mRNA

To determine if PC3 cells could express message for receptors that bind the CXC-chemokines, mRNA was isolated from PC3 cells and RT-PCR was performed for CXCR1 and CXCR2 receptors, using primers from unique areas in the receptor sequences. Primers were chosen so that the resulting amplified DNA would be 967 bp for CXCR2 and 518 bp for CXCR1. CXCR1 and CXCR2 RNA transcripts were detected in the PC3 cells (Fig. 1). Neutrophils were used as a positive control and, as expected, expressed mRNA for both receptors. Control reactions without reverse transcriptase did not have amplified message.

CXC-Chemokines, IL-8, and GROα Stimulate Invasion Through a Reconstituted Basement Membrane

The basement membrane underlies the endothelium in the prostate, presenting a barrier that the prostate carcinoma cell must cross in order to metastasize. Invasion through a reconstituted basement membrane is one of the best in vitro indicators of tumor progres-

sion [30]. Since PC3 cells express CXCR2, we tested invasion with or without IL-8 and GROα, two ligands for CXCR2 shown to be chemotactic agents in other cell types. PC3 cells were added to the upper chamber of the invasion chambers, and IL-8 or GROα were added as chemoattractants to the lower part of the chamber. After 24 hr, cells that invaded through the reconstituted basement membrane were visually quantified. IL-8 and GROα were both effective in increasing PC3 invasion, stimulating invasion 1.8-fold ($P < 0.03$) and 1.7-fold ($P < 0.05$) over untreated controls, respectively (Fig. 2). GROα and IL-8 did not stimulate growth, as measured by accessing cell number in the PC3 cells under conditions similar to those in the invasion assay, indicating that chemokine-stimulated invasion is not due to increased cell proliferation (data not shown). As found in neutrophils, IL-8-induced migration is chemotactic in nature, since IL-8-induced migration was higher if an IL-8 gradient was established rather than if IL-8 was added together with the cells to stimulate random migration (data not shown). IL-8 has been shown to increase the expression of adhesion receptors in neutrophils; therefore, we examined whether IL-8 or GROα stimulated changes in the integrins which bind laminin and type IV collagen, major components of the basement membrane. PC3 cells stimulated with GROα or IL-8 did not change their expression of β_1, β_4, α_2, α_3, or α_6 integrins as measured by flow cytometry (data not shown).

IL-8 and GROα Stimulate Migration on Laminin, a Major Component of the Basement Membrane

CXC-chemokines have been shown to stimulate migration in a variety of cell types. In order to determine if chemotactic properties could contribute to the IL-8 stimulation of invasion, we assessed the ability of IL-8 to stimulate PC3 migration. Laminin, a major component of the basement membrane, was coated on both sides of the migration filter. This provided a relevant matrix to support cellular migration. However, since it was coated on both sides of the filter, it did not act as a haptotactic reagent. Also, suboptimal concentrations of laminin were used to minimize the potential contribution of spontaneous random migration on laminin. At these concentrations, LMN was able to support low levels of random migration. IL-8 was added to the lower compartment of a modified Boyden chamber to act as a chemotactic agent, and PC3 cells were added to the upper compartment and allowed to migrate for 6 hr. Over a range of 0.2–20 nM, IL-8 was chemotactic for PC3 cells migrating on laminin ($P < 0.05$ at 0.2 nM and $P < 0.001$ at 2 and 20 nM) (Fig. 3). IL-8 concentrations used for stimulating PC3 cell migration were similar to concentrations of IL-8 used to stimulate neutrophil and T-cell transmigration through endothelial cells [9,10,31]. IL-8-stimulated migration was inhibited by anti-IL-8 mAbs, demonstrating the specificity of the reaction (data not shown). IL-8 therefore acts as a chemoattractant for PC3 prostate carcinoma cells under these conditions.

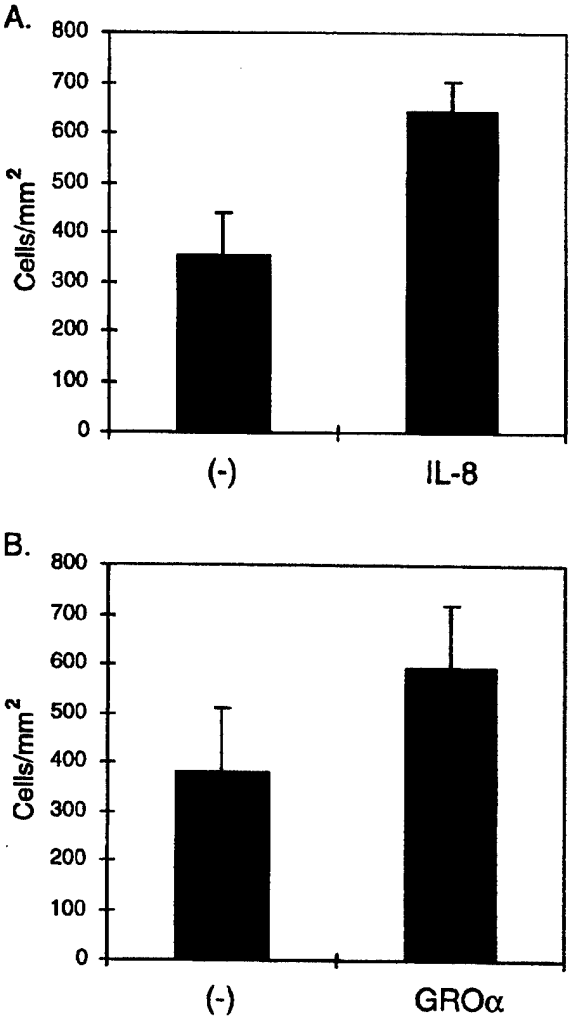

Fig. 2. IL-8 and GROα stimulate invasion through a reconstituted basement membrane. PC3 cells were added to the upper well of the invasion chamber and allowed to invade through the reconstituted basement membrane towards **(A)** 36 nM IL-8 or **(B)** 13 nM GROα. Invasion assays were for 30 hr. Cells that invaded attached to the bottom of the supporting filter, which was coated with fibronectin. Cells were stained and visually quantified. Data represent the means of triplicate determinations plus or minus the standard error of the mean.

To examine if another member of the CXC-chemokine family could also stimulate migration, we tested whether GROα could also stimulate migration. At the nanomolar concentrations used in these experi-

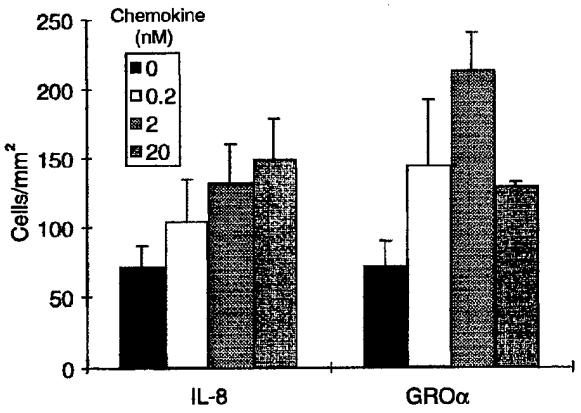

Fig. 3. IL-8 and GROα are chemotactic for PC3 cells migrating on laminin. Chemokines at the indicated concentrations were added to the lower well of a modified Boyden chamber. The wells were overlaid with filters coated on both sides with 5 μg/ml laminin. PC3 cells were added to the upper wells and incubated for 6 hr, and cells that migrated through the filter were stained and visually quantitated. Data are from representative experiments and are the means of triplicate plus or minus the standard deviation of the mean.

ments, GROα acts through CXCR2 and does not bind CXCR1 [16]. GROα also stimulated PC3 chemotaxis on laminin, indicating that CXCR2 is functional in PC3 cells (Fig. 3). At 0.2 nM, GROα PC3 cells responded with a 1.7-fold increase in migration toward the chemokine over basal migration ($P < 0.01$), with maximal response at 2 nM GROα ($P < 0.001$). The decrease in GROα stimulation of chemotaxis at 20 nM was occasionally seen at higher concentrations of both IL-8 and GROα, and is seen in other systems [32].

IL-8 and GROα Stimulate Transient Changes in Adhesion to Laminin

Changes in the adhesive phenotype can contribute to an increase in migration behavior. Therefore we looked at whether IL-8 stimulates laminin-mediated adhesion in a short-term adhesion assay. PC3 cells were pretreated for 0–30 min with 18 nM IL-8, added to laminin-coated wells, and allowed to adhere for 35 min. Suboptimal laminin concentrations were used so that when no chemokine was added, the laminin concentration supported only very low levels of cell adhesion. Preincubation with IL-8 for 15 min resulted in a 2-fold increase in adhesion ($P < 0.01$) (Fig. 4A). The increase in adhesion was transient, as the cells did not continue to respond to IL-8, returning to unstimulated levels after 30 min of IL-8 treatment.

GROα stimulation of adhesion was also observed, but was greater than that observed with IL-8 (8.9-fold

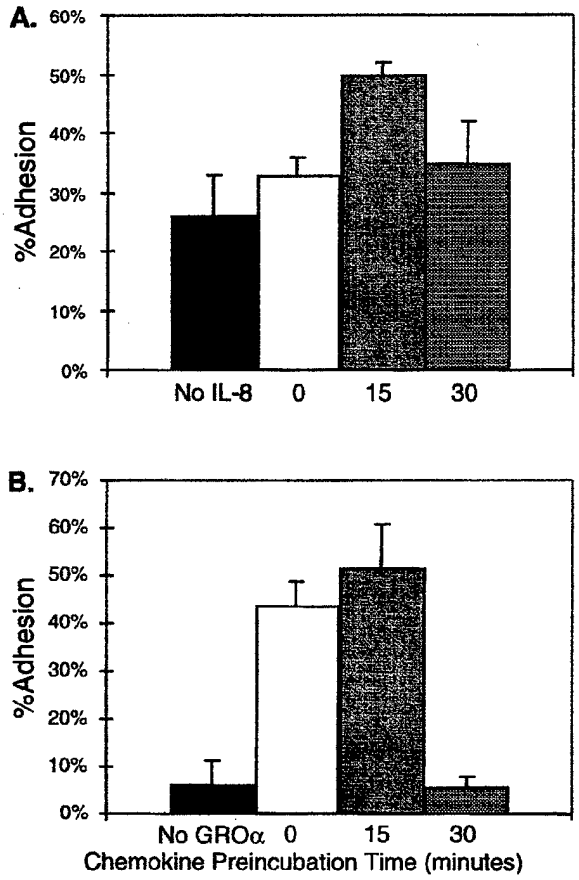

Fig. 4. IL-8 and GROα stimulate PC3 adhesion to laminin. Fluorescently labeled PC3 cells were pretreated with **(A)** 18 nM IL-8 or **(B)** 4 nM GROα for the indicated times (in min) and then added to microtiter plates coated with laminin. Cells were allowed to adhere for 30 min and then were washed, and adherent cells were quantified with a fluorescent plate-reader. Cells with no preincubation had chemokine added at the start of the assay. Adhesion of treated cells is compared to untreated PC3 cells.

vs. 2-fold, Fig. 4B). GROα increased PC3 adhesion to laminin when added at the start of the adhesion assay. Although GROα stimulated PC3 adhesion laminin more rapidly than did IL-8 (Fig. 4), this difference was not routinely observed (data not shown). In all experiments, the IL-8- or GROα-stimulated increase in adhesion was transient, as adhesion returned to prestimulation levels after 30 min. The laminin adhesion receptor levels did not change over the time course of the adhesion assay as measured by flow cytometry, and anti-α6 or anti-β1 integrin antibodies inhibited prostate cell adhesion to laminin in the presence or absence of chemokines (data not shown). These results indicate that chemokine-stimulated increases in laminin-mediated adhesion require laminin-specific inte-

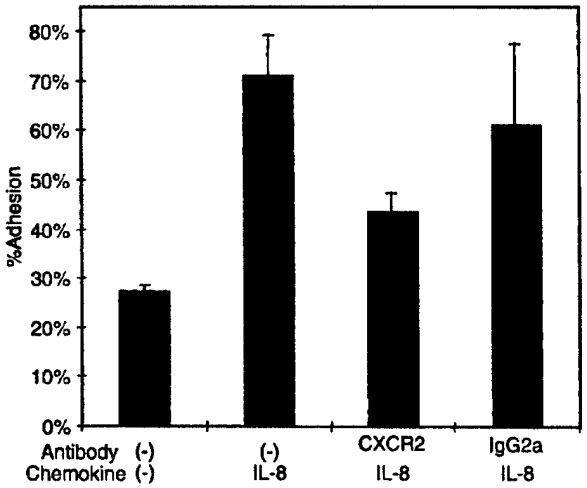

Fig. 5. Neutralizing antibodies to CXCR2 inhibit IL-8 stimulation of adhesion to laminin. PC3 cells, preincubated with or without 0.5 μg/ml anti-CXCR2 mAb or control isotype-matched antibody, were stimulated with 10 nM IL-8 for 10 min and added to adhesion wells coated with 2.5 μg/ml laminin, and then were incubated for 35 min, washed, and quantified.

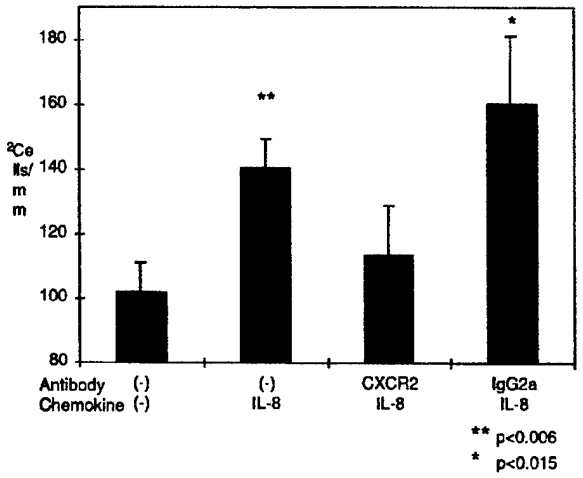

Fig. 6. Neutralizing antibodies to CXCR2 inhibit IL-8 stimulation of chemotaxis. PC3 cells, preincubated with or without 0.5 μg/ml anti-CXCR2 mAb or control isotype-matched antibody, IgG2a, were added to the chemotaxis assay in which 10 nM of IL-8 were added to the lower chamber. Migration was for 6 hr on a filter coated on both sides with 7.5 μg/ml LMN. *$P < 0.015$. **$P < 0.006$.

grins, and they suggest that chemokines stimulate functional changes in these integrins.

IL-8 Utilizes the CXCR2 Receptor to Stimulate Adhesion and Migration

IL-8 binds to both CXCR1 and CXCR2 with high affinity, and both receptors are able to signal adhesion and chemotaxis. As PC3 cells express message for CXCR2 and respond to chemokines which bind only CXCR2 at nanomolar concentrations, we used neutralizing antibodies for CXCR2 in the adhesion and chemotaxis assays to block IL-8 stimulation of adhesion and migration. The IL-8 adhesion was mediated by the CXCR2 receptor, as neutralizing antibodies to the receptor inhibited 65% of the IL-8 stimulation of adhesion ($P < 0.003$) (Fig. 5). The CXCR2 antibody also inhibited 70% of the IL-8 stimulation of migration (Fig. 6).

GROα-Stimulated Migration of Prostate Carcinoma Cells Through $\alpha_6\beta_1$ Integrin

PC3 cells use $\alpha_{6\beta1}$ integrin to adhere and migrate on laminin. The β_1 integrins are a major family of adhesion molecules used to bind to matrix molecules such as laminin. The CXC-chemokines have been shown to stimulate adhesion through the β_1 integrins on T lymphocytes [8,33]. Neutralizing antibodies to β_1 integrin and α_6 integrin subunits inhibit both basal migration and GROα-stimulated migration of PC3 cells, indicating that prostate carcinoma cells treated with GROα use $\alpha_6\beta_1$ integrin to migrate on laminin (Fig. 7). Further experiments with inhibiting antibodies to integrins did not suggest a role for α_2, α_3, α_4, α_5, or β_4 integrin subunits in chemokine-induced PC3 cell migration on laminin (Data not shown). In addition, inhibiting antibodies showed that the $\alpha_6\beta_1$ integrin was used for IL-8-stimulated migration and adhesion on laminin (data not shown). IL-8 and GROα also both stimulated migration on fibronectin at 2 and 20 nM chemokine ($P < 0.01$) (Fig. 8), possibly through effects on the fibronectin integrins $\alpha_5\beta_1$ and $\alpha_3\beta_1$, both of which are expressed by PC3 cells. This suggests that the CXC-chemokines may act on the β_1 integrins to enhance migration and invasion. As was observed for $\alpha_6\beta_1$ integrin, cell surface levels of the fibronectin integrins $\alpha_5\beta_1$ and $\alpha_3\beta_1$ did not change as a function of chemokine treatment. These results suggest that IL-8 and GROα stimulate migration of PC3 cells by modifying the function of the existing β_1 integrins rather than by upregulating expression of new adhesion receptors, as has been demonstrated in leukocytes.

DISCUSSION

Chemokines are important for stimulating cell adhesion, chemotaxis, and invasion of inflammatory cells [1]. Chemokines also promote adhesion and migration of other cell types, including breast carcinoma

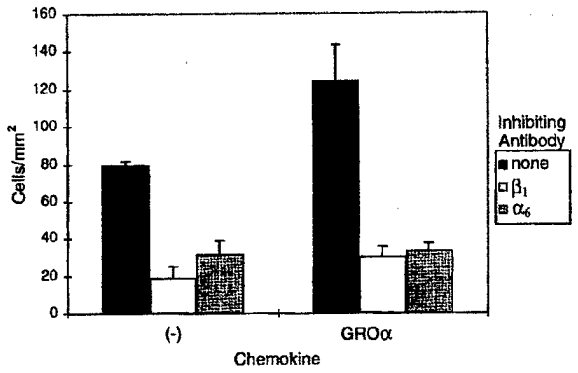

Fig. 7. Neutralizing antibodies to β_1 integrin and α_6 integrin inhibit GROα stimulation of chemotaxis. PC3 cells preincubated with or without 0.5 μg/ml anti-integrin mAbs were added to the chemotaxis assay in which no chemokine or 2.5 nM GROα were added to the lower chamber. Migration was for 6 hr on a filter coated on both sides with 7.5 μg/ml LMN.

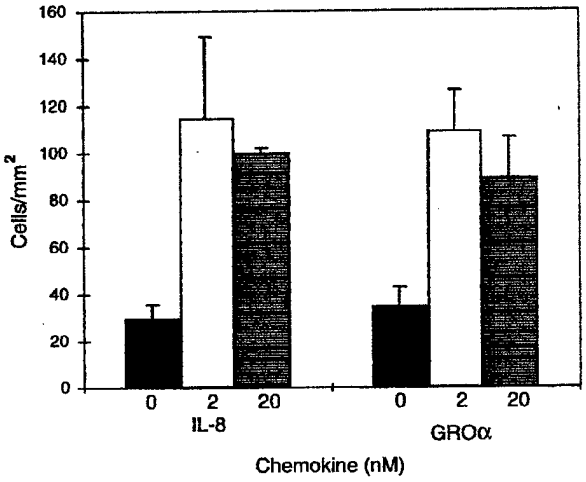

Fig. 8. IL-8 and GROα are chemotactic for PC3 cells migrating on fibronectin. PC3 cells were incubated for 6 hr in modified Boyden chambers with filters coated with 5 μg/ml fibronectin and chemokine in the lower well as the chemoattractant.

and melanoma cells, indicating a role for these chemotactic cytokines in tumor migration and invasion [9,10]. We therefore examined whether two CXC-chemokines, IL-8 and GROα, could promote prostate carcinoma-cell invasion, migration, and adhesion. CXC-chemokines, IL-8 and GROα, stimulate PC3 carcinoma-cell invasion through reconstituted basement membrane. The increase in invasion is accompanied by an IL-8- and GROα-stimulated increases in chemotaxis of cells on laminin, a major component of the basement membrane. In addition to stimulation of invasion and migration, which take place over a period of 6–24 hr, the CXC-chemokines stimulate transient increases in adhesion, which are maximal at 15 min.

Several lines of evidence demonstrate that the chemokine receptor, CXCR2, contributes to these biological effects. First, PC3 cells express mRNA for CXCR2. Next, neutralizing antibodies to CXCR2 inhibit 60% of the IL-8 stimulation of adhesion and migration. Also, CXCR2 is the only known receptor to bind GROα and stimulate migration at the concentrations used in these experiments. While CXCR2 is the predominantly active receptor in stimulating CXC-chemokine activity in PC3 cells, CXCR1 could also contribute to the IL-8 stimulation of adhesion and migration. Indeed, preliminary experiments suggest that CXCR1 contributes to IL-8-induced adhesion and migration, as anti-CXCR1 mAbs inhibit adhesion and migration when used together with CXCR2 antibodies (data not shown). Additional studies using alternate approaches to selectively isolate the two different receptors' functions are in progress to evaluate their relative contributions to chemokine-enhanced adhesion, migration, and invasion.

The mechanism by which IL-8 and GROα stimulate invasion is not known. The transient nature of the adhesion effect may be important for regulating chemotaxis and invasion, as the migration of cells involves both adhesive and deadhesive events. Transient stimulation of adhesion would allow the cell to attach at the leading edge and then migrate, rather than remain firmly attached in one place. It has been proposed that chemokines stimulate more than one signal transduction pathway, leading to the same chemokine being able to stimulate both short-term adhesion and long-term migration and invasion [33]. In addition to adhesion and migration, degradation of the matrix is also an important step in invasion. IL-8 and GROα are known to stimulate neutrophils to release preformed granules containing proteinases [34]. Whether the CXC-chemokines stimulate protease expression or activity on prostate carcinoma cells is not known. PC3 cells are invasive without the addition of chemokines, although at reduced levels, indicating that sufficient proteases are present for invasion. Additional protease release or activation could increase the invasiveness of the cells. However, as PC3 cell motility is increased by chemokine treatment, this suggests that increased migration contributes to increased invasion. The increased tumor migration and invasiveness could translate into increased metastasis of a prostate tumor in vivo when it results in cells moving away from the tumor into new tissues.

Multiple potential sources of CXC-chemokines are present in the prostate and in prostate carcinoma. Tumors are heterogeneous mixtures of cells, including immune cells that infiltrate in response to the tumor,

which could also secrete a number of chemokines. IL-8 is present in sites of inflammation, being secreted by activated monocytes, macrophages, neutrophils, endothelial cells, fibroblasts, and mitogen-activated T lymphocytes [1,35]. Macrophages, a potential source of IL-8 in prostate carcinoma, are present at higher levels in highly metastatic prostate carcinoma than in locally invasive carcinoma [36]. Although the macrophage could act in pleiotrophic ways to promote prostate tumor progression, secretion of IL-8 and the CXC-chemokines could stimulate migratory and invasive phenotypes in prostate carcinoma cells. In addition to the immune cells that produce chemokines, cells normally within the prostate also may produce CXC-chemokines [37]. In this regard, IL-8 has also been shown to be produced by stromal cells cultured from prostates, although the exact cell type(s) producing IL-8 in these cultures was not identified [37].

The CXC-chemokines could stimulate autocrine activity, as tumor cells themselves are possible sources of IL-8 and GROα [1]. IL-8 expression in tumors can be upregulated by inflammatory cytokines [38]. IL-8 expression can also be upregulated at the site of tumor implantation [39], and in areas of necrosis which are accompanied by hypoxia and ischemia [40]. Prostate adenocarcinoma cells implanted orthotopically express more IL-8 mRNA than cells placed ectopically, indicating that the microenvironment of the prostate is capable of stimulating the carcinoma cells to produce IL-8 [4]. GROα is produced by a variety of cancer cell types and is also present at sites of inflammation [1,41]. GROα has not yet been identified in the prostate or prostate carcinoma; however, it is found in seminal fluid, which is produced in part by the prostate gland [42]. The PC3 cells used in these studies expressed IL-8 protein, as determined by ELISA (personal communication from Dr. Joseph E. De Larco), and this chemokine production could contribute to the basal migration seen on laminin. Thus, IL-8 and GROα could act in an autocrine fashion to stimulate basal migration of prostate carcinoma, either in the primary tumor site or at distant sites. In addition to IL-8 and GROα, NAP-2, ENA 78, GCP-2, GROβ, and GROγ all bind to the CXCR2 receptor and are possible additional sources of chemotactic activity for prostate carcinoma in vivo [14,15]. During the course of tumor progression, as prostate tumors invade locally or metastasize to a distant site, the tumor may use CXCR2 to respond to several members of the CXC-chemokine family, depending on which chemokine family member is present at a particular site.

IL-8 and GROα stimulate prostate carcinoma chemotaxis on laminin-coated substrata through $\alpha_6\beta_1$ integrin, which has been linked to prostate tumor progression [43]. Although no clear changes in β_1 integrin expression have been found during prostate cancer progression, several reports have described relative decreases in β_4 expression in advanced prostate carcinoma compared to normal tissue [44,45]. The α_6 integrin associates with both β_4 and β_1 integrin. In more advanced prostate cancer, β_4 integrin is downregulated and the α_6 subunit preferentially associates with β_1 [46]. The relative increase in $\alpha_6\beta_1$ expression may lead to increased malignant behavior, since it was previously shown that the expression of $\alpha_6\beta_1$ integrin causes an increase in the invasiveness of the prostate cells in an in vivo experimental model [43]. IL-8 and GROα stimulation of adhesion and migration is not limited to $\alpha_6\beta_1$ integrin-specific ligands, as these chemokines also stimulate adhesion and migration on fibronectin, which binds $\alpha_5\beta_1$ and perhaps $\alpha_3\beta_1$ integrin. This suggests IL-8 and GROα may stimulate β_1 integrin-mediated events in general rather than acting through one particular α/β integrin heterodimer. As a result, chemokines may act to stimulate invasion of prostate carcinoma cells through multiple tissues and basement membranes, thus contributing to metastasis during several stages of the process.

IL-8 and GROα stimulate adhesion and migration through modulation of the activation state of β_1 integrins, rather than by changing the surface expression levels of these integrins. In other cell types, the CXC-chemokines stimulate β_1 integrin-mediated adhesion and migration on matrix components. IL-8 has been shown to stimulate T-cell [8], neutrophil [47], and sickle erythrocyte [48] migration or adhesion on fibronectin and fibrinogen. β_1 integrin receptor expression is not profoundly changed by the chemokines, and this has led to the proposal that the β_1 integrins are functionally activated by the CXC-chemokines [47]. In prostate carcinoma cells, this is supported in part by the observations that IL-8 and GROα can transiently induce high levels of PC3 cell adhesion at laminin concentrations that normally support only low levels of adhesion. Also, PC3 cells use the same integrins for chemokine-induced migration as for basal migration. Finally, IL-8 and GROα do not upregulate β_1 integrin expression in prostate carcinoma cells. Therefore it may be possible that changes in receptor affinity or avidity rather than expression account for the stimulation in prostate carcinoma cells. The $\alpha_6\beta_1$ integrin can be activated by stimulating inside-out signaling pathways [49,50], and studies are in progress to evaluate if chemokine treatment alters the relative affinity of PC3 cells for laminin. Alternatively, the chemokines could be changing integrin avidity or they may impact on signal pathways downstream of the integrin to enhance integrin-mediated matrix interactions.

The chemokines are known to stimulate signal

transduction pathways that are linked to integrin activation. IL-8 and GROα stimulate intracellular calcium release [51], PI3 kinase [52], and Rho activity [22], which are also linked to increased integrin-mediated adhesion, cytoskeletal changes, and integrin activation [22,53–55]. Inhibiting the IL-8 signal transduction pathways that have been linked to integrins inhibits the ability of the chemokine to stimulate migration and adhesion. For example, inhibiting PI3 kinase inhibits IL-8-stimulated migration [52], and inhibiting Rho inhibits IL-8-stimulated adhesion of lymphocytes transfected with IL-8 receptors [22]. Chemokines have been demonstrated to increase T lymphocyte β_1 integrin-mediated adhesion [33,56] and migration [33] to matrix molecules without changes in integrin expression, suggesting changes in integrin activity [56]. Chemokine stimulation of migration and adhesion in T lymphocytes (similar to results with prostate cells) suggests that chemokines use more than one signal transduction pathway to stimulate such a broad range of effects [33]. By using more than one signal transduction pathway in tumors, the CXC-chemokines could stimulate both more long-term (invasion, migration) and short-term (adhesion) effects.

In conclusion, the CXC-chemokines, which stimulate PC3 prostatic carcinoma cells to adhere to, migrate on, and invade the basement membrane, could be important in signaling the tumor cell to become invasive. The CXCR2 receptor, present on PC3 cells, mediates the CXC-chemokine stimulation of adhesion, migration, and invasion. As the CXCR2 receptor binds many members of the CXC-chemokine family, prostate cells could respond to a variety of CXC-chemokines, allowing the tumor to take advantage of different chemokines at different points in tumor progression. Focusing on how the receptor signals tumor cells may provide basic insights into how tumors invade surrounding tissue. In particular, it will be important to understand CXC-chemokine receptor-signaling in prostate cancer and to define the relationship of this receptor to β_1 integrin-mediated adhesion and migration. Factors that change integrin activity rather than gross changes in integrin expression may play an important role in signaling the adhesion and migration changes required for the prostate carcinoma to become invasive. Understanding pathways between the CXC-chemokines and integrin action may provide better diagnoses or may lead to an effective therapy for the management of prostate cancer patients.

ACKNOWLEDGMENTS

The authors thank Dr. Joseph E. De Larco for excellent advice during the course of these studies. This research was supported by National Cancer Institute/National Institutes of Health grant CA29995 to L.T.F. and DOD grant PC970519 to J.B.M.

REFERENCES

1. Baggiolini M, Dewald B, Moser B. Interleukin-8 and related chemotactic cytokines—CXC and CC chemokines. Adv Immunol 1994;55:97–109.
2. Oppenheim JJ, Zachariae CO, Mukaida N, Matsushima K. Properties of the novel proinflammatory supergene "intercrine" cytokine family. Annu Rev Immunol 1991;9:617–648.
3. Arenberg DA, Kunkel SL, Polverini PJ, Glass M, Burdick MD, Strieter RM. Inhibition of interleukin-8 reduces tumorigenesis of human non-small cell lung cancer in SCID mice. J Clin Invest 1996;97:2792–2802.
4. Greene GF, Kitadai Y, Pettaway CA, von Eschenbach AC, Bucana CD, Fidler IJ. Correlation of metastasis-related gene expression with metastatic potential in human prostate carcinoma cells implanted in nude mice using an in situ messenger RNA hybridization technique. Am J Pathol 1997;150:1571–1582.
5. Mattei S, Colombo MP, Melani C, Silvani A, Parmiani G, Herlyn M. Expression of cytokine/growth factors and their receptors in human melanoma and melanocytes. Int J Cancer 1994;56:853–857.
6. Singh RK, Gutman M, Radinsky R, Bucana CD, Fidler IJ. Expression of interleukin 8 correlates with the metastatic potential of human melanoma cells in nude mice. Cancer Res 1994;54:3242–3247.
7. Geiser T, Dewald B, Ehrengruber MU, Clark-Lewis I, Baggiolini M. The interleukin-8-related chemotactic cytokines GRO alpha, GRO beta, and GRO gamma activate human neutrophil and basophil leukocytes. J Biol Chem 1993;268:15419–15424.
8. Somersalo K, Carpen O, Saksela E. Stimulated natural killer cells secrete factors with chemotactic activity, including NAP-1/IL-8, which supports VLA-4- and VLA-5-mediated migration of T lymphocytes. Eur J Immunol 1994;24:2957–2965.
9. Youngs SJ, Ali SA, Taub DD, Rees RC. Chemokines induce migrational responses in human breast carcinoma cell lines. Int J Cancer 1997;71:257–266.
10. Wang JM, Taraboletti G, Matsushima K, Van Damme J, Mantovani A. Induction of haptotactic migration of melanoma cells by neutrophil activating protein/interleukin-8. Biochem Biophys Res Commun 1990;169:165–170.
11. Koch AE, Polverini PJ, Kunkel SL, Harlow LA, DiPietro LA, Elner VM, Elner SG, Strieter RM. Interleukin-8 as a macrophage-derived mediator of angiogenesis [see comments]. Science 1992;258:1798–1801.
12. Balentien E, Mufson BE, Shattuck RL, Derynck R, Richmond A. Effects of MGSA/GRO alpha on melanocyte transformation. Oncogene 1991;6:1115–1124.
13. Olbina G, Cieslak D, Ruzdijic S, Esler C, An Z, Wang X, Hoffman R, Seifert W, Pietrzkowski Z. Reversible inhibition of IL-8 receptor B mRNA expression and proliferation in non-small cell lung cancer by antisense oligonucleotides. Anticancer Res 1996;16:3525–3530.
14. Wuyts A, Van Osselaer N, Haelens A, Samson I, Herdewijn P, Ben-Baruch A, Oppenheim JJ, Proost P, Van Damme J. Characterization of synthetic human granulocyte chemotactic protein 2: usage of chemokine receptors CXCR1 and CXCR2 and in vivo inflammatory properties. Biochemistry 1997;36:2716–2723.
15. Ahuja SK, Murphy PM. The CXC chemokines growth-regulated oncogene (GRO) alpha, GRObeta, GROgamma, neutrophil-activating peptide-2, and epithelial cell-derived neutrophil-activating peptide-78 are potent agonists for the type B, but not

the type A, human interleukin-8 receptor. J Biol Chem 1996;271: 20545–20550.
16. Loetscher P, Seitz M, Clark-Lewis I, Baggiolini M, Moser B. Both interleukin-8 receptors independently mediate chemotaxis. Jurkat cells transfected with IL-8R1 or IL-8R2 migrate in response to IL-8, GRO alpha and NAP-2. FEBS Lett 1994;341:187–192.
17. Hammond ME, Lapointe GR, Feucht PH, Hilt S, Gallegos CA, Gordon CA, Giedlin MA, Mullenbach G, Tekamp-Olson P. IL-8 induces neutrophil chemotaxis predominantly via type I IL-8 receptors. J Immunol 1995;155:1428–1433.
18. Norgauer J, Metzner B, Schraufstatter I. Expression and growth-promoting function of the IL-8 receptor beta in human melanoma cells. J Immunol 1996;156:1132–1137.
19. Wu D, LaRosa GJ, Simon MI. G protein-coupled signal transduction pathways for interleukin-8. Science 1993;261:101–103.
20. Bacon KB, Flores-Romo L, Life PF, Taub DD, Premack BA, Arkinstall SJ, Wells TN, Schall TJ, Power CA. IL-8-induced signal transduction in T lymphocytes involves receptor-mediated activation of phospholipases C and D. J Immunol 1995;154:3654–3666.
21. Johnston JA, Ferris DK, Wang JM, Longo DL, Oppenheim JJ, Kelvin DJ. Staurosporine restores signaling and inhibits interleukin-8-induced chemotactic desensitization. Eur J Immunol 1994;24:2556–2562.
22. Laudanna C, Campbell JJ, Butcher EC. Role of Rho in chemoattractant-activated leukocyte adhesion through integrins. Science 1996;271:981–983.
23. Norgauer J, Krutmann J, Dobos GJ, Traynor-Kaplan AE, Oades ZG, Schraufstatter IU. Actin polymerization, calcium-transients, and phospholipid metabolism in human neutrophils after stimulation with interleukin-8 and N-formyl peptide. J Invest Dermatol 1994;102:310–314.
24. Smith CW, Kishimoto TK, Abbassi O, Hughes B, Rothlein R, McIntire LV, Butcher E, Anderson DC, Abbassi O. Chemotactic factors regulate lectin adhesion molecule 1 (LECAM-1)-dependent neutrophil adhesion to cytokine-stimulated endothelial cells in vitro. J Clin Invest 1991;87:609–618 [published erratum appears in J Clin Invest 1991;87:1873].
25. Detmers PA, Lo SK, Olsen-Egbert E, Walz A, Baggiolini M, Cohn ZA. Neutrophil-activating protein 1/interleukin 8 stimulates the binding activity of the leukocyte adhesion receptor CD11b/CD18 on human neutrophils. J Exp Med 1990;171:1155–1162.
26. Detmers PA, Powell DE, Walz A, Clark-Lewis I, Baggiolini M, Cohn ZA. Differential effects of neutrophil-activating peptide 1/IL-8 and its homologues on leukocyte adhesion and phagocytosis. J Immunol 1991;147:4211–4217.
27. Herbst TJ, McCarthy JB, Tsilibary EC, Furcht LT. Differential effects of laminin, intact type IV collagen, and specific domains of type IV collagen on endothelial cell adhesion and migration. J Cell Biol 1988;106:1365–1373.
28. McCarthy JB, Skubitz AP, Palm SL, Furcht LT. Metastasis inhibition of different tumor types by purified laminin fragments and a heparin-binding fragment of fibronectin. J Natl Cancer Inst 1988;80:108–116.
29. Wayner EA, Gil SG, Murphy GF, Wilke MS, Carter WG. Epiligrin, a component of epithelial basement membranes, is an adhesive ligand for alpha 3 beta 1 positive T lymphocytes. J Cell Biol 1993;121:1141–1152.
30. Albini A, Iwamoto Y, Kleinman HK, Martin GR, Aaronson SA, Kozlowski JM, McEwan RN. A rapid in vitro assay for quantitating the invasive potential of tumor cells. Cancer Res 1987;47: 3239–3245.
31. Santamaria Babi LF, Moser B, Perez Soler MT, Moser R, Loetscher P, Villiger B, Blaser K, Hauser C. The interleukin-8 receptor B and CXC chemokines can mediate transendothelial migration of human skin homing T cells. Eur J Immunol 1996; 26:2056–2061.
32. Ben-Baruch A, Grimm M, Bengali K, Evans GA, Chertov O, Wang JM, Howard OM, Mukaida N, Matsushima K, Oppenheim JJ. The differential ability of IL-8 and neutrophil-activating peptide-2 to induce attenuation of chemotaxis is mediated by their divergent capabilities to phosphorylate CXCR2 (IL-8 receptor B). J Immunol 1997;158:5927–5933.
33. Campbell JJ, Qin S, Bacon KB, Mackay CR, Butcher EC. Biology of chemokine and classical chemoattractant receptors: differential requirements for adhesion-triggering versus chemotactic responses in lymphoid cells. J Cell Biol 1996;134:255–266.
34. Boxer LA, Smolen JE. Neutrophil granule constituents and their release in health and disease. Hematol Oncol Clin North Am 1988;2:101–134.
35. Proost P, Wuyts A, van Damme J. The role of chemokines in inflammation. Int J Clin Lab Res 1996;26:211–223.
36. Vukanovic J, Isaacs JT. Linomide inhibits angiogenesis, growth, metastasis, and macrophage infiltration within rat prostatic cancers. Cancer Res 1995;55:1499–1504.
37. Degeorges A, Tatoud R, Fauvel-Lafeve F, Podgorniak MP, Millot G, de Cremoux P, Calvo F. Stromal cells from human benign prostate hyperplasia produce a growth-inhibitory factor for LNCaP prostate cancer cells, identified as interleukin-6. Int J Cancer 1996;68:207–214.
38. Singh RK, Gutman M, Llansa N, Fidler IJ. Interferon-beta prevents the upregulation of interleukin-8 expression in human melanoma cells. J Interferon Cytokine Res 1996;16:577–584.
39. Gutman M, Singh RK, Xie K, Bucana CD, Fidler IJ. Regulation of interleukin-8 expression in human melanoma cells by the organ environment. Cancer Res 1995;55:2470–2475.
40. Desbaillets I, Diserens AC, Tribolet N, Hamou MF, Van Meir EG. Upregulation of interleukin 8 by oxygen-deprived cells in glioblastoma suggests a role in leukocyte activation, chemotaxis, and angiogenesis. J Exp Med 1997;186:1201–1212.
41. Yang SK, Eckmann L, Panja A, Kagnoff MF. Differential and regulated expression of C-X-C, C-C, and C-chemokines by human colon epithelial cells. Gastroenterology 1997;113:1214–1223.
42. Rajasekaran M, Hellstrom W, Sikka S. Quantitative assessment of cytokines (GRO alpha and IL-10) in human seminal plasma during genitourinary inflammation. Am J Reprod Immunol 1996;36:90–95.
43. Rabinovitz I, Nagle RB, Cress AE. Integrin alpha 6 expression in human prostate carcinoma cells is associated with a migratory and invasive phenotype in vitro and in vivo. Clin Exp Metastasis 1995;13:481–491.
44. Nagle RB, Knox JD, Wolf C, Bowden GT, Cress AE. Adhesion molecules, extracellular matrix, and proteases in prostate carcinoma. J Cell Biochem [Suppl] 1994;19:232–237.
45. Knox JD, Cress AE, Clark V, Manriquez L, Affinito KS, Dalkin BL, Nagle RB. Differential expression of extracellular matrix molecules and the alpha 6-integrins in the normal and neoplastic prostate. Am J Pathol 1994;145:167–174.
46. Cress AE, Rabinovitz I, Zhu W, Nagle RB. The alpha 6 beta 1 and alpha 6 beta 4 integrins in human prostate cancer progression. Cancer Metastasis Rev 1995;14:219—228.
47. Loike JD, el Khoury J, Cao L, Richards CP, Rascoff H, Mandeville JT, Maxfield FR, Silverstein SC. Fibrin regulates neutrophil migration in response to interleukin 8, leukotriene B4, tumor necrosis factor, and formyl-methionyl-leucyl-phenylalanine. J Exp Med 1995;181:1763–1772.
48. Kumar A, Eckmam JR, Swerlick RA, Wick TM. Phorbol ester stimulation increases sickle erythrocyte adherence to endothelium: a novel pathway involving alpha 4 beta 1 integrin recep-

tors on sickle reticulocytes and fibronectin. Blood 1996;88:4348–4358.
49. Delwel GO, Hogervorst F, Kuikman I, Paulsson M, Timpl R, Sonnenberg A. Expression and function of the cytoplasmic variants of the integrin alpha 6 subunit in transfected K562 cells. Activation-dependent adhesion and interaction with isoforms of laminin. J Biol Chem 1993;268:25865–25875.
50. Shaw LM, Messier JM, Mercurio AM. The activation dependent adhesion of macrophages to laminin involves cytoskeletal anchoring and phosphorylation of the alpha 6 beta 1 integrin. J Cell Biol 1990;110:2167–2174.
51. L'Heureux GP, Bourgoin S, Jean N, McColl SR, Naccache PH. Diverging signal transduction pathways activated by interleukin-8 and related chemokines in human neutrophils: interleukin-8, but not NAP-2 or GRO alpha, stimulates phospholipase D activity. Blood 1995;85:522–531.
52. Knall C, Worthen GS, Johnson GL. Interleukin 8-stimulated phosphatidylinositol-3-kinase activity regulates the migration of human neutrophils independent of extracellular signal-regulated kinase and p38 mitogen-activated protein kinases. Proc Natl Acad Sci USA 1997;94:3052–3057.
53. Hartfield PJ, Greaves MW, Camp RD. Beta 1 integrin-mediated T cell adhesion is regulated by calcium ionophores and endoplasmic reticulum Ca(2+)-ATPase inhibitors. Biochem Biophys Res Commun 1993;196:1183–1187.
54. Sjaastad MD, Lewis RS, Nelson WJ. Mechanisms of integrin-mediated calcium signaling in MDCK cells: regulation of adhesion by IP3- and store-independent calcium influx. Mol Biol Cell 1996;7:1025–1041.
55. Shimizu Y, Mobley JL, Finkelstein LD, Chan AS. A role for phosphatidylinositol 3-kinase in the regulation of beta 1 integrin activity by the CD2 antigen. J Cell Biol 1995;131:1867–1880.
56. Lloyd AR, Oppenheim JJ, Kelvin DJ, Taub DD. Chemokines regulate T cell adherence to recombinant adhesion molecules and extracellular matrix proteins. J Immunol 1996;156:932–938.

THE JOURNAL OF BIOLOGICAL CHEMISTRY
Vol. 276, No. 21, Issue of May 25, pp. 17949–17957, 2001
Printed in U.S.A.

Hyaluronan Synthase Elevation in Metastatic Prostate Carcinoma Cells Correlates with Hyaluronan Surface Retention, a Prerequisite for Rapid Adhesion to Bone Marrow Endothelial Cells*

Received for publication, November 6, 2000, and in revised form, February 20, 2001
Published, JBC Papers in Press, March 5, 2001, DOI 10.1074/jbc.M010064200

Melanie A. Simpson‡, Jane Reiland‡, Scott R. Burger‡, Leo T. Furcht‡, Andrew P. Spicer§, Theodore R. Oegema, Jr.¶‖, and James B. McCarthy‡**

From the Departments of ‡Laboratory Medicine and Pathology, ¶Orthopaedic Surgery and ‖Biochemistry, University of Minnesota, Minneapolis, Minnesota 55455 and the §Rowe Program in Genetics, Department of Biological Chemistry, University of California, Davis, California 95616

Bone marrow is the primary site of metastasis in patients with advanced stage prostate cancer. Prostate carcinoma cells metastasizing to bone must initially adhere to endothelial cells in the bone marrow sinusoids. In this report, we have modeled that interaction *in vitro* using two bone marrow endothelial cell (BMEC) lines and four prostate adenocarcinoma cell lines to investigate the adhesion mechanism. Highly metastatic PC3 and PC3M-LN4 cells were found to adhere rapidly and specifically (70–90%) to BMEC-1 and trHBMEC bone marrow endothelial cells, but not to human umbilical vein endothelial cells (15–25%). Specific adhesion to BMEC-1 and trHBMEC was dependent upon the presence of a hyaluronan (HA) pericellular matrix assembled on the prostate carcinoma cells. DU145 and LNCaP cells were only weakly adherent and retained no cell surface HA. Maximal BMEC adhesion and HA encapsulation were associated with high levels of HA synthesis by the prostate carcinoma cells. Up-regulation of HA synthase isoforms Has2 and Has3 relative to levels expressed by normal prostate corresponded to elevated HA synthesis and avid BMEC adhesion. These results support a model in which tumor cells with up-regulated HA synthase expression assemble a cell surface hyaluronan matrix that promotes adhesion to bone marrow endothelial cells. This interaction could contribute to preferential bone metastasis by prostate carcinoma cells.

Prostate cancer is the second leading cause of cancer death in men (1). In metastatic prostate cancer, peripheral tumor cells undergo phenotypic changes that facilitate invasion of surrounding organ tissues, entry into the lymphatic system and/or the bloodstream, and colonization of other tissues in the body. Their ability to establish growth in a remote site is dependent upon a specific recognition process involving an initial rapid adhesion of the circulating tumor cell to endothelial cells lining the bone marrow microvasculature (2), transmigration through the endothelial cell barrier, and subsequent lodgment in the stroma (3, 4). Remote metastases in prostate cancer often occur in bone marrow, suggesting tissue or endothelial cell-specific factors may contribute to prostate cancer metastasis to bone (2, 5).

Bone marrow endothelial cells (BMEC)[1] maintain a specialized endothelium that must allow cell trafficking in and out of the bone marrow (3, 4, 6). In addition to regulating the egress of mature myeloid and lymphoid cells, BMEC selectively allow transmigration of progenitor cells from a circulating population, indicating that specific receptors regulate the movement of cells through the endothelium (7). Studies have shown that the transmigrating cells move directly through an endothelial cell in a process that involves specific adhesive interactions (Ref. 3 and references therein). BMEC constitutively express adhesion receptors such as VCAM-1 (8, 9), E-selectin (9), and P-selectin (10), which are not expressed in large vein endothelia unless activated by cytokines (6). Specific adhesive interactions between hemopoietic cells and BMEC thought to be important for homing include endothelial lectins and progenitor glycoproteins (11–14), VCAM/VLA-4 (11–13), and CD44/hyaluronan (15). Initial adhesion may be mediated primarily through selectins and glycoproteins. BMEC-associated chemokines such as SDF-1 (stromal-derived factor) can then stimulate integrin ligation, leading to progenitor arrest (16, 17).

Because the bone marrow microvasculature presents the first site of interaction for circulating tumor cells metastasizing to the bone marrow, it is likely that mechanisms of metastasis may parallel those employed by homing progenitors. In fact, tumor cells have been shown to bind and transmigrate through BMEC (17–19). The adhesion molecules implicated in these processes, CD44/hyaluronan, VLA-4/VCAM, and LFA-1/ICAM, are also involved in homing and extravasation of circulating lymphocytes and progenitor cells.

Hyaluronan (HA) is a ubiquitous high molecular weight glycosaminoglycan polymer required for growth, development, cell motility, and cushioning of joints (20, 21). Elevated levels of HA are associated with various pathologies, such as arthritis, inflammation, and several cancers (22–24), including prostate (25, 26). Melanoma cells selected for high expression of HA were more metastatic when injected into nude mice than cells

* This work was supported by NCI, National Institutes of Health Grant CA29995, National Research Service Award 1F32-CA84619-01 (to M. A. S.), and U.S. Army Medical Research Grant PC970519. The costs of publication of this article were defrayed in part by the payment of page charges. This article must therefore be hereby marked "*advertisement*" in accordance with 18 U.S.C. Section 1734 solely to indicate this fact.

** To whom correspondence should be addressed: Dept. of Laboratory Medicine and Pathology, University of Minnesota, Box 609 Mayo, 420 Delaware St. S.E., Minneapolis, MN 55455. Tel.: 612-625-7454; Fax: 612-625-1121; E-mail: mccar001@tc.umn.edu.

[1] The abbreviations used are: BMEC, bone marrow endothelial cells; HUVEC, human umbilical vein endothelial cells; BMSC, bone marrow stromal cells; HA, hyaluronan; HAase, hyaluronidase; HAS, hyaluronan synthase; VCAM/ICAM, vascular/intercellular cell adhesion molecule; GAPDH, glyceraldehyde-3-phosphate dehydrogenase; RT-PCR, reverse transcription followed by polymerase chain reaction; PBS, phosphate-buffered saline; FBS, fetal bovine serum; SFM, serum free medium; HRP, horseradish peroxidase; OPD, *ortho*-phenylenediamine; PAGE, polyacrylamide gel electrophoresis; BSA, bovine serum albumin.

that expressed low amounts of HA (27). Furthermore, overexpression of HA biosynthetic enzymes in tumor cell lines has been shown to increase tumorigenicity and metastatic potential (28, 29).

To investigate the molecular mechanism of initial adhesion to bone marrow endothelium, we modeled adhesion *in vitro* using the bone marrow endothelial cell lines BMEC-1 and trHBMEC and four prostate adenocarcinoma cell lines, PC3, PC3M-LN4, DU145, and LNCaP. Highly metastatic PC3 and PC3M-LN4 cells adhered rapidly to BMEC-1 but not to large vein endothelial cells (HUVEC). DU145 and LNCaP cells, in contrast, were poorly adherent to endothelial cells. Maximal BMEC adhesion was inhibited by addition of excess exogenous hyaluronan, and by hyaluronidase digestion of pericellular HA, found assembled specifically on PC3 and PC3M-LN4 cells. Presence of pericellular HA was correlated with elevated levels of HA synthesis and expression of HA synthase. Our data relate HA synthase overexpression to metastatic potential of prostate tumor cells and represent the first report of such a correlation. Collectively, our results implicate tumor cell-associated HA and up-regulation of HA synthase in prostate cancer progression and may directly impact metastatic potential or preferential tissue colonization of individual tumor cells.

EXPERIMENTAL PROCEDURES

Cell Culture and Reagents—PC3, DU-145, and LNCaP human prostate adenocarcinoma cell lines were purchased from ATCC (Manassas, VA). PC3 and DU145 cells were maintained in MEM supplemented with 10% FBS, 1 mM sodium pyruvate and non-essential amino acids. LNCaP cells were cultured in RPMI containing 10% FBS. The PC3 derivative cell line, PC3M-LN4, was kindly provided by Dr. Isaiah J. Fidler (M. D. Anderson Hospital Cancer Center, Houston, TX), and was maintained in the media described above for PC3 cells. Prostate carcinoma cells were plated 2 days prior to experiments and used at ~70% confluence. The BMEC-1 human bone marrow endothelial cell line was a gift from Dr. S. Rafii (Cornell University Medical Center, New York, NY) and were maintained in M199 containing 20% FBS (30). trHBMEC human bone marrow endothelial cells were a gift from Dr. Karin Schweitzer (Free University Hospital Amsterdam, The Netherlands) and were maintained in RPMI containing 10% FBS (11). HUVEC were purchased from Clonetics and cultured in endothelial cell growth medium, EGM-2, as recommended by the vendor. Human bone marrow stromal cells (31) were cultured and generously provided by Nisha Shah and Dr. Tucker LeBien (University of Minnesota, Minneapolis, MN). Aggrecan was prepared as previously described (32) from Swarm rat chondrosarcoma.

Cell Adhesion Assay—Subconfluent prostate carcinoma cells were PBS-EDTA-released, washed with adhesion medium (RPMI with 0.1% BSA and 20 mM Hepes, pH 7.4, maintained throughout the assay at 37 °C), and resuspended at 1×10^6 cells/ml in adhesion medium. Cells were incubated with 25 μg/ml calcein-AM (Molecular Probes, Eugene, OR), a compound that is converted to a fluorophore only upon uptake and metabolism by living cells, for 20 min, washed with adhesion medium, and resuspended at 1×10^5 cells/ml. BMEC-1 or HUVEC were seeded 100% confluent (about 40,000 cells/well) in 48-well plates for 2 days and washed twice with adhesion medium prior to the assay. trHBMEC were similarly prepared, but seeded only overnight prior to the assay. Prostate carcinoma cells (300 μl/well) were added to the confluent endothelial cell monolayers and incubated for 12 min at 37 °C unless otherwise indicated. Non-adherent cells were removed with two gentle washes of adhesion medium. Viability of non-adherent cells was verified by trypan blue exclusion. Adherent cells were solubilized with PBS containing 0.2 N NaOH/1% SDS and quantified in a Cytofluor II fluorescence plate reader at 485/530 nm (Biosearch Inc., Bedford, MA).

Inhibition of Cell Adhesion—Calcein-AM-labeled prostate carcinoma cell suspensions, at 5×10^5 cells/ml, were preincubated with 16 units/ml *Streptomyces* hyaluronidase (HAase, Calbiochem, San Diego, CA) for 25 min and diluted to 1×10^5 cells/ml with adhesion medium prior to the assay. BMEC-1 monolayers were pretreated with 16 units/ml HAase in adhesion medium for 25 min where indicated. In the case of determining the cell type retaining surface HA, the HAase was removed from each cell type before the assay. In the other experiments, the HAase was present throughout the assay.

To determine the effect of exogenous HA on intercellular adhesion, trHBMEC were seeded at 100% confluence overnight in 48-well tissue culture plates. Prior to the assay, the cell monolayers were washed twice in adhesion medium and preincubated for 30 min in 100 μl of adhesion medium containing the indicated concentrations of high molecular weight human umbilical cord HA (Sigma H1751). Prostate carcinoma cells were labeled and pretreated in the absence or presence of HAase as described above. Labeled cells were then washed, resuspended in adhesion medium containing the appropriate concentration of HA, and immediately added to the endothelial cell monolayers (30,000 cells/well).

Particle Exclusion Assay—Pericellular HA matrices were visualized as described previously (33). Briefly, prostate carcinoma cells cultured in 48-well plates overnight prior to the assay were treated for 25 min in the absence or presence of 16 units/ml *Streptomyces* hyaluronidase in phenol red-free MEM with 0.1% BSA at 37 °C. This medium was removed and cells were incubated 90 min with 2 mg/ml aggrecan in MEM/0.1% BSA at 37 °C. The aggrecan solution was removed and 1×10^8 glutaraldehyde-fixed sheep red blood cells (Accurate Chemical and Scientific Corp.) in PBS/1% BSA were added, allowed to settle for 15 min and then viewed with phase-contrast microscopy. The HA matrix was evidenced by halos surrounding the cells from which the fixed erythrocytes were excluded. Representative cells were photographed at 400× magnification. To quantify matrix retention, outlines of matrices and cellular boundaries from 20 individual cells of each type were traced and relative areas calculated using IMAGE software (National Institutes of Health). Relative matrix areas from similar tracings of each cell type following HAase digestion were subtracted, and HA matrix thickness was reported as the ratio of matrix area to cell area for each cell type. A ratio of 1 indicates complete absence of pericellular clearing.

HA Synthesis Quantitation—The concentration of HA in cell culture supernatants was determined in a competitive binding assay (34). 96-well Immulon microtiter plates were coated with human umbilical cord HA at 25 μg/ml in 200 mM carbonate buffer (pH 9.6) for 4 h at 37 °C. Excess HA was removed with four washes of PBS/0.05% Tween 20. Prostate carcinoma cells (5000/well) were plated overnight in 12-well plates. 24-h conditioned culture media were harvested, and cell counts were determined by trypsin release and manual counting in a hemacytometer. Serial dilutions of cell culture supernatant (100 μl of total volume in PBS/Tween 20) were combined with 100 μl of a 1 μg/ml solution of biotinylated hyaluronic acid-binding protein (Seikagaku) and incubated in the HA-precoated wells at room temperature overnight. The plate was washed 4× with PBS/Tween 20, developed using an avidin-biotin HRP system (Vector Laboratories ABC-HRP kit PK-4000) with OPD (Sigma P8287) as substrate, and read at 490 nm. HA concentration was interpolated from a standard curve generated by plotting HA standards against absorbance values. The mean HA concentration for each sample of culture supernatant was calculated, and the results were normalized to cell number. Data are presented as mass of HA (in μg) per 10^6 cells.

Determination of HA Synthase Expression—HA synthase isoform and relative level of expression in prostate carcinoma cell lines was semi-quantitatively assayed by RT-PCR. Poly(A)$^+$ RNA was isolated from subconfluent PC3M-LN4, PC3, DU145, and LNCaP cell lines with the Oligotex mRNA isolation kit (Qiagen) and quantitated by Ribogreen fluorescence (Molecular Probes). Normal prostate poly(A)$^+$ RNA was purchased from CLONTECH. 25 ng of each mRNA template was reverse-transcribed with an oligo(dT) primer using the Superscript II first strand cDNA synthesis kit (Life Technologies, Inc.). PCR oligonucleotides specific for Has1, Has2, and Has3 messages were designed from the sequence data base; exact sequences are given in Table I along with relative positions in the reported sequences and expected product sizes. Glyceraldehyde-3-phosphate dehydrogenase (GAPDH) was amplified with each reaction to standardize conditions using oligos available from Life Technologies. Cycling conditions for Has2 and Has3 were optimized independently as follows: 1-min initial denaturation at 95 °C; 33 cycles (Has2) or 27 cycles (Has3) of 30-s denaturation, 30-s annealing at 60 °C, and 30-s polymerization at 72 °C; 5-min final extension at 72 °C. 15 μl of each reaction was electrophoresed on a 3% agarose gel, stained with ethidium bromide, and digitally photographed. To determine relative expression levels, digital images were integrated using Molecular Analyst software, and band intensities were normalized to the corresponding GAPDH band. Levels are reported as the fold expression relative to that determined for normal prostate.

TABLE I
RT-PCR primers

	Oligo sequences	Sequence position	Product length
			bp
HAS 1			
Forward	5′ CTGAGGATCCGTCTGTGACTCGGAC 3′	737	246
Reverse	5′ GACTAAGCTTCTAGAGGACCGCTG 3′	963	
HAS 2			
Forward	5′ GTATCAGTTTGGTTTACAATC 3′	1441	207
Reverse	5′ GCACCATGTCATATTGTTGTC 3′	1648	
HAS 3			
Forward	5′ GTGCAGTGTATTAGTGGGCCCT 3′	839	414
Reverse	5′ GCTGCACCGTCAGCAGGAAGAGG 3′	1253	
GAPDH			
Forward	5′ TGAAGGTCGGAGTCAACGGATTTGGT 3′	44	982
Reverse	5′ CATGTGGGCCATGAGGTCCACCAC 3′	1026	

RESULTS

PC3M-LN4 Cells Adhere Rapidly and Specifically to BMEC-1 Bone Marrow Endothelial Cells—Prostate adenocarcinoma cells have been reported to adhere preferentially to bone marrow-derived microvascular endothelial cells relative to endothelial cells from a large vein source (HUVEC). This preference implies a specific intercellular recognition process dictated in part by heterogeneous expression of endothelial cell surface adhesion receptors. To investigate the molecular interactions underlying this process, we initially chose PC3M-LN4, a human prostate adenocarcinoma cell line derived from PC3 cells. This subline was clonally selected for enhanced metastatic propensity in mice and, in particular, was shown to be capable of metastasis to bone upon intracardial injection (35). We determined a time course for adhesion of PC3M-LN4 cells to BMEC-1 bone marrow endothelial cells and compared it with adhesion to HUVEC. Within 10 min, 70% of the cells were adherent on BMEC-1 relative to 16% on HUVEC (Fig. 1). After 30 min, nearly 100% of the cells adhered to BMEC-1 compared with only 25% on HUVEC. PC3M-LN4 cells, therefore, demonstrate preferential rapid adhesion to BMEC-1 bone marrow microvascular endothelial cells.

Hyaluronan Presented by the Prostate Carcinoma Cells Mediates Adhesion to BMEC-1—Several surface-borne adhesion molecules have been implicated in homing of circulating cells to the bone marrow, including VLA-4 ($\alpha_4\beta_1$ integrin), LFA-1 ($\alpha_L\beta_2$ integrin), CD44 proteoglycan, and the high molecular weight glycosaminoglycan hyaluronan (HA). Pretreatment of PC3M-LN4 cells with blocking antibodies directed against α_4, β_1, α_L, or β_2 integrin subunits, or against CD44, had no effect on adhesion of these cells to BMEC-1 (data not shown). To assess the relevance of HA to prostate carcinoma cell adhesion, we pretreated PC3M-LN4 or BMEC-1 cells individually or simultaneously with hyaluronidase (HAase) enzyme and assayed initial rapid adhesion at a 12-min time point. As above, ~70% of PC3M-LN4 cells were adherent at this time point in the absence of enzymatic digestion (Fig. 2). Pretreatment of BMEC-1 cells with HAase had no effect on this adhesion. However, treatment of PC3M-LN4 or both cell types reduced adhesion to about 35%, indicating that cell surface HA promotes this rapid intercellular interaction. Furthermore, the HA required for maximum adhesion is carried by the prostate carcinoma cells.

HA-mediated Adhesion of Prostate Carcinoma Cells Is Specific for Bone Marrow-derived Endothelial Cells—Because endothelial cell types of different origin exhibit differences in HA binding (36), we assayed the specificity of hyaluronidase-sensitive prostate tumor cell adhesion to endothelial cells. PC3M-LN4 cells were preincubated in the absence or presence of hyaluronidase and allowed to adhere to BMEC-1, HUVEC, or bone marrow-derived stromal cells (BMSC). Consistent with the above results, PC3M-LN4 cells adhered rapidly to BMEC-1 and adhesion was inhibited by 50% in the presence of HAase (Fig. 3). Cells adhered weakly to HUVEC, and adhesion was not inhibited by enzyme treatment. Although adhesion of PC3M-LN4 cells to BMSC was efficient and rapid, it was not inhibited by HAase digestion, suggesting cell surface HA was not mediating this adhesion. Collectively, these results imply that heterogeneous expression of HA receptors among endothe-

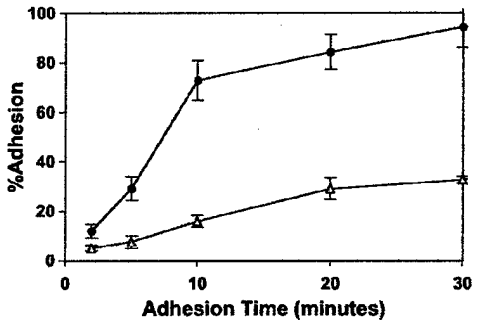

FIG. 1. **Time course for adhesion of PC3M-LN4 prostate carcinoma cells to BMEC-1 and HUVEC.** Calcein-AM-labeled PC3M-LN4 cells were added in a single cell suspension to confluent BMEC-1 (*closed symbols*) or HUVEC (*open symbols*) monolayers in a 48-well plate. At the indicated times, wells were washed to remove nonadherent cells, and adherent cells were lysed and quantified in a fluorescence plate reader. Results are presented as the mean percentage of input cells from triplicate wells ± standard error of the mean (S.E.).

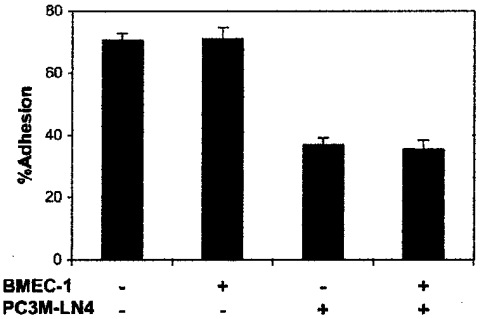

FIG. 2. **HA on the PC3M-LN4 cells is required for adhesion to BMEC-1.** BMEC-1 monolayers and/or calcein-AM-labeled PC3M-LN4 cell suspensions were treated where indicated with 16 units/ml hyaluronidase for 25 min. The hyaluronidase was removed, and the PC3M-LN4 cells were added to the BMEC-1 for 12 min at 37 °C. Nonadherent cells were removed by washing, and adherent cells were quantified in a fluorescence plate reader. Each *bar* represents the mean of triplicate wells assayed ± S.E., reported as percentage of input cells.

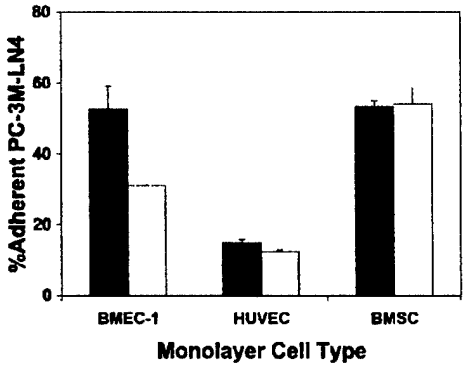

FIG. 3. **Enzymatic removal of HA inhibits PC3M-LN4 adhesion to BMEC-1 but not HUVEC or BMSC.** Calcein-AM-labeled PC3M-LN4 suspensions were pretreated for 25 min at 37 °C in the absence (*solid bars*) or presence (*open bars*) of 16 units/ml *Streptomyces* hyaluronidase. The cells were diluted 5-fold with adhesion medium and added to BMEC-1, HUVEC, or BMSC monolayers in a 48-well plate for 12 min at 37 °C. Nonadherent cells were removed by washing, and adherent cells were lysed and quantified in a fluorescence plate reader. Each *bar* represents the mean ± S.E. of quadruplicate wells assayed, reported as percentage of input cells. Each assay was repeated three times.

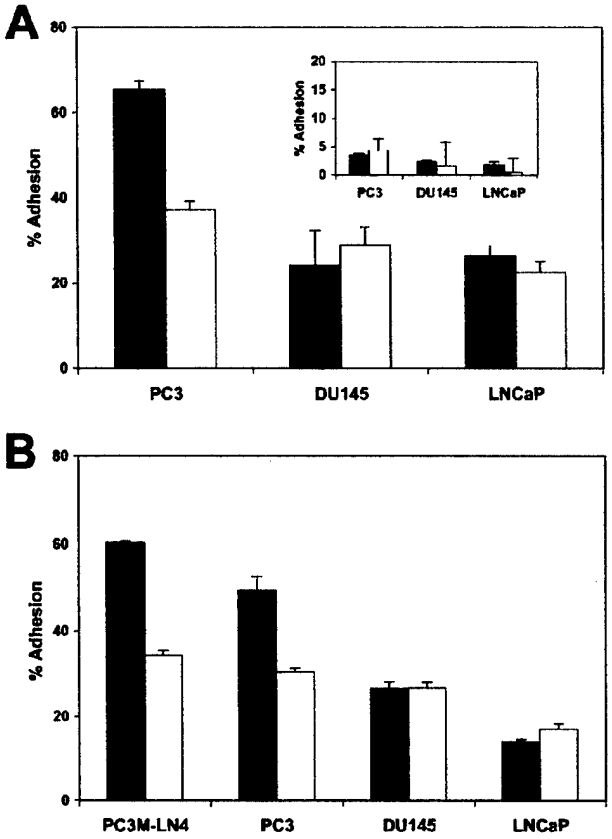

FIG. 4. **Adhesion of prostate carcinoma cell lines to bone marrow endothelial cells is differentially HA dependent.** PC3, DU145, LNCaP (*A* and *B*), and PC3M-LN4 (*B*) cell suspensions were calcein-AM-labeled, pretreated in the absence (*solid bars*) or presence (*open bars*) of 16 units/ml *Streptomyces* hyaluronidase. Cells were then diluted in adhesion medium and added to confluent washed monolayers of BMEC-1 (*A*), HUVEC (*panel A, inset graph*), or trHBMEC (*B*) in a 48-well plate for 12 min at 37 °C. Nonadherent cells were removed by washing, and adherent cells were lysed and quantified in a fluorescence plate reader. Each *bar* represents the mean ± S.E. of quadruplicate wells assayed, reported as a percentage of input cells determined separately for each cell type. Each assay was repeated three times.

lial cell types may dictate specific recognition of prostate carcinoma cells, although different molecules may dominate their interactions with other bone marrow-derived cells.

Rapid, Specific Prostate Carcinoma Cell Adhesion to Bone Marrow Endothelial Cells Is Differentially Sensitive to Hyaluronidase and Exogenous Hyaluronan—To examine whether HA would generally promote adhesion of prostate carcinoma cell lines to bone marrow endothelial cells, we measured HAase-sensitive BMEC-1 adhesion of the commercially available cell lines PC3, DU145, and LNCaP. As demonstrated above with PC3M-LN4 cells, about 60–70% of PC3 cells adhered to BMEC-1 monolayers and adhesion was inhibited 40–50% by HAase treatment (Fig. 4*A*). In contrast, DU145 and LNCaP cells adhered very poorly (about 25%), and the low level of adhesion was not altered by HAase treatment. None of the cell lines adhered well to HUVEC, and adhesion to HUVEC was not sensitive to HAase (Fig. 4*A*, *inset*). These results were replicated in similar experiments using another human bone marrow endothelial cell line, trHBMEC. As presented in Fig. 4*B*, PC3 and PC3M-LN4 cells exhibited comparable levels of HAase-sensitive adhesion to trHBMEC, whereas very few DU145 or LNCaP cells were adherent, and their adhesion was unaffected by HAase treatment. HA, therefore, is required for maximal rapid interaction between prostate carcinoma cells and bone marrow endothelial cells.

To further establish the requirement for direct HA recognition by the BMEC as a component of preferential adhesion to prostate carcinoma cells, we pretreated trHBMEC monolayers with increasing concentrations of exogenous high molecular weight HA. PC3M-LN4 cells were incubated with or without HAase, which was then removed. Cells were resuspended in the respective concentrations of HA and added to the BMEC. As before, about 80% of the cells were adherent after 12 min, and adhesion was reduced to 35% by HAase digestion (Fig. 5). Preincubation of the BMEC with 10 μg/ml of HA modestly increased adhesion of untreated cells, but rather strikingly increased adhesion of HAase-treated cells to about 60%. However, a dose-dependent inhibition was observed at higher concentrations, with adhesion almost completely inhibited at 500 μg/ml HA. This effect was more greatly manifested in HAase-treated cells, suggesting the residual adhesion observed for these cells may be due to incompletely digested HA or HA resynthesis during the time of the assay. When DU145 cells were similarly incubated with pretreated trHBMEC (Fig. 5, *inset graph*), no effect of exogenous HA was observed. This confirms that the inhibitory effect of HA is not occurring indirectly by destabilizing the BMEC monolayer, and that other receptor interactions are promoting the less rapid adhesion of DU145 cells to BMEC.

Prostate Carcinoma Cell Surface HA Retention Correlates to BMEC Adhesion—If HA was mediating the differential BMEC adhesion observed among the various prostate carcinoma cell lines, then these differences should be manifested in varied levels of HA retained on the surface of prostate carcinoma cells. Therefore, we used a particle exclusion assay to visualize the cell surface HA. In these experiments, surface-associated HA was first amplified by addition of aggrecan, a large multivalent proteoglycan that specifically associates with HA at the cell surface, surrounding the cell with a highly hydrated gel-like envelope. HA is thereby detected as a pericellular clear zone upon addition of fixed red blood cells, which cannot settle directly at the cell surface. Cells that lack HA do not exhibit these cleared halos, and the blood cell particles contact the cell perimeter. PC3M-LN4 cells were surrounded by a large matrix

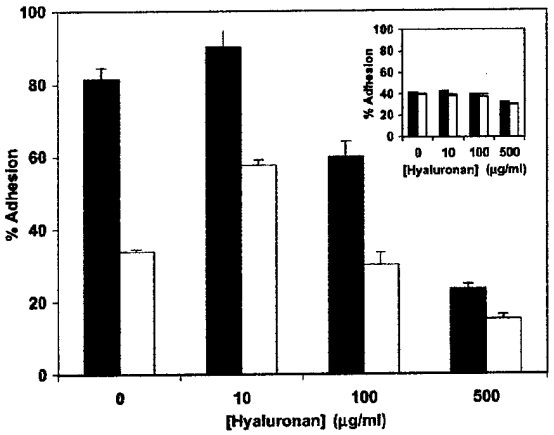

FIG. 5. **Effect of exogenous hyaluronan addition on PC3M-LN4 adhesion to trHBMEC.** Calcein-AM-labeled PC3M-LN4 suspensions or DU145 suspensions (*inset graph*) were pretreated for 25 min at 37 °C in the absence (*solid bars*) or presence (*open bars*) of 16 units/ml *Streptomyces* hyaluronidase. Cells were then washed and resuspended in the indicated concentrations of hyaluronan and added to confluent monolayers of trHBMEC cells preincubated for 30 min in the same hyaluronan concentrations. Nonadherent cells were removed after incubation for 12 min at 37 °C and remaining adherent cells were lysed and quantified by fluorescence plate reader. Each *bar* represents the mean ± S.E. of quadruplicate wells assayed, reported as a percentage of input cells determined separately for each cell type.

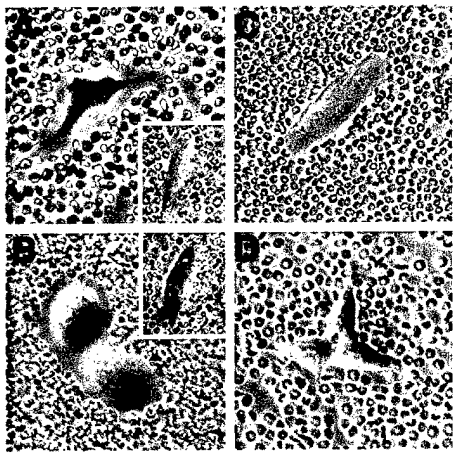

FIG. 6. **Visualization of prostate carcinoma cell surface HA.** Subconfluent PC3M-LN4 (*A*), PC3 (*B*), DU145 (*C*), or LNCaP (*D*) cells were incubated with 2 mg/ml aggrecan for 90 min, followed by addition of 1×10^8 fixed red blood cells and incubation at 37 °C for 15 min. HA-aggrecan coats evidenced by halos surrounding the cells were photographed at 400× magnification. Hyaluronidase treatment eliminated the pericellular matrices of PC3M-LN4 (*panel A inset*) and PC3 (*panel B inset*) cells, verifying their HA composition.

(Fig. 6*A*) that disappeared quantitatively after HAase treatment (Fig. 6*A*, *inset*). Similarly, PC3 cell surfaces bore a matrix (Fig. 6*B*) that was removed by HAase treatment (Fig. 6*B*, *inset*). In contrast, neither DU145 cells nor LNCaP cells retained HA on the cell surface (Fig. 6, *C* and *D*). Average ratios of matrix area with respect to cell area, obtained by integrating individual tracings of each cell type (Table II), were 1:1 for DU145 and LNCaP and 2:1 for PC3 and PC3M-LN4. Presence of cell surface HA, therefore, correlated with rapid, specific adhesion to BMEC. Conversely, its absence corresponded to weak adhesion.

Prostate Carcinoma Cell HA Synthesis Correlates to Presence of a Pericellular HA Matrix and Adhesion to BMEC—Elevated levels of HA have been reported to correlate with progression of several tumor types, including prostate. Furthermore, high levels of HA synthesis are necessary and sufficient for production of a pericellular HA coat. To address the possibility that the prostate carcinoma cells used in our study could be synthesizing large amounts of HA but differentially retaining it at the cell surface, we quantitated the HA synthesized by each cell line. HA synthesis occurs at the plasma membrane, concurrent with extrusion of HA from the cell, such that the majority of cellular HA is shed into the culture medium. Overnight culture media from each cell type were accordingly analyzed for HA content by a competitive binding assay and HA level was normalized to cell count (Fig. 7). PC3 and PC3M-LN4 cell culture supernatants were found to contain high levels of HA (~5 and 6 $\mu g/10^6$ cells, respectively, Table II) whereas DU145 culture medium had very little (1 $\mu g/10^6$ cells), and levels in LNCaP culture were virtually undetectable. These results are consistent with high levels of HA synthesis contributing to cell surface HA retention, promoting adhesion to bone marrow endothelial cells.

Elevated Levels of HA Synthase Expression by Prostate Carcinoma Cells Correlate to HA Production and Adhesion to BMEC—HA synthesis is catalyzed by one or more isoforms of three homologous HA synthase enzymes: Has1, Has2, and Has3. We used RT-PCR to determine initially which isoform(s) were expressed by each prostate carcinoma cell line, in an attempt to correlate elevated HA synthesis and BMEC adhesion with presence of a specific message. We were unable to detect Has1 message in any cell line using any set of oligonucleotide primers, although we could amplify a product from a Has1 cDNA control plasmid (data not shown). However, expression of Has2 and Has3 was detectable in most of the cell lines. Because the presence or absence of message for a particular isoform did not appear to correlate with either HA matrix formation or BMEC adhesion, we developed a semi-quantitative approach to look at relative message levels. Equal amounts of input mRNA from normal prostate (CLONTECH) and each of the prostate carcinoma cell lines were reverse-transcribed and used as templates for PCR amplification of Has2 (Fig. 8*A*, *lanes 8–14*) or Has3 (Fig. 8*B*, *lanes 8–14*), concurrent with a GAPDH housekeeping control message (Fig. 8, *lanes 2–6*). Product yields were normalized to GAPDH and presented as fold expression relative to normal prostate in Table II.

Results of this assay showed that PC3 (*lanes 4* and *10*) and PC3M-LN4 cells (*lanes 3* and *9*) expressed higher levels of both Has2 and Has3 than DU145 (*lanes 5* and *11*), or LNCaP (*lanes 6* and *12*), consistent with higher levels of HA synthesis and rapid adhesion to BMEC by those cell lines. Has2 was virtually absent in DU145 cells and undetectable in normal prostate (*lanes 2* and *8*) or LNCaP cells. Has3 expression was dramatically increased in the most highly metastatic line, PC3M-LN4, followed by PC3 and DU145. Has3 expression was very low in normal prostate or LNCaP cells. Although DU145 cells appeared to express significant levels of Has3, this cell line was found to be a heterogeneous population in which about 2–10% carry surface associated HA (in contrast to PC3 and PC3M-LN4, in which >99% of the cells carry abundant surface HA). This was visualized by phase contrast microscopy at the level of individual cells using biotinylated HA binding protein, followed by streptavidin-HRP detection with diaminobenzidine precipitation (data not shown). The apparent Has3 cDNA level amplified from this cell line may be anomalously high due to those specific cells and not representative of the overall phenotype of the cell line, which probably expresses lower message levels. Collectively, these results demonstrate that HA synthesis correlates very well to HA synthase expression level, which in

TABLE II

Elevated HA synthase expression correlates to prostate carcinoma cell surface HA, adhesion to BMEC-1, and previously reported metastatic potential

	PC3M-LN4	PC3	DU145	LNCaP
HA coat[a]	1.94 ± 0.03	1.89 ± 0.04	1.02 ± 0.02	1.01 ± 0.01
HA synthesis[b]	6.38 ± 1.01	4.74 ± 0.61	1.19 ± 0.41	0.64 ± 0.21
HAS expression[c]				
Has2	2	6	0.2	0.1
Has3	20	17	10	0.5
BMEC adhesion[d]	71 ± 2	65 ± 8	24 ± 2	26 ± 3
Metastatic potential[e]	High	High	Moderate	Low/none

[a] Pericellular clear zones and cell perimeters of 20 individual cells were traced in NIH IMAGE, the relative ratio was calculated, and the corresponding ratio for HAase treated cells was subtracted. A value of 1 denotes a cell completely lacking pericellular matrix.
[b] Values presented are those plotted in Fig. 7 (in micrograms per 10^6 cells).
[c] Derived from Fig. 8. Data are shown as -fold expression relative to levels in normal prostate, normalized to GAPDH.
[d] Presented as percentage of input cells. The value for PC3M-LN4 cells is extracted from Fig. 2, and the other values from Fig. 4*A*.
[e] Cited in "Discussion."

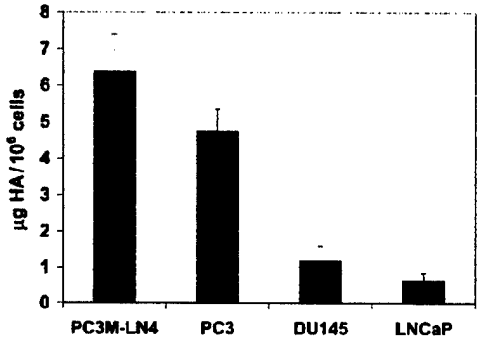

FIG. 7. **HA synthesis and secretion by prostate carcinoma cells in culture.** Equal numbers of prostate carcinoma cells were seeded overnight then given fresh culture medium. After an additional 24 h, supernatants were harvested and cells were trypsin-released and counted. HA-containing culture media were serially diluted, incubated with biotinylated HA binding protein, and applied to HA-coated plates. Bound HA binding protein was detected, following extensive washes, with streptavidin-HRP conjugate and OPD substrate, and quantified spectrophotometrically. Total HA in the culture media was determined by interpolation from a concurrent HA standard curve and plotted relative to cell number in the original culture.

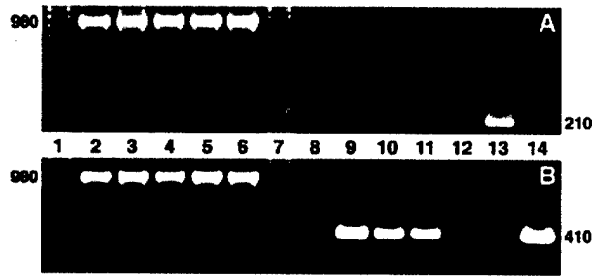

FIG. 8. **HA synthase expression in prostate adenocarcinoma cell lines.** HA synthase isoform and level of expression was determined for each of the four prostate carcinoma cell lines PC3M-LN4, PC3, DU145, and LNCaP, and for normal prostate, by RT-PCR as described under "Experimental Procedures." *A*, RT-PCR amplification of Has2 and GAPDH control messages; *B*, Has3 and GAPDH. Anticipated product sizes (in base pairs) are indicated adjacent to the figure: Has2 is ~210 bp, Has3 is ~410 bp, and GAPDH is ~980 bp. *Lanes* are numbered as follows: *lanes 1* and *7*, 100-base pair DNA ladder; *lanes 2* and *8*, normal prostate; *lanes 3* and *9*, PC3M-LN4; *lanes 4* and *10*, PC3; *lanes 5* and *11*, DU145; *lanes 6* and *12*, LNCaP; *lane 13*, Has2 control plasmid; *lane 14*, Has3 control plasmid.

turn may dictate adhesion to bone marrow endothelial cells. Furthermore, it is clear that HA synthesis and HA synthase expression are dramatically up-regulated in aggressive prostate adenocarcinoma cells, with overall HA production and HAS expression levels correlating directly to metastatic potential.

DISCUSSION

Bone metastasis is an eventuality of advanced stage prostate cancer that results in severely reduced quality of life and ultimate morbidity. Metastasis is preceded by initial adhesion of circulating tumor cells to endothelial cells lining the vasculature of the secondary site. Because prostate carcinoma metastasizes to bone, we modeled this initial event using prostate carcinoma cell lines and the transformed bone marrow sinusoidal endothelial cell lines, trHBMEC and BMEC-1. In this study we demonstrate that highly metastatic prostate carcinoma cells adhere to bone marrow endothelial cells through pericellular hyaluronan (HA). Unlike reports of other model system interactions requiring this molecule, we find that the prostate carcinoma cells present the HA recognized by the BMEC. The HA-mediated adhesion shows endothelial source specificity, because PC3M-LN4 cells do not adhere rapidly to HUVEC, another endothelial cell type. Furthermore, HA-mediated adhesion exhibits specificity among bone-derived cell types: Although adhesion of PC3M-LN4 cells to bone marrow stromal cells is rapid, HA does not appear to be involved, suggesting other receptor interactions contribute to this process. Up-regulation of HA synthase in prostate tumor cells may promote bone marrow metastasis by specifically arresting those cells on the bone endothelium.

The bone marrow microvasculature is a specialized network of venules and fenestrated sinusoids permeable to low molecular weight fluorophores but impenetrable by larger macromolecular conjugates and cellular bodies (10). However, the bone marrow as the site of hemopoiesis must be capable of progenitor cell flux across its protective endothelial layer, a function not required or desirable in other types of endothelium. Endothelial cell types exhibit heterogeneity in cytokine response (11, 37), receptor expression (9, 11, 36), and signaling pathways (38). In the absence of specific stimuli, endothelial heterogeneity alone is able to influence homing of circulating progenitor cells to the bone marrow through differential expression of selectins (10, 39, 40), glycoproteins (14), and VCAM-1 and CD44 (15). Receptor expression and adhesion of circulating leukocytes to sites of inflammation is further regulated through endothelial activation by inflammatory cytokines (41, 42). These cell surface differences may translate into preferential adhesion of circulating tumor cells to endothelial cells in specific tissues.

Transformed BMEC lines recently developed have facilitated exploration of the mechanisms by which endothelial adhesion receptors may dictate tumor preference for specialized endothelia. Results presented in this study demonstrate that prostate cancer cells adhere rapidly to bone marrow but not large vein endothelial cells. This is in agreement with observations by other investigators that prostate adenocarcinoma cell lines

adhere preferentially to cell cultures enriched for BMEC over components of the bone marrow or hepatic endothelial cells (2). In another study, adhesion of prostate carcinoma cells to a cell line immortalized from isolated BMEC was shown to be inhibited by preincubation of BMEC with monoclonal anti-LFA-1 antibodies or polyclonal anti-galectin-3 (43), but it was unclear which cell type expressed LFA-1 because neither has been previously reported to do so. We have used two transformed bone marrow endothelial cell lines, BMEC-1 (30) and trHBMEC (11), which express the same cell adhesion molecules and synthesize the same cytokines as the primary endothelial cells with minor differences in level of expression, to determine that HA on the prostate tumor cells mediates adhesion to BMEC. However, this does not exclude the possibility of other interactions. We expect that, like progenitor arrest, adhesion and migration of prostate tumor cells on BMEC involves multiple adhesive interactions that may or may not be interdependent.

HA is a ubiquitous polysaccharide component of extracellular and cell-associated matrices (44, 45), essential for growth and motility. HA is required for normal ductal branching in the developing prostate gland (46), underscoring its vital role in cell migration (47). In some cell types, this requirement entails assembly of an HA pericellular matrix for proliferation and migration (33, 48). Cell-associated HA may facilitate growth and motility by stimulating detachment of rounded, dividing cells and the trailing edges of migrating cells, respectively. HA exhibits further functional complexity as an adhesion molecule involved in recruitment of circulating lymphocytes to inflamed tissues through the action of cell surface HA receptors (38). The structure of HA, consisting of many thousand repetitions of a disaccharide motif, is well-suited to serve as a multivalent ligand for coordinate binding by many simultaneous adhesion receptors or for providing a scaffold for cellular movement.

Cellular behaviors contributing to cancer progression include unrestricted growth, motility, and ability to circulate and colonize new tissues. Because HA is a normal component of such processes, it is not surprising that elevated levels correlate with cancer progression (21, 49, 50). High levels of serum HA, for example, correlated with disseminated carcinoma in general (51, 52) and, specifically, with tumor progression to metastatic disease in malignant lymphoma (53) and breast carcinoma (54). In human breast carcinoma, HA is more concentrated in areas where the tumor is invading into the surrounding tissue (22), and elevated stromal and cell-associated HA correlates with malignancy (55). Elevated stromal and epithelial HA are also indicative of poor survival rate in patients with ovarian and colorectal cancers (23, 24). In animal models, tumor cells with high levels of HA expression were more metastatic than cells expressing lower levels of HA (27, 29, 56, 57). Interestingly, both high and low HA-expressing cells have the same growth rate *in vitro* and at the primary injection site (27). This correlation of HA with metastasis but not growth rate suggests that HA may be more critical to endothelial adhesion and/or the infiltration of the cells into tissues.

PC3M-LN4 cell adhesion to BMEC *in vitro* was both enhanced and inhibited by the addition of high molecular weight HA. At low concentrations comparable to those secreted into the culture medium of the cells during growth, adhesion of hyaluronidase-treated tumor cells to BMEC was significantly enhanced by HA preincubation. HA prebinding by the BMEC may restore adhesion by replacing the cross-bridging ligand normally presented by the prostate tumor cells via its own cell surface HA receptors. When BMEC were precoated with higher levels of HA, PC3M-LN4 cell adhesion was almost entirely precluded, regardless of HAase treatment. This suggests that BMEC and prostate HA receptors have been saturated and are no longer able to cross-link. HA has been previously reported to enhance/inhibit intercellular adhesion in this fashion in development of chick limb buds (58). Rapid intercellular adhesion was synergistically inhibited by HAase treatment and high exogenous HA, suggesting the incomplete HAase effect is probably due to HA resynthesis during the assay. By contrast, DU145 cell adhesion was not affected by addition of HA at any concentration, and therefore, these cells most likely lack active cell surface HA binding proteins.

PC3 (59) and PC3M-LN4 (35) prostate carcinoma cells are highly metastatic in mouse models and are shown in this report to produce a dense pericellular HA matrix that mediates adhesion to bone marrow endothelial cells. DU145 (60) and LNCaP (61) cell lines, by contrast, are poorly metastatic in mice, produce very little HA, and do not adhere well to BMEC. It is worth noting the origins and characteristics of the four cell types: PC3 is from a human bone metastasis; its derivative, PC3M-LN4, metastasizes to mouse bone; DU145 and LNCaP are from a human brain and a human lymph node metastasis, respectively, and their interaction with bone has never been documented. The correlation between high metastatic potential as reported in the literature, up-regulated HA synthesis and expression of HA biosynthetic enzymes is summarized in Table II. This correlation is consistent with a putative role for HA as a component of prostate cancer metastasis. In fact, HA overproduction is thought to be directly involved in prostate cancer progression. Histological sections of normal adult prostate tissue demonstrate the presence of HA in the prostate stroma (25, 46). In cancerous human prostates, HA expression levels are increased on the carcinoma cells and correspond to dedifferentiation of the cancer (25, 26).

Synthesis and secretion of HA is catalyzed in vertebrates by a family of three HA synthases: Has1 (62), Has2 (63), and Has3 (64), each of which is capable of conferring HA synthesis and pericellular HA retention to transfected cells (for a review of HA synthases, see Ref. 65). HAS expression is ubiquitous, but isoforms exhibit temporal and tissue-specific distribution. Targeted disruption of the *has2* gene is an embryonic lethal mutation in mice, which fail to produce HA essential for pericardial endothelial cell migration and endothelial/mesenchymal transformation during cardiac development (66). Has2 is also specifically up-regulated in response to wounding in a mesothelial cell model (67). Because HAS expression is critical during periods of normal tissue remodeling, understanding its dysregulation in tumors may be important in controlling tumor growth and metastasis. HAS expression is regulated by glucocorticoids (68), growth factors such as platelet-derived growth factor (69), transforming growth factor β1 (70), and pro-inflammatory cytokines (71). Expression of HAS appears to correlate directly to HA synthesis (69), suggesting regulation occurs at the level of transcription. To date, there is no evidence for post-transcriptional mechanisms. Elevated HA in tumor cells is, therefore, probably a reflection of HAS gene expression. In support of this, we have determined that Has2 and Has3 are strongly up-regulated in highly metastatic prostate tumor cells. HAS up-regulation in prostate cancer progression may be dictated in part by factors such as those described above, produced and secreted by prostate stromal or epithelial cells.

HA synthase enzymes have been implicated in tumorigenesis and metastasis in mouse models. Overexpression of Has2 in fibrosarcoma cells yields significantly larger subcutaneous tumors (28). Mammary carcinoma cells transfected with *has1* were more metastatic than control cells (29). In a melanoma model, tumor cells selected for high cell surface expression of HA were highly tumorigenic and metastatic, whereas tumor

cells bearing little or no surface HA, although equally tumorigenic, did not metastasize (27). In the latter model, however, *has* isoform expression was not characterized. Our data present the first characterization of *has* expression in prostate carcinoma cells and reveal a possible correlation of Has3 overexpression with tumor cell metastatic potential. Collectively, these results suggest involvement of HA in tumor growth and metastasis, and imply that specific HA synthase isoforms and/or expression levels of those isoforms may mediate these processes.

Both Has2 and Has3 are capable of synthesizing HA with an average molecular mass of 1–2 million Da (72), the average size of the exogenous HA used to enhance/inhibit adhesion (Fig. 5). This would suggest that the products of both enzymes are capable of supporting intercellular adhesion. DU145 cells, however, appear to express elevated Has3 but synthesize little HA and retain no matrix. One possible explanation may be that Has3 message is transcribed but not translated in these cells or that the protein made is inactive. Alternatively, there may be a requisite maximum threshold of HAS expression for maintenance of a pericellular matrix. Levels of Has3 expression sufficient to promote matrix retention may occur in only a subset of DU145 cells, with the remaining cells expressing it at lower levels. This may also be the case for Has2 expression. If production of an HA matrix enhances arrest in the bone marrow sinusoids, the cell population would have significantly diminished propensity to do so, relative to PC3 or PC3M-LN4 cells, which could then translate to reduced bone metastatic proclivity. Both enzymes are up-regulated in highly metastatic cells, which may implicate HAS up-regulation in prostate cancer progression. Has3 overexpression most consistently corresponds to aggressive potential, but intrinsic heterogeneity within the cell lines renders assignment of such a correlation premature.

Another factor to consider is that DU145 cells may lack surface receptors to anchor the matrix, because exogenous HA could restore adhesion of HAase-inhibited PC3M-LN4 cells, which are normally able to maintain an HA coat, but not enhance adhesion of DU145 cells. It is important to recognize that, although HA produced by prostate tumor cells may facilitate metastasis to bone marrow by initially attaching to the endothelium in the bone marrow, changes in matrix-associated HA binding proteins could also modify prostate tumor cell behavior. Because HA is secreted as a free glycosaminoglycan and is not attached to a core protein, its retention at the cell surface is achieved through accessory proteins such as versican, which contribute to the matrix, specifically binding and cross-linking the multivalent HA into a dense network (33, 48). Elevated levels of versican are associated with prostate carcinoma progression, but it is not known if its HA binding properties are responsible (73).

However, in addition to the HA binding proteins in the extracellular matrix, HA is specifically recognized by a widely expressed transmembrane receptor, CD44. Bone marrow and umbilical vein endothelial cells BMEC-1, trHBMEC, and HUVEC express cell surface CD44 but exhibit different affinity for PC3M-LN4 cells. Preincubation of BMEC-1 cells with various reported anti-CD44 blocking monoclonal antibodies failed to impact prostate tumor cell interaction (data not shown). Nonetheless, regulation of CD44 activation state with respect to HA binding occurs on many levels and probably contributes to endothelial adhesive preference. CD44 and HA interactions may be important for metastasis. CD44-mediated migration and invasion of glioma cell lines is stimulated by HA (74) and inhibiting CD44/HA interactions *in vivo* inhibits metastasis (75, 76). HA clusters CD44 resulting in stimulation of signal transduction pathways and engagement of adhesion molecules such as integrins (77), which could either strengthen adhesion or lead to transmigration of the prostate cells through the endothelium.

Alternatively, HA binding proteins on the surface of BMEC-1 other than CD44 may contribute to rapid adhesion. One candidate protein is the receptor for HA-mediated motility (RHAMM), which has not been reported on BMEC surfaces but has been shown to mediate differential HA binding by endothelial cells of different vascular origin (36). It is therefore possible that differences in vascular endothelial RHAMM expression could be promoting the recognition of prostate carcinoma cells bearing surface-associated HA. Other recently described cell surface HA receptors include the lymph vessel endothelial-specific LYVE-1 (78), and the HA receptor for endocytosis thought to be specific for clearance of circulating HA through the liver and spleen (79).

In this report, we have surveyed established prostate carcinoma cell lines for common molecular interactions governing preferential adhesion to bone marrow endothelial cells and discovered a correlation between metastatic potential and elevated HA synthase. We have delineated a mechanism in which prostate cancer cells adhere to bone marrow endothelial cells via tumor cell-associated HA. It will be important to extend these findings to establish whether this adhesive interaction contributes to prostate cancer metastasis. With this goal, we are currently manipulating HA levels on prostate carcinoma cells in HA synthase transfectants, which should enable us to determine if HA changes the metastatic potential of prostate carcinoma cells in an animal model and whether a specific HA synthase isoform is responsible. Furthermore, this approach will allow us to study the impact of HA overproduction on activation of adhesion receptors and signal transduction pathways in HA-mediated adhesion of prostate carcinoma cells to bone marrow endothelium.

Acknowledgments—We acknowledge Christopher M. Wilson for excellent technical assistance and Dr. Joseph Barycki for many thoughtful discussions.

REFERENCES

1. Landis, S. H., Murray, T., Bolden, S., and Wingo, P. A. (1999) *CA-Cancer J. Clin.* **49**, 8–31
2. Haq, M., Goltzman, D., Tremblay, G., and Brodt, P. (1992) *Cancer Res.* **52**, 4613–4619
3. Tavassoli, M., and Hardy, C. L. (1990) *Blood* **76**, 1059–1070
4. Mohle, R., Bautz, F., Rafii, S., Moore, M. A., Brugger, W., and Kanz, L. (1999) *Ann. N. Y. Acad. Sci.* **872**, 176–85.; discussion 185–6
5. Scher, H. I., and Chung, L. W. (1994) *Semin. Oncol.* **21**, 630–656
6. Mazo, I. B., and von Andrian, U. H. (1999) *J. Leukoc. Biol.* **66**, 25–32
7. Mohle, R., Moore, M. A., Nachman, R. L., and Rafii, S. (1997) *Blood* **89**, 72–80
8. Jacobsen, K., Kravitz, J., Kincade, P. W., and Osmond, D. G. (1996) *Blood* **87**, 73–82
9. Schweitzer, K. M., Drager, A. M., van der Valk, P., Thijsen, S. F., Zevenbergen, A., Theijsmeijer, A. P., van der Schoot, C. E., and Langenhuijsen, M. M. (1996) *Am. J. Pathol.* **148**, 165–175
10. Mazo, I. B., Gutierrez-Ramos, J. C., Frenette, P. S., Hynes, R. O., Wagner, D. D., and von Andrian, U. H. (1998) *J. Exp. Med.* **188**, 465–474
11. Schweitzer, K. M., Vicart, P., Delouis, C., Paulin, D., Drager, A. M., Langenhuijsen, M. M., and Weksler, B. B. (1997) *Lab. Invest.* **76**, 25–36
12. Papayannopoulou, T., Craddock, C., Nakamoto, B., Priestley, G. V., and Wolf, N. S. (1995) *Proc. Natl. Acad. Sci. U. S. A.* **92**, 9647–9651
13. Papayannopoulou, T., and Craddock, C. (1997) *Acta Haematol. (Basel)* **97**, 97–104
14. Kataoka, M., and Tavassoli, M. (1985) *Blood* **65**, 1163–1171
15. Vermeulen, M., Le Pesteur, F., Gagnerault, M. C., Mary, J. Y., Sainteny, F., and Lepault, F. (1998) *Blood* **92**, 894–900
16. Peled, A., Grabovsky, V., Habler, L., Sandbank, J., Arenzana-Seisdedos, F., Petit, I., Ben-Hur, H., Lapidot, T., and Alon, R. (1999) *J. Clin. Invest.* **104**, 1199–1211
17. Mohle, R., Bautz, F., Rafii, S., Moore, M. A., Brugger, W., and Kanz, L. (1998) *Blood* **91**, 4523–4530
18. Turner, M. L., Masek, L. C., Hardy, C. L., Parker, A. C., and Sweetenham, J. W. (1998) *Br. J. Haematol.* **100**, 112–122
19. Okada, T., Hawley, R. G., Kodaka, M., and Okuno, H. (2000) *Clin. Exp. Metastasis* **17**, 625–631
20. Fraser, J. R., Laurent, T. C., and Laurent, U. B. (1997) *J. Intern. Med.* **242**, 27–33

21. Laurent, T. C., Laurent, U. B., and Fraser, J. R. (1996) *Immunol. Cell Biol.* **74,** A1–A7
22. Bertrand, P., Girard, N., Delpech, B., Duval, C., d'Anjou, J., and Dauce, J. P. (1992) *Int. J. Cancer* **52,** 1–6
23. Anttila, M. A., Tammi, R. H., Tammi, M. I., Syrjanen, K. J., Saarikoski, S. V., and Kosma, V. M. (2000) *Cancer Res.* **60,** 150–155
24. Ropponen, K., Tammi, M., Parkkinen, J., Eskelinen, M., Tammi, R., Lipponen, P., Agren, U., Alhava, E., and Kosma, V. M. (1998) *Cancer Res.* **58,** 342–347
25. De Klerk, D. P. (1983) *Prostate* **4,** 73–81
26. De Klerk, D. P., Lee, D. V., and Human, H. J. (1984) *J. Urol.* **131,** 1008–1012
27. Zhang, L., Underhill, C. B., and Chen, L. (1995) *Cancer Res.* **55,** 428–433
28. Kosaki, R., Watanabe, K., and Yamaguchi, Y. (1999) *Cancer Res.* **59,** 1141–1145
29. Itano, N., Sawai, T., Miyaishi, O., and Kimata, K. (1999) *Cancer Res.* **59,** 2499–2504
30. Candal, F. J., Rafii, S., Parker, J. T., Ades, E. W., Ferris, B., Nachman, R. L., and Kellar, K. L. (1996) *Microvasc. Res.* **52,** 221–234
31. Shah, N., Oseth, L., and LeBien, T. W. (1998) *Blood* **92,** 3817–3828
32. Knudson, C. B. (1993) *J. Cell Biol.* **120,** 825–834
33. Knudson, C. B., and Toole, B. P. (1985) *Dev. Biol.* **112,** 308–318
34. Lokeshwar, V. B., Obek, C., Soloway, M. S., and Block, N. L. (1997) *Cancer Res.* **57,** 773–777
35. Pettaway, C. A., Pathak, S., Greene, G., Ramirez, E., Wilson, M. R., Killion, J. J., and Fidler, I. J. (1996) *Clin. Cancer Res.* **2,** 1627–1636
36. Lokeshwar, V. B., and Selzer, M. G. (2000) *J. Biol. Chem.* **275,** 27641–27649
37. Favaloro, E. J. (1993) *Immunol. Cell Biol.* **71,** 571–581
38. Mohamadzadeh, M., DeGrendele, H., Arizpe, H., Estess, P., and Siegelman, M. (1998) *J. Clin. Invest.* **101,** 97–108
39. Naiyer, A. J., Jo, D. Y., Ahn, J., Mohle, R., Peichev, M., Lam, G., Silverstein, R. L., Moore, M. A., and Rafii, S. (1999) *Blood* **94,** 4011–4019
40. Frenette, P. S., Subbarao, S., Mazo, I. B., von Andrian, U. H., and Wagner, D. D. (1998) *Proc. Natl. Acad. Sci. U. S. A.* **95,** 14423–14428
41. DeGrendele, H. C., Estess, P., and Siegelman, M. H. (1997) *Science* **278,** 672–675
42. Siegelman, M. H., DeGrendele, H. C., and Estess, P. (1999) *J. Leukoc. Biol.* **66,** 315–321
43. Lehr, J. E., and Pienta, K. J. (1998) *J. Natl. Cancer Inst.* **90,** 118–123
44. Reed, R. K., Lilja, K., and Laurent, T. C. (1988) *Acta Physiol. Scand.* **134,** 405–411
45. Laurent, T. C., and Fraser, J. R. (1992) *FASEB J.* **6,** 2397–2404
46. Gakunga, P., Frost, G., Shuster, S., Cunha, G., Formby, B., and Stern, R. (1997) *Development* **124,** 3987–3997
47. Fujimoto, T., Hata, J., Yokoyama, S., and Mitomi, T. (1989) *J. Pediatr. Surg.* **24,** 550–556
48. Evanko, S. P., Angello, J. C., and Wight, T. N. (1999) *Arterioscler. Thromb. Vasc. Biol.* **19,** 1004–1013
49. Delpech, B., Girard, N., Bertrand, P., Courel, M. N., Chauzy, C., and Delpech, A. (1997) *J. Intern. Med.* **242,** 41–48
50. Toole, B. P. (1997) *J. Intern. Med.* **242,** 35–40
51. Manley, G., and Warren, C. (1987) *J. Clin. Pathol.* **40,** 626–630
52. Wilkinson, C. R., Bower, L. M., and Warren, C. (1996) *Clin. Chim. Acta* **256,** 165–173
53. Hasselbalch, H., Hovgaard, D., Nissen, N., and Junker, P. (1995) *Am. J. Hematol.* **50,** 231–233
54. Delpech, B., Chevallier, B., Reinhardt, N., Julien, J. P., Duval, C., Maingonnat, C., Bastit, P., and Asselain, B. (1990) *Int. J. Cancer* **46,** 388–390
55. Auvinen, P., Tammi, R., Parkkinen, J., Tammi, M., Agren, U., Johansson, R., Hirvikoski, P., Eskelinen, M., and Kosma, V. M. (2000) *Am. J. Pathol.* **156,** 529–536
56. Kimata, K., Honma, Y., Okayama, M., Oguri, K., Hozumi, M., and Suzuki, S. (1983) *Cancer Res.* **43,** 1347–1354
57. Turley, E. A., and Tretiak, M. (1985) *Cancer Res.* **45,** 5098–5105
58. Maleski, M. P., and Knudson, C. B. (1996) *Exp. Cell Res.* **225,** 55–66
59. Ware, J. L., Paulson, D. F., Mickey, G. H., and Webb, K. S. (1982) *J. Urol.* **128,** 1064–1067
60. Powell, W. C., Knox, J. D., Navre, M., Grogan, T. M., Kittelson, J., Nagle, R. B., and Bowden, G. T. (1993) *Cancer Res.* **53,** 417–422
61. Dumont, P., Petein, M., Lespagnard, L., Tueni, E., and Coune, A. (1993) *In Vivo* **7,** 167–170
62. Shyjan, A. M., Heldin, P., Butcher, E. C., Yoshino, T., and Briskin, M. J. (1996) *J. Biol. Chem.* **271,** 23395–23399
63. Watanabe, K., and Yamaguchi, Y. (1996) *J. Biol. Chem.* **271,** 22945–22948
64. Spicer, A. P., and McDonald, J. A. (1998) *J. Biol. Chem.* **273,** 1923–1932
65. Weigel, P. H., Hascall, V. C., and Tammi, M. (1997) *J. Biol. Chem.* **272,** 13997–14000
66. Camenisch, T. D., Spicer, A. P., Brehm-Gibson, T., Biesterfeldt, J., Augustine, M. L., Calabro, A., Jr., Kubalak, S., Klewer, S. E., and McDonald, J. A. (2000) *J. Clin. Invest.* **106,** 349–360
67. Yung, S., Thomas, G. J., and Davies, M. (2000) *Kidney Int.* **58,** 1953–1962
68. Zhang, W., Watson, C. E., Liu, C., Williams, K. J., and Werth, V. P. (2000) *Biochem. J.* **349,** 91–97
69. Jacobson, A., Brinck, J., Briskin, M. J., Spicer, A. P., and Heldin, P. (2000) *Biochem. J.* **348,** 29–35
70. Usui, T., Amano, S., Oshika, T., Suzuki, K., Miyata, K., Araie, M., Heldin, P., and Yamashita, H. (2000) *Invest. Ophthalmol. Vis. Sci.* **41,** 3261–3267
71. Kaback, L. A., and Smith, T. J. (1999) *J. Clin. Endocrinol. Metab.* **84,** 4079–4084
72. Itano, N., Sawai, T., Yoshida, M., Lenas, P., Yamada, Y., Imagawa, M., Shinomura, T., Hamaguchi, M., Yoshida, Y., Ohnuki, Y., Miyauchi, S., Spicer, A. P., McDonald, J. A., and Kimata, K. (1999) *J. Biol. Chem.* **274,** 25085–25092
73. Ricciardelli, C., Mayne, K., Sykes, P. J., Raymond, W. A., McCaul, K., Marshall, V. R., and Horsfall, D. J. (1998) *Clin. Cancer Res.* **4,** 963–971
74. Koochekpour, S., Pilkington, G. J., and Merzak, A. (1995) *Int. J. Cancer* **63,** 450–454
75. Guo, Y., Ma, J., Wang, J., Che, X., Narula, J., Bigby, M., Wu, M., and Sy, M. S. (1994) *Cancer Res.* **54,** 1561–1565
76. Yu, Q., Toole, B. P., and Stamenkovic, I. (1997) *J. Exp. Med.* **186,** 1985–1996
77. Siegelman, M. H., Stanescu, D., and Estess, P. (2000) *J. Clin. Invest.* **105,** 683–691
78. Banerji, S., Ni, J., Wang, S. X., Clasper, S., Su, J., Tammi, R., Jones, M., and Jackson, D. G. (1999) *J. Cell Biol.* **144,** 789–801
79. Zhou, B., Oka, J. A., Singh, A., and Weigel, P. H. (1999) *J. Biol. Chem.* **274,** 33831–33834

THE JOURNAL OF BIOLOGICAL CHEMISTRY
Vol. 277, No. 12, Issue of March 22, pp. 10050–10057, 2002
Printed in U.S.A.

Manipulation of Hyaluronan Synthase Expression in Prostate Adenocarcinoma Cells Alters Pericellular Matrix Retention and Adhesion to Bone Marrow Endothelial Cells*

Received for publication, October 18, 2001, and in revised form, December 19, 2001
Published, JBC Papers in Press, January 14, 2002, DOI 10.1074/jbc.M110069200

Melanie A. Simpson‡, Christopher M. Wilson‡, Leo T. Furcht‡, Andrew P. Spicer§, Theodore R. Oegema, Jr.¶‖, and James B. McCarthy‡**

From the Departments of ‡Laboratory Medicine and Pathology, ¶Orthopedic Surgery, and ‖Biochemistry, University of Minnesota, Minneapolis, Minnesota 55455 and the §Institute of Biosciences and Technology, Texas A&M University, College Station, Texas 77843

Prostate cancer metastasis to bone marrow involves initial adhesion of tumor cells to the bone marrow endothelium, followed by transmigration and proliferation within the marrow. Rapid, specific adhesion of highly metastatic prostate adenocarcinoma cells (PC3M-LN4) to bone marrow endothelial cell (BMEC) lines requires a pericellular hyaluronan (HA) matrix and correlates with dramatically up-regulated HA synthase (HAS) expression. Non-metastatic prostate tumor cells (LNCaP) do not assemble a HA matrix, adhere poorly to BMECs, and express normal levels of HAS. Preferential bone metastasis of prostate carcinoma cells may therefore be facilitated by tumor cell HA biosynthesis. In this report, HAS gene expression was manipulated to investigate the direct impact of prostate tumor cell HA production on adhesion to BMECs. PC3M-LN4 cells stably transfected with antisense HAS2 and HAS3 failed to form pericellular matrices. Adhesion of these transfectants to BMECs was significantly diminished, comparable to the low level exhibited by LNCaP cells. Upon transfection with full-length HAS2 or HAS3, the non-adherent LNCaP cells retained pericellular HA and adhered to BMECs. The results of this study are consistent with a model in which HA matrix formation, BMEC adhesion, and metastatic potential are mediated by HAS expression.

Prostate cancer mortality is frequently the result of bone metastasis. The preferential homing of circulating prostate tumor cells to bone marrow is thought to involve an initial rapid adhesion to cells of the bone marrow endothelium, followed by transmigration of the endothelium, engagement of specific receptors, and subsequent proliferation within the bone marrow microenvironment. Molecular mechanisms underlying these processes are poorly understood, but there is evidence that tumor cells may exploit existing pathways utilized by circulating blood cell progenitors to gain access to bone marrow.

To identify potential cell adhesion molecules involved in prostate tumor bone metastasis, research in our laboratory has focused on the interaction of prostate carcinoma cells with bone marrow endothelial cells (BMECs).[1] Highly metastatic PC3M-LN4 cells (1) were found to adhere rapidly to human bone marrow-derived sinusoidal endothelial cell lines, whereas poorly metastatic LNCaP cells were only weakly adherent (2). This adhesion, specific for BMECs relative to other endothelial cells, was subsequently found to depend upon the presence of a pericellular hyaluronan (HA) matrix assembled on the PC3M-LN4 cells. The presence of pericellular HA further correlated with elevated HA synthesis and expression of HA biosynthetic enzymes in the metastatic cells. Collectively, our results may implicate tumor cell-associated HA and up-regulation of HA synthase (HAS) in prostate cancer progression, possibly by facilitating arrest in the bone microvasculature and/or preferential tissue colonization of individual tumor cells.

HA is a ubiquitous polysaccharide component of extracellular and cell-associated matrices (3, 4), essential for growth and motility of both normal and transformed cells (3, 5–7). In some cell types, this requirement entails assembly of a pericellular HA matrix (8, 9). Cell-associated HA is thought to stimulate cellular detachment during proliferation and migration, and HA deposition is associated with normal and transformed cell growth and migration in several species (10). Elevated levels of HA in urine and serum often correlate with advanced cancer (11, 12). Production of HA is thought to be directly involved in prostate cancer progression. In human cancerous prostates, HA levels are increased on the carcinoma cells and correspond to dedifferentiation of the cancer (13, 14).

HA biosynthesis is catalyzed by transmembrane HAS enzymes (15). Three human isoforms have been identified and cloned (*HAS1* (16), *HAS2* (17), and *HAS3* (18)). The cDNA of each isoform is capable of conferring HA synthesis and pericellular HA retention to transfected cells. HAS expression is ubiquitous, but isoforms exhibit temporal and tissue-specific distribution. HAS2, for example, is essential for mouse pericardial endothelial cell migration and transformation to mesenchyme during cardiac development (19). HAS2 is also specifically up-

* This work was supported by United States Army Medical Research and Materiel Command Grant DA/DAMD 17-99-A-9029, NCI Grant CA21463 from the National Institutes of Health, and National Research Service Award Grant 1F32-CA84619-01 (to M. A. S.). The costs of publication of this article were defrayed in part by the payment of page charges. This article must therefore be hereby marked "*advertisement*" in accordance with 18 U.S.C. Section 1734 solely to indicate this fact.

** To whom correspondence should be addressed: Dept. of Laboratory Medicine and Pathology, University of Minnesota, P. O. Box 609 UMHC, 420 Delaware St. S. E., Minneapolis, MN 55455. Tel.: 612-625-7454; Fax: 612-625-1121; E-mail: mccar001@tc.umn.edu.

[1] The abbreviations used are: BMECs, bone marrow endothelial cells; TrHBMECs, transformed human bone marrow endothelial cells; HA, hyaluronan; HAS, hyaluronan synthase; HAase, hyaluronidase; HABP, hyaluronan-binding protein; RT-PCR, reverse transcription-polymerase chain reaction; GFP, green fluorescent protein; Hyg, hygromycin; FACS, fluorescence-activated cell sorting; GAPDH, glyceraldehyde-3-phosphate dehydrogenase; PBS, phosphate-buffered saline; BSA, bovine serum albumin; MEM, minimal essential medium; streptavidin per CP, streptavidin-peridinin chlorophyll-α protein conjugate.

regulated in response to wounding in a mesothelial cell model (20). Overexpression of HAS2 in fibrosarcoma cells or HAS3 in prostate carcinoma cells yields significantly larger subcutaneous tumors in nude mice (21, 22). Mammary carcinoma cells transfected with HAS1 are more metastatic than control cells (23). In a melanoma model, tumor cells selected for abundant cell-surface HA were highly tumorigenic and metastatic, whereas tumor cells bearing little or no surface HA, although equally tumorigenic, did not metastasize (6). In the latter model, however, HAS isoform expression was not characterized. Collectively, these results suggest involvement of HA in tumor growth and metastasis and imply that specific HAS isoforms and/or expression levels of those isoforms may mediate these processes. Expression of HAS appears to correlate directly with HA synthesis (24), suggesting that elevated HA in tumor cells is probably a reflection of HAS gene expression.

In our previous report, we determined that HAS2 and HAS3, normally present at low levels in the prostate, are strongly up-regulated in metastatic prostate tumor cells (2). In this report, we have used the *in vitro* BMEC adhesion model to examine the role of these enzymes and their product in prostate cancer bone metastasis. Specifically, we have manipulated expression of HAS2 and HAS3 in tumor cell lines and evaluated them for HA synthesis, pericellular HA retention, and HA-dependent adhesion to BMECs. Individual inhibition of HAS2 or HAS3 expression in metastatic PC3M-LN4 cells was found to diminish pericellular HA retention and BMEC adhesion; however, complete inhibition of HA-mediated adhesion was obtained by double antisense expression. Conversely, we found that overexpression of either HAS2 or HAS3 in non-metastatic LNCaP cells conferred pericellular HA retention and HA-mediated adhesion to BMECs. These results definitively implicate HAS expression in rapid adhesion of prostate carcinoma cells to BMECs, which may thereby impact the bone metastatic potential of circulating tumor cells.

EXPERIMENTAL PROCEDURES

Cell Culture and Reagents—LNCaP human prostate adenocarcinoma cells were purchased from American Type Culture Collection (Manassas, VA) and cultured in RPMI 1640 medium containing 10% fetal bovine serum. The PC3 derivative cell line PC3M-LN4 (also a human prostate adenocarcinoma cell line) was kindly provided by Dr. Isaiah J. Fidler (M. D. Anderson Hospital Cancer Center, Houston, TX) and was maintained in MEM containing 10% fetal bovine serum, sodium pyruvate, and nonessential amino acids. Prostate carcinoma cells were plated 2 days prior to experiments and used at ~70% confluence. Transformed human BMECs (TrHBMECs) were a gift from Dr. Karin Schweitzer (Free University Hospital Amsterdam, Amsterdam, The Netherlands) and were maintained in RPMI 1640 medium containing 10% fetal bovine serum (25). Aggrecan was prepared as previously described (26) from Swarm rat chondrosarcoma.

Plasmid Construction—Full-length human HAS3 cDNA was subcloned by PCR using oligonucleotides that incorporated flanking *Sac*I and *Eco*RI restriction sites. HAS2 cDNA was amplified by RT-PCR from PC3M-LN4 mRNA using oligonucleotides that incorporated *Nhe*I and *Bam*HI restriction sites. Full-length cDNAs were inserted in pIRES2-EGFP (CLONTECH) via the *NheI*/*Bam*HI (HAS2) or *SacI*/*Eco*RI (HAS3) restriction sites. The sequences were verified and found to be identical to the published sequence. For antisense constructs, HAS2 or HAS3 plasmid DNA was used as the template to amplify the first 300 bases of each isoform sequence, including the ATG start codon, which was then subcloned in the antisense orientation into pIRES-Hyg (CLONTECH). For double antisense HAS inhibition, we expressed antisense HAS2 as a bicistronic message with GFP (pIRES2-EGFP vector) and antisense HAS3 with hygromycin resistance (pIRES-Hyg).

Transfection of Prostate Carcinoma Cells—LNCaP cells were transfected with Lipofectin reagent (Invitrogen) in serum-free medium according to the manufacturer's protocol and allowed to recover in complete standard culture medium for 24–48 h before assaying. GFP expression was verified in LNCaP cells by flow cytometry, and expression of HAS2 and HAS3 RNAs was ascertained by RT-PCR as described below. PC3M-LN4 cells were incubated for 30 min in serum-free minimal essential medium containing 0.5 units/ml chondroitinase ABC (Sigma) to remove inhibitory glycosaminoglycans and subsequently transfected with FuGENE 6 liposome-mediated transfection reagent (Roche Molecular Biochemicals).

Preparation of Stable Antisense HAS Transfectants—PC3M-LN4 cells were cotransfected with pIRES2-EGFP and pIRES-Hyg for the vector-transfected control, termed GFP. Individual antisense HAS2 or HAS3 transfectants were created by cotransfection of pIRES2-EGFP and HAS2-Hyg or HAS3-Hyg, respectively. Double antisense HAS transfectants received HAS2-GFP and HAS3-Hyg. All transfectants were selected through multiple rounds of fluorescence-activated cell sorting (FACS) and antibiotic selection in 1 mg/ml G418 and 0.8 mg/ml hygromycin until the final cell populations were 85–95% positive for GFP expression. Once established, stable transfectants were maintained in the parental medium supplemented with 1 mg/ml G418 and 0.5 mg/ml hygromycin.

Determination of HAS Expression—HAS isoform and relative level of expression in prostate carcinoma cell lines was semiquantitatively assayed by RT-PCR as previously described (2). Briefly, poly(A)$^+$ RNA was isolated from subconfluent LNCaP and PC3M-LN4 transfectants with the Oligotex mRNA isolation kit (QIAGEN Inc.) and quantitated by Ribogreen fluorescence (Molecular Probes, Inc., Eugene, OR). 20 ng of each mRNA template was reverse-transcribed with an oligo(dT) primer using the Sensiscript kit (QIAGEN Inc.). PCR oligonucleotides specific for HAS2 and HAS3 messages were designed from the sequence data base; expected product sizes are 980 base pairs for glyceraldehyde-3-phosphate dehydrogenase (GAPDH) message, 210 base pairs for HAS2 message, and 410 base pairs for HAS3 message. GAPDH was amplified with each reaction to standardize conditions using oligonucleotides available from Invitrogen. Cycling conditions for HAS2 and HAS3 amplification from PC3M-LN4 cells were optimized independently as follows: 1-min initial denaturation at 95 °C; 33 cycles (HAS2) or 25 cycles (HAS3) of 30-s denaturation, 30-s annealing at 60 °C, and 30-s polymerization at 72 °C; and 5-min final extension at 72 °C. For cDNA amplification from LNCaP transient transfectant mRNA, 30 cycles of the above conditions were uniformly employed. A 15-μl aliquot of each reaction was electrophoresed on a 3% agarose gel, stained with ethidium bromide, and digitally photographed.

Flow Cytometric Assay for Surface HA Retention—LNCaP transfectants were analyzed in suspension for the retention of cell-surface HA. 2 days post-transfection, cells were released with PBS containing 3 mM EDTA, washed with FACS buffer (PBS containing 1 mM $CaCl_2$ and 1 mM $MgCl_2$), passed twice through a mesh cell filter to remove aggregates, and resuspended at 5×10^5 cells/ml in FACS buffer with or without 16 units/ml *Streptomyces* hyaluronidase (HAase) (Calbiochem). Cells were incubated at 37 °C for 30 min and then washed and resuspended in FACS buffer containing biotinylated HA-binding protein (HABP) (Seikagaku America, Inc.) at a final concentration of 2 μg/ml. Following a 90-min room temperature incubation with agitation, cells were washed with FACS buffer, resuspended in streptavidin-conjugated perCP (PharMingen) at a final dilution of 1:200, and incubated for an additional 1 h under the same conditions. After a final wash in FACS buffer, cells were resuspended in 0.3 ml of FACS buffer and immediately analyzed by flow cytometry. Results were gated to include only GFP-fluorescing cells and plotted as a histogram for HABP positivity.

HA Synthesis Quantitation—The concentration of HA in transfected cell culture supernatants was determined in a competitive binding assay (27). Immulon 96-well microtiter plates were coated with human umbilical cord HA at 50 μg/ml in 200 mM carbonate buffer (pH 9.6) overnight at 4 °C. Excess HA was removed, and wells were blocked with four washes of Pierce Superblock reagent. Prostate carcinoma cells (30,000 cells/well) were plated overnight in 24-well plates. Cells were washed, given fresh media, and incubated for an additional 20–24 h. Overnight conditioned culture media were harvested, and cell counts were determined by trypsin release and manual counting in a hemocytometer. Cell culture supernatants were centrifuged to remove cellular material or particulates, boiled for 20 min to inactivate protein components, and serially diluted in PBS and 0.05% Tween 20. Equal volumes of each dilution were combined with biotinylated HABP (Seikagaku America, Inc.) to a final HABP concentration of 1 μg/ml and incubated in the HA-precoated wells at room temperature for 6–8 h. The plate was washed four times with PBS and Tween 20 and developed using an avidin-biotin-horseradish peroxidase system (Vector Laboratories ABC-HRP PK-4000 kit) with tetramethylbenzidine (Sigma) as substrate, and absorbance was read at 650 nm. HA concentration was interpolated from a standard curve of absorbance values corresponding to known HA quantities. The mean HA concentration for each sample of culture supernatant was calculated, and results were normalized to cell num-

ber. Data are presented as mass of HA (in micrograms)/10^6 cells.

Cell Adhesion Assay—Subconfluent prostate carcinoma cells were PBS/EDTA-released, washed with adhesion medium (RPMI 1640 medium with 0.1% BSA and 20 mM HEPES (pH 7.4), maintained throughout the assay at 37 °C), and resuspended at 1×10^6 cells/ml in adhesion medium. Cells were incubated with 25 μg/ml calcein/AM (Molecular Probes, Inc.; a compound that is converted to a fluorophore only upon uptake and metabolism by living cells) for 20 min, washed with adhesion medium, and resuspended at 1×10^5 cells/ml. TrHBMECs were seeded 100% confluent (~40,000 cells/well) in 48-well plates overnight and washed twice with adhesion medium prior to the assay. Prostate carcinoma cells (300 μl/well) were added to the confluent endothelial cell monolayers and incubated for 12 min at 37 °C unless otherwise indicated. Non-adherent cells were removed with two washes done by gently pipetting 2×0.5 ml of adhesion medium and immediately decanting. Viability of non-adherent cells was verified by trypan blue exclusion. Adherent cells were solubilized with PBS containing 0.2 N NaOH and 1% SDS and quantified in a Cytofluor II fluorescence plate reader at 485/530 nm (Biosearch Inc., Bedford, MA).

Inhibition of Cell Adhesion—Calcein/AM-labeled prostate carcinoma cell suspensions (5×10^5 cells/ml) were preincubated with 16 units/ml *Streptomyces* HAase for 25 min and diluted to 1×10^5 cells/ml with adhesion medium prior to the assay. HAase was present throughout the assay.

Particle Exclusion Assay—Pericellular HA matrices were visualized as described (8). Briefly, prostate carcinoma cells cultured overnight in 48-well plates were washed and treated for 25 min at 37 °C in the absence or presence of *Streptomyces* HAase (16 units/ml in phenol red-free MEM with 0.1% BSA). This medium was removed, and cells were incubated for 90 min with 2 mg/ml aggrecan in MEM and 0.1% BSA at 37 °C. The aggrecan solution was removed, and 1×10^8 glutaraldehyde-fixed sheep red blood cells (Accurate Chemical & Scientific Corp.) in PBS and 1% BSA were added, allowed to settle for 15 min, and then viewed by phase-contrast microscopy. The HA matrix was evidenced by halos surrounding the cells from which the fixed erythrocytes were excluded. Representative cells were photographed at a magnification of ×400. To quantify matrix retention, outlines of matrices and cellular boundaries from 10–15 individual cells of each type were traced, and relative areas were calculated using NIH Image software. HA matrix thickness is presented as the ratio of matrix area to cell area for each transfectant or condition. Values for individual cell tracings were plotted, with mean values represented in each distribution by a *horizontal bar*. A ratio of 1 indicates complete absence of pericellular clearing.

RESULTS

HAS Overexpression and Antisense Inhibition Strategy—In our previous work (2), we correlated overexpression of mRNA for HAS2 and HAS3 with aggressive prostate carcinoma cell lines. We reasoned that altered HA synthesis and/or pericellular HA matrix assembly by prostate carcinoma cells could contribute to tumorigenic or metastatic behavior, either by overall HAS expression level or in an isoform-specific fashion. To establish a functional correlation, we decided to overexpress full-length cDNA for HAS2 or HAS3 in LNCaP cells, which synthesize little or no HA, and to inhibit HAS2 or HAS3 expression in PC3M-LN4 cells, which have a thick pericellular HA matrix. We chose the pIRES2-EGFP eukaryotic expression vector, which expresses inserted cDNA as a bicistronic message with GFP, so cells expressing GFP can be separated from untransfected cells by flow cytometry. Expression of GFP therefore requires the transcription of HAS message and provides a useful detection mechanism for transfected cells expressing high levels of that message. This is particularly critical for antisense RNA expression, where it is frequently difficult to verify the presence of antisense message. The vector also provides an antibiotic resistance gene for stable selection.

HAS2 or HAS3 Overexpression in LNCaP Cells Confers Upregulated HA Synthesis and Pericellular HA Retention—LNCaP cells were transiently transfected with vector alone (GFP) or with vector containing cDNA encoding full-length human HAS2 or HAS3. Transfection efficiencies in the population as measured by flow cytometric analysis of GFP expression were consistently 7–10% for HAS2 cDNA and 15–20% for HAS3 cDNA. Expression of HAS mRNA in the transfected cells was verified by RT-PCR (Fig. 1). Consistent with our previous characterization of the LNCaP cell line (2), GFP control transfectants did not yield detectable amounts of HAS2 product and only small quantities of HAS3 (*lanes 4* and *9*, respectively). Easily amplified HAS2 and HAS3 products were found only in the respective transfected cell types: *lanes 5* and *10* in Fig. 1 correspond to HAS2 transfectants, and *lanes 6* and *11* are HAS3 transfectants. Simultaneous control amplification of the GAPDH housekeeping gene from each transfectant is provided in *lanes 1–3*, and HAS2 (*lanes 7* and *8*) and HAS3 (*lanes 12* and *13*) plasmid constructs were amplified as positive controls for specificity of the reactions.

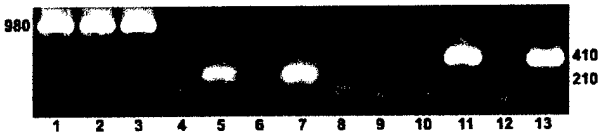

FIG. 1. **LNCaP cells transiently transfected with HAS2 or HAS3 cDNA express the respective message.** LNCaP cells were transfected as described under "Experimental Procedures." 2 days after transfection, poly(A)$^+$ RNA was isolated from each transfectant, reverse-transcribed, and amplified by PCR with primers specific for GAPDH (980 bp; *lanes 1–3*), HAS2 (210 bp; *lanes 4–8*), and HAS3 (410 bp; *lanes 9–13*). *Lanes 1*, *4*, and *9* correspond to GFP control transfectants. *Lanes 2*, *5*, and *10* contain products amplified from HAS2-transfected cells. *Lanes 3*, *6*, and *11* are from HAS3 transfectants. *Lanes 7* and *12* (HAS2) and *lanes 8* and *13* (HAS3) are plasmid DNA controls.

To evaluate functionality of the expressed HAS2 and HAS3 proteins, HA synthesis was measured. It has been shown previously that the majority of HA synthesized by cells in culture is secreted to the culture medium (17). We analyzed HA secretion by LNCaP transient transfectants in a competitive enzyme-linked immunosorbent assay-like assay as described under "Experimental Procedures." LNCaP GFP transfectant culture supernatants were found to contain ≈0.5 μg of HA/10^6 cells (Fig. 2), in close agreement with levels detected in untransfected LNCaP cultures. Following transfection with HAS2 and HAS3 constructs, culture media contained nearly 3- and 4-fold increased HA levels, respectively, confirming enzymatic activity of the transfected cDNA products. Remarkably, the quantity of HA detected in HAS-transfected supernatants was greater by 1–1.5 μg/10^6 cells than in controls. Normalized to the 10–15% transfection efficiency of the cells, this HA increase corresponds to a synthesis rate of ≈10–15 μg/10^6 transfected cells, which is on the order of catalysis measured for the PC3M-LN4 cell line (see Fig. 7).

To assess potential cell-surface HA retention resulting from enhanced HA production, we used particle exclusion. In this assay, cells were preincubated with a specific HA-binding proteoglycan (aggrecan), and small red blood cells were allowed to settle around the much larger prostate cells. Those cells with surface-associated HA exhibited surrounding clear zones. Both the HAS2- and HAS3-transfected LNCaP cells were clearly observed to have a halo (Fig. 3, *B* and *C*, respectively), whereas the GFP control (Fig. 3*A*) lacked such a pericellular zone of exclusion, indicating that transfection of LNCaP cells with HAS2 or HAS3 also conferred surface HA retention. Cells did not appear to exhibit any isoform specificity with regard to the thickness of the matrix as measured in this assay. However, there was a definite correlation between intensity of GFP fluorescence (indicative of transfected cells) and matrix size (data not shown). To verify the HA content of the matrices produced by HAS-transfected cells, transfectants were digested with HAase prior to addition of aggrecan, upon which the pericellular clear zones were no longer visible (Fig. 3, *D–F*).

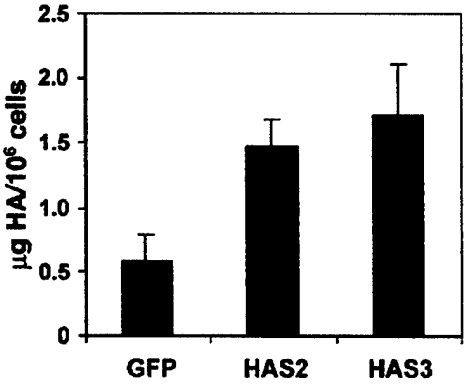

FIG. 2. **HA synthesis and secretion are elevated in LNCaP cells overexpressing HAS2 or HAS3.** LNCaP cells were transfected as described under "Experimental Procedures" with vector alone (GFP) or vector containing full-length cDNA for HAS2 or HAS3. HA synthesis in overnight culture media was assayed by competitive binding assay. Serial dilutions of media were incubated with biotinylated HABP and applied to a 96-well plate coated overnight with 50 μg/ml high molecular mass HA. Wells were washed and detected with streptavidin-conjugated horseradish peroxidase followed by tetramethylbenzidine precipitation. HA levels were interpolated from a concurrent HA standard curve. Assays were performed in triplicate on supernatants from three wells per condition for three separate transient transfections. Levels are plotted in micrograms of HA/10^6 cells.

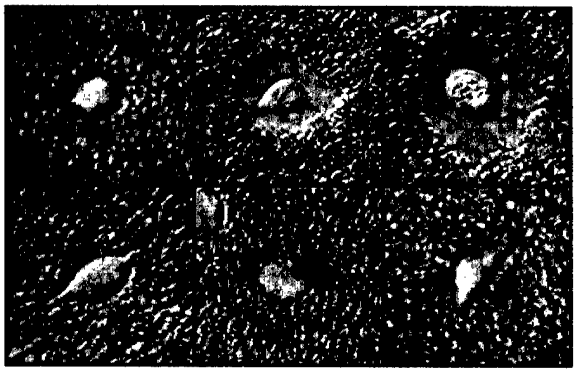

FIG. 3. **Transfection of LNCaP cells with cDNA encoding either HAS2 or HAS3 confers pericellular HA retention.** LNCaP cells were transfected as described under "Experimental Procedures" with vector alone (GFP; *A* and *D*) or vector containing full-length cDNA for HAS2 (*B* and *E*) or HAS3 (*C* and *F*). Overnight cultured cells were washed and incubated at 37 °C for 90 min with 2 mg/ml aggrecan, and HA matrices were visualized as clear zones surrounding the cell perimeter following addition of fixed red blood cells (*A–C*). HA composition of the matrix was verified by digestion with 16 units/ml *Streptomyces* HAase prior to addition of aggrecan (*D–F*).

HAS2- or HAS3-transfected LNCaP Cells Retain Cell-associated HA in Suspension—To verify retention of cell-associated HA in suspended cells, we performed a two-color FACS analysis. Single cell suspensions of LNCaP cells transiently transfected with GFP control, HAS2, or HAS3 constructs were incubated with a biotinylated HABP probe, detected with a streptavidin-conjugated fluorophore, and analyzed by flow cytometry. Cells were gated to include only GFP-positive transfectants and plotted to illustrate HA binding (Fig. 4, *solid line*). HAase sensitivity of the HABP probe demonstrated the specificity of its reactivity with HA and affirmed the HA content of the matrix retained by LNCaP HAS2 and HAS3 transfectants in suspension (*dotted line*). Using this assay, it was apparent that although both HAS transfectants possessed surface HA, LNCaP HAS3 transfectants (Fig. 4*B*), relative to HAS2-transfected cells (Fig. 4*A*), retained considerably more matrix with

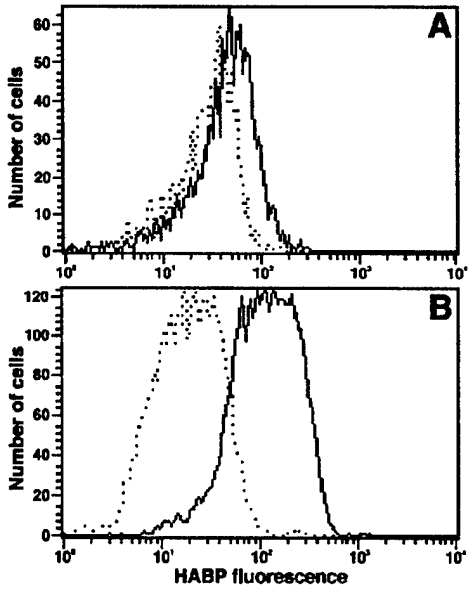

FIG. 4. **HAS2- or HAS3-transfected LNCaP cells retain cell-associated HA in suspension.** HAS2 (*A*)- or HAS3 (*B*)-transfected LNCaP cells were released with PBS containing 3 mM EDTA, filtered twice to obtain single cell suspensions, and incubated with 1 mg/ml biotinylated HABP for 90 min at room temperature with gentle agitation. Cells were centrifuged, washed, and resuspended in PBS with 0.1% BSA. Streptavidin-conjugated perCP in PBS/BSA was added to a final dilution of 1:200 and incubated for 45 min. Cells were washed, resuspended in PBS/BSA, and subjected to two-color FACS analysis. HA composition of the matrix was verified by digestion with 16 units/ml *Streptomyces* HAase prior to addition of HABP. HAase-treated cells are represented in the histograms by *dotted lines*, and untreated cells are indicated by *solid lines*.

HABP-binding potential composed of HAase-sensitive material. Gating on very high GFP-expressing cells, which would be assumed to represent the highest HAS-expressing population, increased the amount of HABP signal intensity in HAS2 transfectants, but not to the level of HAS3 transfectants (data not shown). Reduced apparent transfection efficiency of HAS2 rendered it difficult to obtain significant numbers of highly GFP-positive cells to analyze, however; so this difference may reflect greater transfected message instability rather than inherent isoform-specific matrix formation.

LNCaP HAS2 and HAS3 Transfectants Adhere to BMECs—To determine whether surface HA retention could mediate adhesion to BMECs, LNCaP HAS2 and HAS3 transfectants and corresponding GFP controls were labeled and applied to confluent TrHBMEC monolayers. Like the parental LNCaP cells, adhesion of GFP control transfectants (Fig. 5, *black bars*) was very low and unaffected by HAase digestion (*white bars*). Greater numbers of LNCaP cells transiently transfected with HAS2 (≈8% more, $p = 0.068$ relative to GFP control) and HAS3 (≈12% more, $p < 0.01$ relative to GFP control) were found to adhere to BMECs, and the enhanced adhesion was entirely HAase-sensitive. These increases, although modest, are in close relation to the respective transfection efficiencies of HAS2 and HAS3 constructs. Furthermore, flow cytometric analysis of non-adherent cells relative to total input cells demonstrated removal of GFP-positive cells from the HAS2- and HAS3-transfected populations (data not shown), implying that all transfected cells were adherent. This result is consistent with a direct role for up-regulated HA synthesis and surface HA retention in prostate tumor cell adhesion to BMECs. Furthermore, overexpression of either the HAS2 or HAS3 isoform alone was sufficient to confer these properties to LNCaP cells.

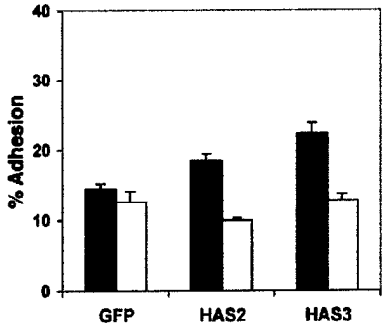

FIG. 5. **HAS overexpression by LNCaP cells confers HA-mediated adhesion to BMECs.** Single cell suspensions of LNCaP GFP control, HAS2, or HAS3 transfectants were calcein-labeled, preincubated in the absence (*black bars*) or presence (*white bars*) of 16 units/ml *Streptomyces* HAase, and applied to confluent TrHBMEC monolayers in a 48-well plate. Non-adherent cells were removed after 15 min, and the remaining adherent cells were lysed and quantified in a fluorescence plate reader.

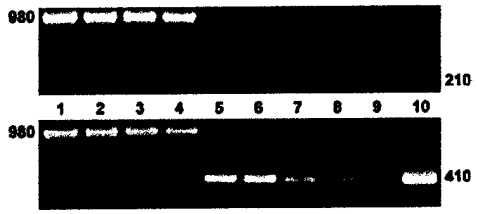

FIG. 6. **Stable expression of antisense HAS RNA in PC3M-LN4 cells reduces steady-state HAS2 and HAS3 message levels.** PC3M-LN4 cells were stably selected for expression of control vectors (*lanes 1* and *5*), vector encoding bicistronic antisense HAS2-GFP (*lanes 2* and *6*), vector encoding bicistronic antisense HAS3-GFP (*lanes 3* and *7*), or vector encoding double antisense HAS2/HAS3 (*lanes 4* and *8*) as described under "Experimental Procedures." Poly(A)$^+$ RNA was isolated from each transfectant, reverse-transcribed, and amplified by PCR with primers specific for GAPDH (980 bp; *lanes 1–4*), HAS2 (210 bp; *upper panel, lanes 5–10*), and HAS3 (410 bp; *lower panel, lanes 5–10*). Plasmids containing full-length HAS2 and HAS3 cDNAs (*lanes 9* and *10*, respectively) were amplified concurrently as controls.

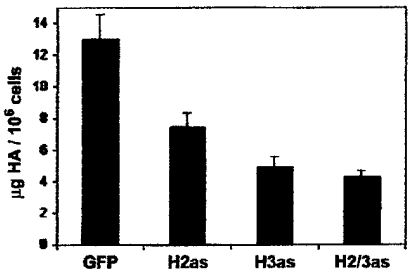

FIG. 7. **Inhibition of HAS2 and/or HAS3 expression in PC3M-LN4 cells by stable antisense transfection reduces HA synthesis and secretion.** PC3M-LN4 cells were selected as described under "Experimental Procedures" for stable expression of control vectors alone (GFP) or vectors encoding antisense HAS2 RNA (H2as), antisense HAS3 RNA (H3as), or double antisense HAS2/HAS3 RNA (H2/3as). Transfectants were seeded in triplicate wells of a 24-well plate (30,000 cells/well). Seeding media were removed the following day; cells were washed; and fresh medium was applied. These overnight conditioned media were then harvested and analyzed for HA content by competitive binding assay as described under "Experimental Procedures." HA quantity was normalized to cell number as determined by trypsin release and manual counting in a hemocytometer. Data are presented as the means ± S.E. of three independent HA quantitations performed on triplicate culture supernatants for each transfectant.

Antisense HAS Expression Diminishes PC3M-LN4 Synthesis and Secretion of HA—To evaluate the effect of antisense HAS mRNA expression on prostate tumor cell behavior, we developed four stably transfected PC3M-LN4 cell lines: GFP, bearing the appropriate vector controls; H2as, expressing only antisense HAS2; H3as, with antisense HAS3 only; and H2/3as, a "double knockout" incorporating both antisense HAS2 and HAS3. We have previously used semiquantitative RT-PCR to demonstrate that PC3M-LN4 cells express relatively high levels of HAS2 and HAS3 mRNAs. By the same methodology, equal amounts of poly(A)$^+$ RNA from each of the four stably transfected cell lines were analyzed by RT-PCR for HAS2 (Fig. 6, *upper panel, lanes 5–10*) and HAS3 (*lower panel, lanes 5–10*) expression. GAPDH was simultaneously amplified with each set of reactions to control for input RNA (*lanes 1–4*). Fig. 6 (*upper panel, lanes 6* and *8*) shows reduced HAS2 message in H2as and H2/3as transfectants, respectively, whereas GFP control and H3as transfectants retained comparable expression (*lanes 5* and *7*). HAS3 expression, unaffected in GFP control or H2as transfectants (*lower panel, lanes 5* and *6*), was significantly diminished in both H3as and H2/3as cells (*lanes 7* and *8*). These results demonstrate efficacy and isoform specificity of antisense HAS inhibition, although endogenous HAS gene expression appeared to be incompletely suppressed.

We next used a competitive binding assay to quantify HA synthesis and secretion by each cell line and to evaluate potential functional differences. As shown in Fig. 7, GFP controls produced ≈13 μg of HA/10^6 cells in 20 h, consistent with our previous results for untransfected PC3M-LN4 cells. H2as transfectants produced about half as much HA as the control cells (≈7 μg/10^6 cells), reflecting the significantly diminished HAS2 expression observed by RT-PCR. H3as transfectants secreted ≈5 μg of HA/10^6 cells in 20 h, and the H2/3as cell supernatants contained <4 μg of HA/10^6 cells. These results show dramatic inhibition of HA synthesis by stable transfection with antisense HAS and possibly suggest that HAS3 may produce more of the cellular HA than HAS2, although it is clear that there is residual HAS expression even in the presence of both antisense messages.

Antisense HAS Expression in PC3M-LN4 Cells Reduces Matrix Thickness—We next evaluated the antisense PC3M-LN4 cell lines by particle exclusion to determine whether antisense HAS transfection affected cell-surface HA retention. The vector control transfectants retained HAase-sensitive matrices (Fig. 8*A* and *inset*) of comparable thickness to the parental PC3M-LN4 cells (Fig. 8*E*). Antisense HAS2 or HAS3 transfectants (Fig. 8, *B* and *C*), although still surrounded by pericellular HA, appeared to have matrices of diminished thickness. H2/3as cells (Fig. 8*D*) did not appear to retain HA at the cell surface (compare with 8*A*, *inset*, HAase-treated). To quantify matrix thickness, outlines of matrices and cellular boundaries from 10 individual cells were traced, and relative areas were calculated using NIH Image software. Coat thickness was plotted as the ratio of matrix area to cell area (coat/cell area ratio) for each transfectant as well as for the parental PC3M-LN4 cell line with and without HAase treatment (Fig. 8*E*). The mean ratio for each condition is indicated by a *horizontal bar*. The parental cell line bore a very thick coat, with coat/cell area ratios averaging 2.6. HAase treatment reduced this ratio to ~1.3, demonstrating virtually complete removal of HA from the cell surface (a ratio of 1 signifies absence of matrix). GFP vector control transfectants had comparable coat/cell area ratios relative to parental cells, but these ratios were significantly reduced in single antisense HAS2 and HAS3 transfectants (≈2 and 1.5, respectively) as well as in the H2/3as cell line (≈1.3). These quantitations correlated well with trends observed in HA synthesis by the respective cells and suggest a direct correlation among HAS expression, HA synthesis levels, and pericellular matrix retention.

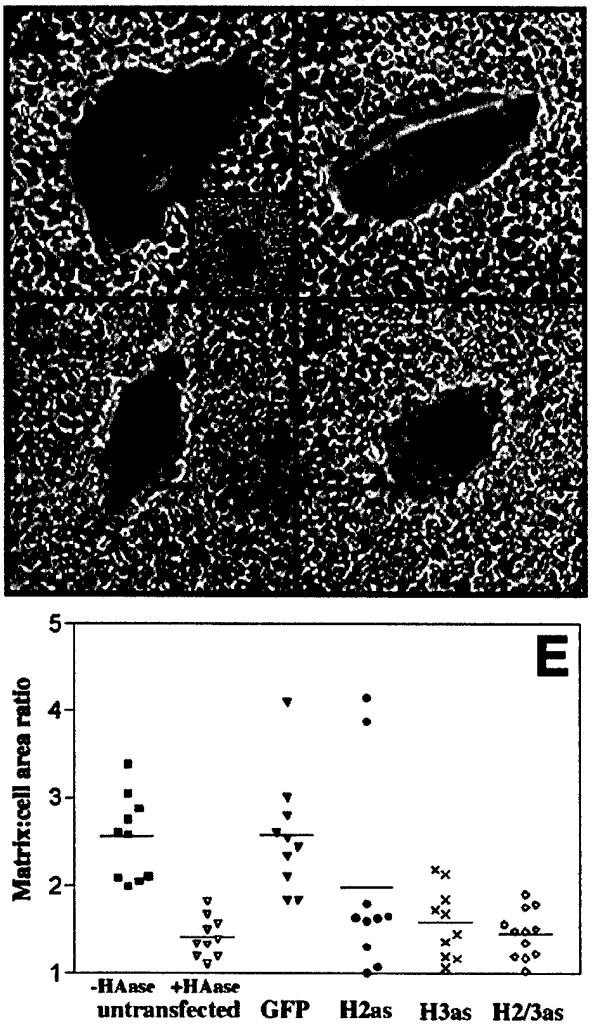

FIG. 8. **Antisense HAS inhibition in PC3M-LN4 cells diminishes pericellular HA matrix retention.** Overnight cultures of PC3M-LN4 stable transfectants were washed and incubated with aggrecan as described under "Experimental Procedures." Surface HA retention was visualized as a clear zone encapsulating the cell upon subsequent addition of fixed red blood cells. Cells were digitally photographed at a magnification of ×400. *A*, GFP control transfectants exhibited halos. HA composition of the matrix was verified by HAase digestion (*inset*). *B–D*, shown are the antisense HAS2, antisense HAS3, and double antisense HAS2/HAS3 transfectants, respectively. *E*, surface HA retention was quantified as the ratio of matrix area to cell area for vector control relative to antisense HAS-inhibited PC3M-LN4 transfectants. Following addition of red blood cells, individual PC3M-LN4 transfectants were traced using NIH Image at the boundary of the clear zone to calculate matrix area and at the cell perimeter to calculate cell area. Coat/cell area ratios are plotted as a distribution, with the mean value represented by a *horizontal bar*.

Antisense Expression Inhibits BMEC Adhesion—To examine the role of HA synthesis and surface retention in PC3M-LN4 intercellular interaction with BMECs, we performed adhesion assays as described under "Experimental Procedures." Inhibition of HAS2 or HAS3 expression individually was observed to diminish adhesion of PC3M-LN4 cells to TrHBMECs (Fig. 9). Adhesion was further inhibited by digestion with HAase, however, suggesting that there is sufficient residual synthesis of HA by the remaining HAS isoform in either the single antisense HAS2 or HAS3 transfectants to promote BMEC adhesion. The greatest inhibition was observed in antisense HAS3, which may imply that although HAS2 is active and sufficient to

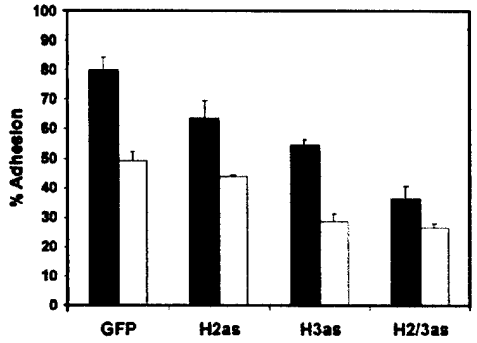

FIG. 9. **Antisense HAS2 and HAS3 inhibition in PC3M-LN4 cells impairs adhesion to BMECs.** Single cell suspensions of PC3M-LN4 stable transfectants were calcein-labeled, incubated in the absence (*black bars*) or presence (*white bars*) of 16 units/ml *Streptomyces* HAase, and applied to confluent TrHBMEC monolayers. After 10 min, nonadherent cells were removed, and the remaining adherent cells were lysed and quantified in a fluorescence plate reader. Results are plotted as percentage of total input cells.

maintain HA synthesis required for BMEC adhesion, HAS3 actually is more critical to the process than HAS2. The level of adhesion following HAase digestion of HAS3 transfectants was also decreased relative to controls (~25% adhesion relative to 45% for vector controls), suggesting that HA-mediated adhesion may be a more significant percentage than is apparent from digestion of parental cells. HA was probably re-synthesized on the time scale of the assay in the parental and vector control cells, whereas antisense HAS slowed the rate of surface matrix replenishment, thus decreasing adhesion to BMECs. This is further supported by the effect of double antisense H2/3as inhibition: adhesion of these transfectants to BMECs was reduced below the level of HAase-inhibited control cell adhesion, and there was a virtual absence of HAase sensitivity. HAase treatment of these cells did not reduce adhesion below levels following HAase digestion of H3as cells, again strongly implying that HAS3 may synthesize most of the overproduced HA required to promote adhesion of PC3M-LN4 cells to BMECs.

DISCUSSION

Prostate cancer bone metastasis is the most frequent cause of mortality in patients with prostate cancer. The origin of preferential bone metastasis by prostate tumor cells may therefore reside in expression of a unique and complementary profile of adhesion molecules and receptors by prostate and bone marrow endothelial cells that would facilitate the arrest of circulating cells in the bone marrow microvasculature. In this report, we have demonstrated the role of two specific genes in modulation of rapid adhesion by prostate tumor cells in suspension to cultured BMEC monolayers. The overproduction of HA induced by transfection of LNCaP cells with HA biosynthetic enzyme isoforms HAS2 and HAS3 was sufficient to enhance HA-mediated adhesion of these cells to TrHBMECs. Conversely, decreased HA production by antisense HAS2 and HAS3 expression in PC3M-LN4 cells eliminated the pericellular HA matrix normally retained by these cells and abolished HA-mediated adhesion to TrHBMECs. Up-regulation of HA biosynthetic enzymes may therefore be one mechanism governing preferential bone metastasis.

Individual HAS isoform expression in LNCaP cells is sufficient for elevated HA synthesis, leading to surface HA retention, which mediates BMEC adhesion. It is worth noting that LNCaP cells do not express CD44, the primary cell-surface receptor for HA (28), shown many times in other studies to be a requisite component of HA matrices. This argues that other

HA receptors must be cross-linking HA into a matrix or that HAS enzymes themselves, when present at high levels in the cell membrane, retain considerable amounts of HA. The presence of HA alone is capable of promoting intercellular adhesion: as a result of its repetitive polymeric structure, it exhibits multivalent binding characteristics, simultaneously ligating receptors on multiple cells. In our studies with LNCaP cells, it was difficult to distinguish the relative effects of the two HAS isoforms. Although it appeared that HAS2 was less active in HA overproduction and surface retention, when normalized to transfection efficiency, both enzymes catalyzed sufficient HA synthesis to mediate equivalent BMEC adhesion, suggesting similarity of the products with regard to ligation of adhesion molecules and/or receptor engagement.

HAS overexpression has been correlated with aggressive cell behaviors in several other model systems. Treatment of mesothelial cells with several pro-inflammatory cytokines (24) increases HAS2 expression, and manual wounding of cultured peritoneal mesothelial cells specifically induces HAS2 up-regulation at the wounded edge of the monolayer (20). HAS2 clearly appears to have a role in wound healing and inflammation and also appears to be the most highly regulated isoform because these studies reported no significant changes in the levels of HAS1 or HAS3 transcripts. Overexpression of HAS1 in a syngeneic mouse mammary carcinoma model resulted in increased lung metastasis following intravenous injection (23). Although human breast cancers also metastasize preferentially to bone marrow, bone metastasis was not addressed in that model. HAS2 overexpression has been shown to promote anchorage-independent growth in HT1080 fibrosarcoma cells (21) and malignant mesotheliomas (29) as well as to increase migration (29) and to enhance subcutaneous tumorigenicity in nude mice (21). HAS3 overexpression in TSU prostate carcinoma cells (22) yields bigger subcutaneous tumors in nude mice, but has no effect on lung metastasis following intravenous injection. HAS enzymes therefore also function to promote growth and motility; however, no studies have addressed the effect of HAS expression on bone metastatic proclivity.

Fewer studies documenting inhibition of HA synthesis have been published. The most conspicuous HAS inhibitors reported to date include hydrocortisone (24), which suppresses HAS2 expression in mesothelial cells almost entirely, and dexamethasone, another glucocorticoid that rapidly down-regulates HAS2 expression in skin fibroblasts (30). The former study again reported no effect on HAS1 or HAS3 message levels, suggesting that HAS2 may be the most transiently regulated of the three genes. Our characterization of prostate carcinoma cell lines by RT-PCR demonstrated elevated expression of both HAS2 and HAS3 relative to normal prostate epithelial cells, with overexpression of HAS3 correlating most closely to the reported metastatic potential of the cell lines. Because HAS3 appears to be less regulated at the transcriptional level, the consequences of its basal overexpression by tumor cells are likely to be dramatic and difficult to alleviate.

To directly ascertain the impact of HAS expression on HA matrix retention and adhesion to BMECs, we employed a 2-fold strategy: up-regulation in cells lacking HA (LNCaP) and inhibition of HAS gene expression in cells with a thick pericellular HA matrix (PC3M-LN4). The latter strategy required stable selection for antisense HAS expression to obtain a significant decrease in HA secretion, reflecting the difficulty of achieving complete knockout. Inhibition of individual HAS isoforms, although able to decrease HA production, matrix retention, and adhesion to BMECs, did not completely abolish these functions, suggesting that each isoform alone actively produces HA in PC3M-LN4 cells. HA production and BMEC adhesion were more significantly reduced in HAS3-inhibited cells, which could be indicative of more efficient HAS3 enzyme catalysis. Kinetic characterizations of HAS in reconstituted liposomes showed equivalent catalytic rates for HAS2 and HAS3 (31), however. Rather, this observation is consistent with greater detectable expression of HAS3 relative to HAS2 (2) and with a potential correlation between adhesive/metastatic potential and levels of HAS3. Because adhesion of double antisense HAS-inhibited tumor cells was almost entirely reduced to a basal percentage, we conclude that surface HA retention is both necessary and sufficient for rapid maximal intercellular adhesion in our cell culture model.

Histopathologic studies of human prostate cancer have shown that HA levels increase in tumors as a function of increasing pathologic grade (13, 14). These data suggest that tumor cells may develop an enhanced capacity to synthesize and retain pericellular HA. Consequently, the cells become surrounded by a hydrated envelope that facilitates invasiveness, perhaps by altering the composition and interfering with the integrity of tissue stromal matrices. This envelope could also permit the tumor cells to evade immune system detection, to adhere to specialized endothelia, and/or to grow in remote sites. Short HA oligosaccharide degradation products have been shown to stimulate angiogenesis (32), and levels may be elevated in the environs of such tumor cells through the action of HAase enzymes (33). Inhibition of HAS enzyme expression within the tumor would then be predicted to decrease angiogenesis and thereby suppress tumor growth. HAS expression has not yet been characterized in human tumor tissue.

Tumor cells may utilize adhesive mechanisms for homing to bone marrow that normally occur for the purpose of regulating homing of hematopoietic progenitor cells. Studies of circulating progenitors have demonstrated the involvement of carbohydrate/lectin interactions as well as intercellular adhesion molecules, VCAM, and integrins. In a metastatic myeloma model (34), CD44/HA was required for transmigration of BMEC monolayers. Furthermore, HA binding to CD44 has also been shown to mediate lymphocyte rolling under shear flow conditions (35). Endothelial adhesion receptor profiles may drive preferential metastasis. Cultured endothelial cells from microvascular *versus* large vein or arterial sources have been shown to bind significantly greater amounts of HA (36), which was attributable to differential expression of the HA receptors CD44 and RHAMM (receptor for HA-mediated motility). Ligation of these receptors has been shown to transduce motility signals (37, 38), perhaps consequently permitting ingress of tumor cells to bone marrow.

The most simple consequence of our results is that tumor cell-associated HA would recognize bone marrow endothelial receptors and arrest the circulating cell in the microvasculature. However, it is possible that this interaction could occur indirectly or be facilitated by indirect interaction with lymphocytes or other CD44-expressing cells in the bloodstream. The presence of such cells in tumor cell aggregates could provide a source of "normal" cross-talk between the tumor cells and the endothelium. Chemokines and their receptors, for example, are required for transendothelial migration of hematopoietic progenitor cells *in vitro* (39). Secretion of chemokines or expression of chemokine receptors within the cell aggregates and recognition by the endothelial cognate receptor or ligand would be one mechanism by which transmigration of a tumor cell could be indirectly orchestrated.

We have demonstrated, by manipulation of gene expression, that up-regulated HAS enzymes in prostate tumor cells are responsible for promoting rapid adhesion to BMECs *in vitro*. This is a novel interaction that has not been previously de-

scribed for prostate carcinoma cells. It will be important to determine whether this adhesive preference *in vitro* translates to preferential arrest and/or homing to the bone marrow microvasculature in a mouse model. We are currently investigating this question. We anticipate that inhibition of HA synthesis by prostate tumor cells or antagonism of HA-mediated adhesion may provide a means of regulating metastatic growth of prostate cancer.

Acknowledgment—We thank Dr. Joseph Barycki for many thoughtful discussions.

REFERENCES

1. Pettaway, C. A., Pathak, S., Greene, G., Ramirez, E., Wilson, M. R., Killion, J. J., and Fidler, I. J. (1996) *Clin. Cancer Res.* **2,** 1627–1636
2. Simpson, M. A., Reiland, J., Burger, S. R., Furcht, L. T., Spicer, A. P., Oegema, T. R., Jr., and McCarthy, J. B. (2001) *J. Biol. Chem.* **276,** 17949–17957
3. Laurent, T. C., and Fraser, J. R. (1992) *FASEB J.* **6,** 2397–2404
4. Reed, R. K., Lilja, K., and Laurent, T. C. (1988) *Acta Physiol. Scand.* **134,** 405–411
5. Papayannopoulou, T., Craddock, C., Nakamoto, B., Priestley, G. V., and Wolf, N. S. (1995) *Proc. Natl. Acad. Sci. U. S. A.* **92,** 9647–9651
6. Zhang, L., Underhill, C. B., and Chen, L. (1995) *Cancer Res.* **55,** 428–433
7. Gakunga, P., Frost, G., Shuster, S., Cunha, G., Formby, B., and Stern, R. (1997) *Development* **124,** 3987–3997
8. Knudson, C. B., and Toole, B. P. (1985) *Dev. Biol.* **112,** 308–318
9. Evanko, S. P., Angello, J. C., and Wight, T. N. (1999) *Arterioscler. Thromb. Vasc. Biol.* **19,** 1004–1013
10. Koochekpour, S., Pilkington, G. J., and Merzak, A. (1995) *Int. J Cancer* **63,** 450–454
11. Delpech, B., Chevallier, B., Reinhardt, N., Julien, J. P., Duval, C., Maingonnat, C., Bastit, P., and Asselain, B. (1990) *Int. J. Cancer* **46,** 388–390
12. Manley, G., and Warren, C. (1987) *J. Clin. Pathol.* **40,** 626–630
13. De Klerk, D. P. (1983) *Prostate* **4,** 73–81
14. De Klerk, D. P., Lee, D. V., and Human, H. J. (1984) *J. Urol.* **131,** 1008–1012
15. Weigel, P. H., Hascall, V. C., and Tammi, M. (1997) *J. Biol. Chem.* **272,** 13997–14000
16. Shyjan, A. M., Heldin, P., Butcher, E. C., Yoshino, T., and Briskin, M. J. (1996) *J. Biol. Chem.* **271,** 23395–23399
17. Watanabe, K., and Yamaguchi, Y. (1996) *J. Biol. Chem.* **271,** 22945–22948
18. Spicer, A. P., and McDonald, J. A. (1998) *J. Biol. Chem.* **273,** 1923–1932
19. Camenisch, T. D., Spicer, A. P., Brehm-Gibson, T., Biesterfeldt, J., Augustine, M. L., Calabro, A., Jr., Kubalak, S., Klewer, S. E., and McDonald, J. A. (2000) *J. Clin. Invest.* **106,** 349–360
20. Yung, S., Thomas, G. J., and Davies, M. (2000) *Kidney Int.* **58,** 1953–1962
21. Kosaki, R., Watanabe, K., and Yamaguchi, Y. (1999) *Cancer Res.* **59,** 1141–1145
22. Liu, N., Gao, F., Han, Z., Xu, X., Underhill, C. B., and Zhang, L. (2001) *Cancer Res.* **61,** 5207–5214
23. Itano, N., Sawai, T., Miyaishi, O., and Kimata, K. (1999) *Cancer Res.* **59,** 2499–2504
24. Jacobson, A., Brinck, J., Briskin, M. J., Spicer, A. P., and Heldin, P. (2000) *Biochem. J.* **348,** 29–35
25. Schweitzer, K. M., Vicart, P., Delouis, C., Paulin, D., Drager, A. M., Langenhuijsen, M. M., and Weksler, B. B. (1997) *Lab. Invest.* **76,** 25–36
26. Knudson, C. B. (1993) *J. Cell Biol.* **120,** 825–834
27. Lokeshwar, V. B., Obek, C., Soloway, M. S., and Block, N. L. (1997) *Cancer Res.* **57,** 773–777
28. Aruffo, A., Stamenkovic, I., Melnick, M., Underhill, C. B., and Seed, B. (1990) *Cell* **61,** 1303–1313
29. Li, Y., and Heldin, P. (2001) *Br. J. Cancer* **85,** 600–607
30. Zhang, W., Watson, C. E., Liu, C., Williams, K. J., and Werth, V. P. (2000) *Biochem. J.* **349,** 91–97
31. Itano, N., Sawai, T., Yoshida, M., Lenas, P., Yamada, Y., Imagawa, M., Shinomura, T., Hamaguchi, M., Yoshida, Y., Ohnuki, Y., Miyauchi, S., Spicer, A. P., McDonald, J. A., and Kimata, K. (1999) *J. Biol. Chem.* **274,** 25085–25092
32. Rooney, P., Kumar, S., Ponting, J., and Wang, M. (1995) *Int. J. Cancer* **60,** 632–636
33. Lokeshwar, V. B., Rubinowicz, D., Schroeder, G. L., Forgacs, E., Minna, J. D., Block, N. L., Nadji, M., and Lokeshwar, B. L. (2001) *J. Biol. Chem.* **276,** 11922–11932
34. Okada, T., Hawley, R. G., Kodaka, M., and Okuno, H. (2000) *Clin. Exp. Metastasis* **17,** 625–631
35. Nandi, A., Estess, P., and Siegelman, M. H. (2000) *J. Biol. Chem.* **275,** 14939–14948
36. Lokeshwar, V. B., and Selzer, M. G. (2000) *J. Biol. Chem.* **275,** 27641–27649
37. Bourguignon, L. Y., Zhu, H., Shao, L., and Chen, Y. W. (2000) *J. Biol. Chem.* **275,** 1829–1838
38. Savani, R. C., Cao, G., Pooler, P. M., Zaman, A., Zhou, Z., and DeLisser, H. M. (2001) *J. Biol. Chem.* **276,** 36770–36778
39. Mohle, R., Bautz, F., Rafii, S., Moore, M. A., Brugger, W., and Kanz, L. (1998) *Blood* **91,** 4523–4530

American Journal of Pathology, Vol. 161, No. 3, September 2002

Inhibition of Prostate Tumor Cell Hyaluronan Synthesis Impairs Subcutaneous Growth and Vascularization in Immunocompromised Mice

Melanie A. Simpson,* Christopher M. Wilson,* and James B. McCarthy*†

From the Department of Laboratory Medicine and Pathology and the University of Minnesota Cancer Center,† University of Minnesota, Minneapolis, Minnesota*

Hyaluronan (HA), a secreted glycosaminoglycan component of extracellular matrices, is critical for cellular proliferation and motility during development. However, elevated circulating and cell-associated levels correlate with various types of cancer, including prostate. We have previously shown that aggressive PC3M-LN4 prostate tumor cells synthesize excessive HA relative to less aggressive cells, and express correspondingly higher levels of the HA biosynthetic enzymes HAS2 and HAS3. Inhibition of these enzymes by stable transfection of PC3M-LN4 cells with antisense HAS2 or HAS3 expression constructs diminishes HA synthesis and surface retention. In this report, we used these HA-deficient cell lines to examine the role of HA in tumorigenicity. Subcutaneous injection of SCID mice with hyaluronan synthase (HAS) antisense-transfected cells produced tumors threefold to fourfold smaller than control transfectants. Tumors from HAS antisense transfectants were histologically HA-deficient relative to controls. HA deficiency corresponded to threefold reduced cell numbers per tumor, but comparable numbers of apoptotic and proliferative cells. Percentages of apoptotic cells in cultured transfectants were identical to those of control cells, but antisense inhibition of HA synthesis effected slower growth rate of cells in culture. Quantification of blood vessel density within tumor sections revealed 70 to 80% diminished vascularity of HAS antisense tumors. Collectively, the results suggest HAS overexpression by prostate tumor cells may facilitate their growth and proliferation in a complex environment by enhancing intrinsic cell growth rates and promoting angiogenesis. Furthermore, this is the first report of a role for inhibition of HA synthesis in reducing tumor growth kinetics. ***(Am J Pathol 2002, 161:849–857)***

Prostate cancer is the second leading cause of cancer death in men.[1] In prostate cancer progression, prostate epithelial cells undergo phenotypic and genotypic changes that facilitate inappropriate proliferation, invasion of surrounding stromal matrices, entry into the lymphatic system and/or the bloodstream, and colonization of other tissues in the body. Understanding the molecular events that mediate these processes is essential to ultimate disease diagnosis, management, and treatment.

Hyaluronan (HA) is a secreted glycosaminoglycan abundant in stromal matrices and important for providing cushion around organ tissue and within joints.[2] However, more active roles for HA have been demonstrated in proliferation, in which its deposition facilitates rounding of mitotic cells;[3] development, in which it is both a scaffold for the movement of differentiating cells and a stimulus for the transformation to a mesenchymal phenotype that precedes cellular migration to form organs such as the heart[4] and prostate;[5] and wound healing, in which accelerated synthesis serves to recruit lymphocytes to the wound through the action of specific HA receptors.[6] Because these functions for HA are also components of aggressive tumor cell behavior, it is not surprising that HA has been implicated in tumorigenicity and metastasis. In fact, HA overproduction is a diagnostic or prognostic factor for several types of cancer, including breast,[7] thyroid,[8] ovarian,[9] colorectal,[10] and bladder cancers.[11] In histopathological analyses of human prostate cancer,[12–14] excessive stromal HA accumulation is detectable in early stages and intensifies throughout progression. Eventually, advanced cancers exhibit tumor cell-associated HA, which correlates to poor patient prognosis.[15]

HA biosynthesis is catalyzed by transmembrane HA synthase (HAS) enzymes.[16] Three human isozymes have been identified and cloned (*has1*,[17] *has2*,[18] *has3*[19]). The cDNA of each isozyme is capable of conferring HA synthesis and pericellular HA retention to transfected cells, and the HA products and rates of synthesis seem to be

Supported by funds from the United States Army Medical Research and Material Command (grants DA/DAMD 17-99-A-9029 and DA/DAMD 17-02-1-0102) and a National Institutes of Health National Research Service Award postdoctoral fellowship 1F32-CA84619-02 (to M. A. S.).

Accepted for publication May 15, 2002.

Present address for Melanie A. Simpson is the Department of Biochemistry, University of Nebraska, Lincoln, NE.

Address reprint requests to Dr. James B. McCarthy, Department of Laboratory Medicine and Pathology, University of Minnesota, Mayo Mail Code 609, 420 Delaware St. S.E., Minneapolis, MN 55455. E-mail: mccar001@tc.umn.edu.

very comparable in these transfectants.[20,21] Manipulation of specific isozyme expression levels has been demonstrated to affect tumorigenicity and metastasis. Overexpression of HAS2 in fibrosarcoma cells or HAS3 in prostate carcinoma cells yields significantly larger subcutaneous tumors in nude mice.[22,23] These results suggest involvement of HA in tumor growth, and imply that specific HAS isozymes and/or expression levels of those isozymes may mediate this process.

Previous work in our laboratory has been directed at determining the role of HA biosynthetic enzymes in prostate cancer. Initially, we demonstrated overexpression of mRNA for HAS isozymes 2 and 3 in PC3M-LN4, an aggressive prostate carcinoma cell line,[24] relative to less aggressive prostate tumor cell lines and normal prostate.[25] Overexpression of HAS2[22] and HAS3[23] has been shown to enhance growth of human tumor cell transfectants in immunocompromised mice, but the effect of inhibited HA production by tumor cells has not been determined. Altered HA synthesis and/or pericellular HA retention by prostate carcinoma cells could contribute to tumorigenic behavior, either by overall HAS expression level or in an isozyme-specific manner. Seeking to establish a functional correlation, we developed and characterized four stably transfected PC3M-LN4 cell lines.[26] An appropriate vector control; H2as, expressing only HAS2 antisense; H3as, with HAS3 antisense only; and H2/3as, a double knockout incorporating antisense for both HAS2 and HAS3. Significant inhibition of HA synthesis and pericellular HA retention was obtained by stable transfection with individual HAS antisense, with double antisense transfectants most dramatically affected.[26]

In this study, our goal was to evaluate the impact of inhibited HA production on prostate tumor cell growth in an animal model. We found the presence of excessive HA was required for efficient tumor growth, and investigated the potential mechanisms by which growth kinetics were altered. Apoptosis was unaffected either in tumor sections or cultured cells. The intrinsic rate of proliferation in culture was modestly reduced by HAS antisense inhibition, although the absolute percentage of proliferating cells within the tumor sections was not impacted. Quantification of blood vessel density among the cell lines revealed significantly reduced vascularization of HAS antisense-inhibited transfectant tumors. We conclude that the role of HA in prostate tumor cell biology is both proliferative and angiogenic.

Materials and Methods

Cell Culture and Reagents

The PC3-derivative cell line, PC3M-LN4 (human prostate adenocarcinoma cells), was kindly provided by Dr. Isaiah J. Fidler (M. D. Anderson Hospital Cancer Center, Houston, TX), and was maintained in minimal essential medium containing 10% fetal bovine serum, sodium pyruvate, and nonessential amino acids. Media supplements, and antibiotics were purchased from Invitrogen (Carlsbad, CA). Stably transfected cells selected as previously described[26] were maintained in the above medium containing 1 mg/ml of G418 and 0.5 mg/ml of hygromycin until one passage before injection, at which time this medium was replaced with standard medium. C.B-17.scid mice were purchased from Charles River, Wilmington, MA.

Mouse Subcutaneous Injection and Analysis

Male SCID mice (five animals per condition in three separate experiments) were injected subcutaneously in each flank with 1×10^6 tumor cells suspended at 10×10^6 cells/ml in standard culture medium. Tumor growth was monitored every 3 to 7 days using digital calipers. After 21 days, mice were sacrificed, a final caliper reading was recorded, and tumors were dissected and weighed. One part of each tumor was snap-frozen in OCT compound on dry ice for subsequent sectioning and CD31 detection. The other part was formalin-fixed, paraffin-embedded, and sectioned for histological analysis. Five sections per tumor type were stained with hematoxylin and eosin (H&E).

Detection of HA in Tumor Sections

HA was specifically detected in tumor sections with a biotinylated HA-binding protein (Seikagaku) at 3 μg/ml in phosphate-buffered saline (PBS)/1% bovine serum albumin overnight at 4°C. Sections were then washed, incubated for 1 hour with avidin-horseradish-peroxidase conjugate (Vector Laboratories, Irvine, CA), developed with the 3,3′-diaminobenzidine tetrahydrochloride liquid substrate system (Sigma Chemical Co., St. Louis, MO) for 10 minutes, hematoxylin-counterstained, and examined microscopically for 3,3′-diaminobenzidine tetrahydrochloride deposition.[15] Representative sections were digitally photographed at ×400 magnification.

Cellularity Determination

Cell counts were determined manually in hematoxylin-stained frozen sections. Five random sections were counted in each of four to five tumors per cell line and averages plotted in a distribution with the mean represented by a horizontal bar. To obtain relative cell numbers per tumor, the average two-dimensional cell counts were integrated to a three-dimensional volumetric density and normalized to the average three-dimensional volume of each tumor.

Apoptosis

Subconfluent cultures of equivalent passages of tumor cell lines were trypsin released, washed twice in PBS, and fixed/permeabilized by addition of ice-cold ethanol. Control aliquots of each cell suspension were incubated with 10 μg/ml of DNase. A terminal dUTP nick-end labeling (TUNEL) assay for DNA fragmentation, an early event in apoptosis, was performed according to the manufac-

turer's protocols using the TUNEL-Red apoptosis detection kit from Boehringer Mannheim, Indianapolis, IN. Cells were analyzed by two-color flow cytometry, gating on GFP-positive cells, and assessing incorporation of the red fluorophore in the FL-2 channel.

Intrinsic Growth Rate

Equivalent passages of each tumor cell line were plated at 2000 cells/well in 48-well plates. At 24-hour intervals up to 6 days, quadruplicate wells of each cell line were released with 150 μl of trypsin, neutralized with 150 μl of serum-containing medium, and manually counted in a hemacytometer.

Angiogenesis Quantification

Vascularization of the tumors was assessed in acetone-fixed frozen sections by antibody staining for CD31, a transmembrane protein specifically expressed by vascular endothelial cells. CD31-phycoerythrin-conjugated antibody (BD Pharmingen) staining was visualized by fluorescence microscopy. Five random sections from each of three tumors per cell line were digitally photographed with 5 seconds of exposure time, saved as TIF files, and processed as previously described.[27] Briefly, images were converted from 16 bit to 8 bit in Adobe Photoshop, red channel fluorescence was specifically isolated, images were converted to grayscale, inverted, and a black-and-white threshold was arbitrarily set to 200 based on levels. The histogram function was then used to determine vessel density as represented by density of black pixels at 0 on the black-to-white scale. Average pixel density for each transfectant tumor section was normalized to the average pixel density for untransfected PC3M-LN4 tumor sections.

Subcutaneous Injection with Exogenous HA

Tumor cells (GFP control and H2/3as cell lines) were resuspended in standard culture medium as above or in medium containing 1 mg/ml of sodium hyaluronate (average molecular size 810 kd; Lifecore, Chaska, MN), solubilized overnight, and filter-sterilized. Male SCID mice (five per condition in two separate experiments) were injected subcutaneously in each flank and monitored as above.

Results

Inhibition of Hyaluronan Synthase (HAS) by Anti-Sense RNA Expression Reduces Growth Rate of Subcutaneous Tumors

In a previous report, we described four stably transfected subline populations of PC3M-LN4 prostate adenocarcinoma cells: GFP, bearing the appropriate vector controls; H2as, expressing HAS2 antisense; H3as, with HAS3 antisense only; and H2/3as, incorporating antisense for both

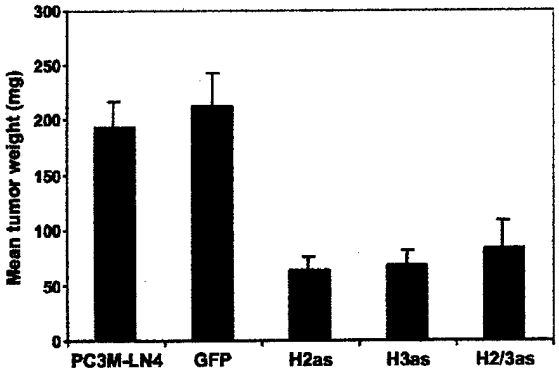

Figure 1. Inhibition of HAS gene expression in PC3M-LN4 cells by stable transfection with antisense constructs impairs tumor growth kinetics in immunocompromised mice. Untransfected, or vector (GFP)-, HAS2 (H2as)-, HAS3 (H3as)-, and HAS double antisense (H2/3as)-transfected tumor cells were suspended in serum-containing medium and injected subcutaneously into the flanks of male SCID mice. Tumors were harvested and weighed after 3 weeks. Data are plotted as the mean tumor wet weight (mg) ± SEM of 10 tumors per condition and are representative of three separate experiments.

HAS2 and HAS3.[26] To evaluate the relevance of tumor cell HA to tumor growth *in vivo*, we performed subcutaneous injections of PC3M-LN4 untransfected cells, control vector-transfected cells, or stable HAS antisense-inhibited transfectants, into flanks of male SCID mice. At 3 weeks after injection, mice were sacrificed, and tumors were dissected and weighed. All tumors appeared encapsulated and no spontaneous metastasis was detected in any of the animals. Vector-transfected control cells formed tumors of comparable size to those of PC3M-LN4-untransfected cells (Figure 1). Expression of either antisense HAS2 or HAS3 individually, or in concert, in these cells, however, reduced the size of resultant tumors by 70 to 75%, suggesting HA overproduction was required for rapid tumor growth.

Tumors Derived from HAS Antisense-Expressing Cells Contain Reduced HA and Diminished Cell Counts

H&E staining of tumor sections derived from control and transfected PC3M-LN4 cells confirmed the encapsulated, locally confined nature of the tumors. There was no evidence of necrosis, invasiveness, or spreading in any of the sections, and no apparent differences in morphology among cell lines. GFP expression within the transfectant tumor sections was verified by antibody staining (data not shown). To assess HA content of subcutaneous PC3M-LN4 tumors, formalin-fixed, paraffin-embedded tumors were sectioned, dewaxed, and probed with biotinylated HA-binding protein. HA appeared as a heavy brown stain interspersed among purple hematoxylin-counterstained tumor cells (Figure 2A). HA content and specificity of the probe was verified by absence of stain when sections were pretreated with hyaluronidase enzyme (Figure 2B). HA content of subcutaneous PC3M-LN4 transfectant tumors was then evaluated and visualized (Figure 2; C to F). As illustrated by the representative

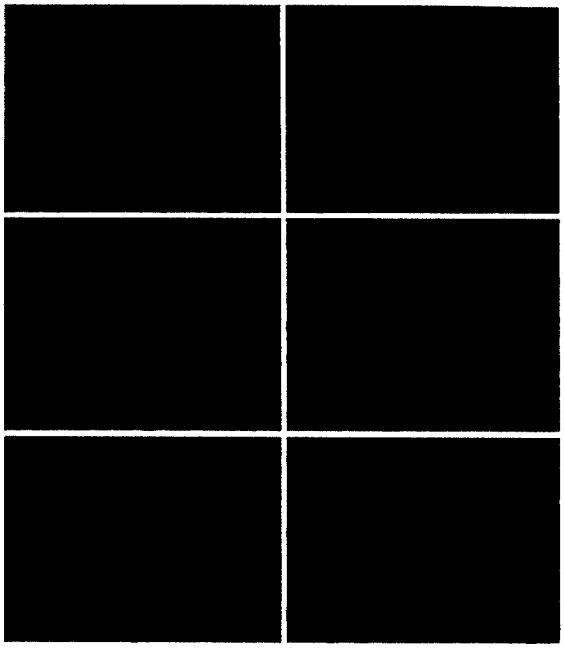

Figure 2. Evaluation of tumor HA content. Formalin-fixed paraffin-embedded sections were dewaxed, rehydrated, hematoxylin-stained, and probed with biotinylated HA-binding protein. After incubation with streptavidin-horseradish peroxidase conjugate, HA was detected by 3,3′-diaminobenzidine tetrahydrochloride precipitation. Representative stained tumor sections from each cell line are shown at ×400 magnification: **A:** PC3M-LN4; **B:** PC3M-LN4, hyaluronidase-treated; **C:** GFP control; **D:** H2as; **E:** H3as; **F:** H2/3as.

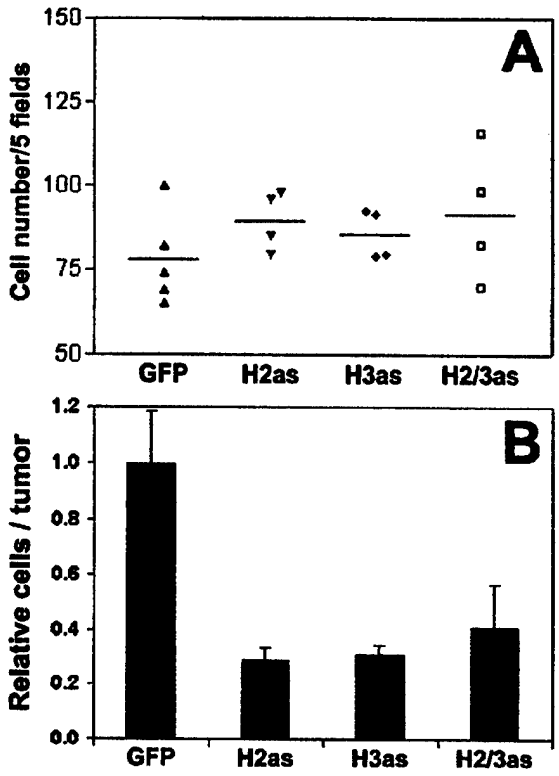

Figure 3. Cell counts in HAS antisense tumors. **A:** Individual cells in hematoxylin-stained frozen sections were manually counted under ×400 magnification and the average number of cells per five random fields was determined. Results of four to five tumors per cell line are plotted as a distribution with the mean represented by a **horizontal bar**. **B:** Two-dimensional average cell densities were integrated to volume densities, normalized to tumor size, and plotted as the mean relative fractional cell number ± SEM.

sections presented, GFP control tumors (Figure 2C) were similarly HA-rich, relative to the untransfected tumors, but individual or double HAS antisense tumors contained little to no intercellular HA (Figure 2; D, E, and F), consistent with reduced production by the tumor cells.

Because massively reduced intercellular HA within the tumors could translate to smaller tumor volumes with equivalent cell numbers, we quantified cellular density of the tumor sections. Cells were manually counted in five random hematoxylin-stained sections from four to five tumors for each cell line. Two-dimensional cell densities (Figure 3A) were only slightly greater in the antisense tumors. However, integration to three dimensions using the relative volumes of the respective tumors (Figure 3B) illustrated 2.5- to 3-fold more cells in control tumors. Hence although cell densities were somewhat increased by the absence of HA within the antisense tumors, the difference in tumor size was primarily the result of reduced cell number.

HAS Antisense Expression Reduces Intrinsic Growth Rate of PC3M-LN4 Cells But Does Not Affect Apoptosis or Proliferation Rate in Tumors

Cell counts in locally confined tumors are the result of a balance between apoptosis and growth in the tumor cell populations. Apoptosis was measured by a TUNEL assay for DNA fragmentation in fixed, permeabilized tissue sections. Sections viewed by fluorescence microscope exhibited virtually no apoptotic cellular staining (data not shown). However, at 3 weeks within the subcutaneous environment, apoptosis may no longer be detectable by this method, so we repeated the assay on cultured cell suspensions. Results were analyzed by flow cytometry (Figure 4; A to D), gating on GFP-positive cells, and detecting red fluorophore incorporation by apoptotic cells in FL-2 (black tracings). Approximately 1 to 2% of the GFP-positive cells were undergoing apoptosis and no differences in this percentage were evident among cell lines. DNase treatment of permeabilized cells was included as a control (gray tracings). Similar results were obtained by annexin-V staining (3 to 4% of GFP-positive cells were annexin-V-positive in all cell lines, data not shown), suggesting inhibition of HA production did not stimulate apoptosis in stably selected cultures.

Intrinsic growth rate of cells in culture was monitored by trypsin release and manual counting each day for 6 days (Figure 4E). Growth of individual HAS antisense transfectants was moderately impaired, and double antisense cell growth rate was 60% of control in the 6-day assay. We evaluated proliferation within tumor sections by staining for the nuclear proliferation antigen Ki-67 (not shown). The average percentage of Ki-67-positive cells

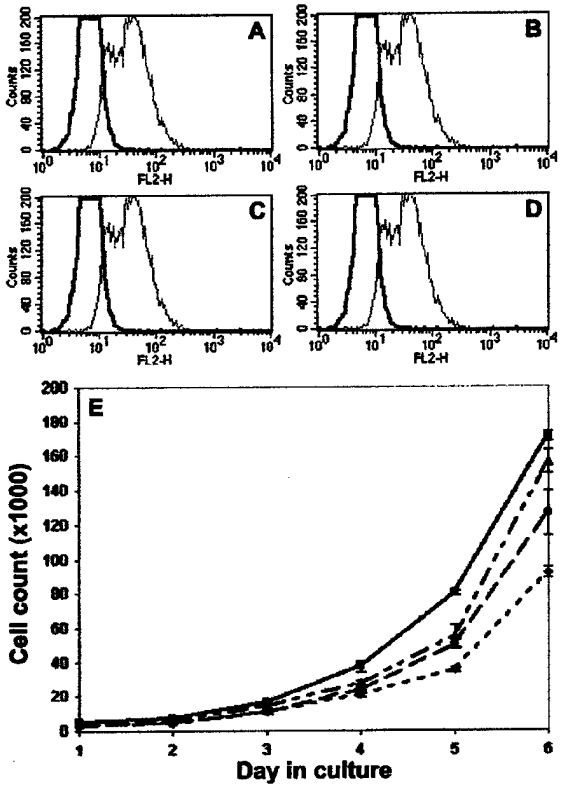

Figure 4. Apoptosis and intrinsic growth of HAS anti-sense cells in culture. **A–D:** Subconfluent cultures of tumor cell lines were trypsin released, washed, fixed, and permeabilized. Control aliquots of each cell suspension were incubated with 10 μg/ml of DNase. Apoptosis was measured by a TUNEL Red assay followed by two-color flow cytometry, gating on GFP-positive cells, and assessing incorporation of the red fluorophore in the FL-2 channel. **Black tracings** represent the FL-2 distribution of GFP (**A**), H2as (**B**), H3as (**C**), and H2/3as (**D**) cell lines. DNase control results are superimposed as **gray tracings**. **E:** Equivalent passages of each tumor cell line were plated in 48-well plates. At 24-hour intervals up to 6 days, quadruplicate wells of each cell line were trypsin released and manually counted in a hemacytometer. Growth curves are shown for GFP controls (**solid line, squares**), H2as (**dotted/dashed line, triangles**), H3as (**dashed line, circles**), H2/3as (**dotted line, diamonds**).

per five random sections of tumor ranged from 35 to 55% and was equivalent in all tumors. The high level of variability in these data among tumors derived from the same cell line suggested no HAS antisense-related trends. Hence, although intrinsic growth rate seemed to be significantly slowed in the HAS antisense-inhibited tumor cell lines, this did not account for the dramatic differences observed in tumor weight and volume.

Reduction of HA Synthesis Inhibits Angiogenesis

Visualized grossly on dissection, control tumors were obviously more vascularized than anti-sense HAS-expressing tumors. Furthermore, there is literature precedent for angiogenic regulation by HA. In particular, its oligomeric degradation products have been shown to mediate endothelial cell motility and proliferation.[28–30] To quantify vascularity, tumors were stained with a phycoerythrin-conjugated antibody to CD31, a vascular endothelial cell surface antigen. Representative grayscale sections of GFP control (Figure 5A) and H2/3as (Figure 5B) tumors illustrate differences in CD31 staining. Digital photographs of five random sections from each of three tumors per cell line were analyzed as TIF files in Adobe Photoshop.[27] Angiogenesis in PC3M-LN4 transfectant tumors is represented by average pixel density and normalized to untransfected control tumors (Figure 5C). Inhibition of HA synthesis in tumor cells reduced blood vessel density by 70 to 80%, despite insignificant differences in cellular density. Therefore, HA overproduction by tumor cells may be required for efficient subcutaneous growth because of its impact on angiogenesis.

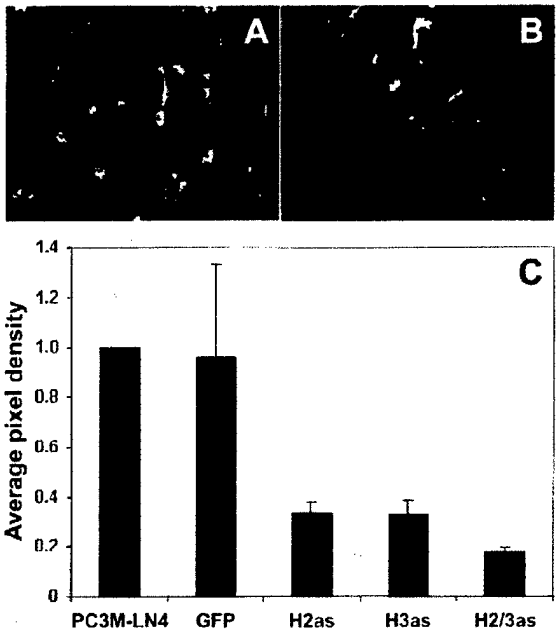

Figure 5. Antisense HAS expression in PC3M-LN4 cells yields poorly vascularized tumors relative to controls. CD31-phycoerythrin-conjugated antibody staining was used to quantify angiogenesis of tumor sections, visualized by fluorescence microscopy. Representative sections from GFP control (**A**) and HAS double antisense (**B**) tumors are shown. **C:** Five random sections from each of three tumors per cell line were digitally photographed and images processed as described in Materials and Methods. Average pixel density for each transfectant tumor section was then normalized to the average pixel density for untransfected PC3M-LN4 tumor sections.

Exogenous HA Restores Subcutaneous Tumor Growth and Vascular Density

If HA production were all that was required for efficient growth of PC3M-LN4 cells, then inclusion of excess quantities in the injection medium of the antisense-inhibited transfectants would be predicted to restore tumor growth kinetics to those of the control cells. Inclusion of 1 mg/ml of exogenous HA in the culture medium of untransfected, control, or HAS antisense-transfected PC3M-LN4 cells had no effect on the two-dimensional growth curves shown in Figure 4E (data not shown). To test this prediction *in vivo*, vector (GFP) and double antisense (H2/3as)-

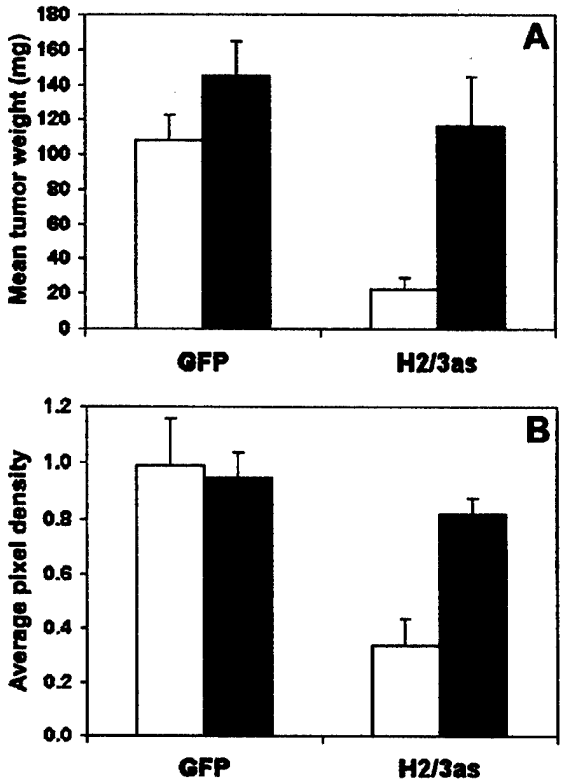

Figure 6. Exogenous HA restores control tumor growth kinetics and vascular density to double HAS antisense-inhibited PC3M-LN4 cells. **A:** Vector (GFP) and HAS double antisense (H2/3as)-transfected tumor cells were suspended in control culture medium (**white bars**) or medium containing 1 mg/ml of sodium hyaluronate (average size, 810 kd), and injected subcutaneously into the flanks of male SCID mice. Tumors were harvested and weighed after 3 weeks. Data are plotted as the mean wet weight (mg) ± SEM of seven to nine tumors per condition. **B:** CD31-phycoerythrin-conjugated antibody staining was used to quantify angiogenesis of tumor sections. Five random sections from each of three tumors per cell line injected in control medium (**white bars**) or HA-containing medium (**black bars**) were analyzed as described in Materials and Methods. Average pixel density of each section was normalized to that of untransfected PC3M-LN4 tumor sections.

transfected cells were suspended in standard medium (control) or medium containing 1 mg/ml of HA (average molecular weight, 810 kd) before subcutaneous injection as described. Tumors were harvested and weighed at 21 days (Figure 6A). Growth of control transfectants was slightly, but not significantly, stimulated by addition of HA to the injection medium. Inhibited growth of HAS double antisense cells, however, was enhanced to match growth of the controls. This confirmed the specific nature of the antisense inhibition and the requirement only for the product of the HAS isozymes, not for production by the tumor cell, retention at the surface by HAS, or expression of a specific isozyme.

The efficacy of growth restoration *in vivo*, but not in cultured cells, implies a more complex requirement for HA than to modify intrinsic growth rate of the cells, and is consistent with a putative role in angiogenesis. To investigate this possibility, we quantified vascular density of GFP control and H2/3as tumors injected in standard or HA-containing medium by CD31-phycoerythrin staining as described above. Average CD31-positive pixel density was comparable for GFP controls cells irrespective of injection medium (Figure 6B). However, the low vascular densities observed for H2/3as tumors injected in standard medium were entirely restored to control levels by addition of exogenous HA. This result provides direct support for the involvement of HA in tumor vascularization.

Discussion

Prostate cancer progression occurs with elevated HA deposition in the prostate stroma and tumor cell-associated HA is a bad prognostic factor. HA overproduction and cell surface retention correlates with malignant prostate tumor cell phenotype. In this report, we have used PC3M-LN4 aggressive prostate tumor cells selected for stable expression of antisense HAS constructs to assess the impact of inhibited HA production on tumorigenic behavior *in vivo*. Diminished HA synthesis resulting from reduced expression of either or both HAS enzyme isoforms significantly altered the growth kinetics of the tumor cells (75% reduction). Intrinsic proliferation and apoptosis in two-dimensional cell cultures were not sufficiently different to account for this observation. However, blood vessel densities within the HAS antisense-inhibited tumors reflected the same 75 to 80% reduction exhibited by tumor growth. These results strongly imply that the elevated HA levels produced by PC3M-LN4 cells function both to enhance cell growth within the tumor and to promote its vascularization.

Ample evidence exists for the function of HA in growth and development. HA is deposited in large quantities by cells undergoing mitosis, and facilitates both cell rounding and ultimate separation of the daughter cells.[3] Addition of HA to explanted embryonic mouse prostate tissue was required for ductal branching.[5] Targeted disruption of HAS2 is an embryonic lethal mutation in mice as a result of cessation in heart development.[4] Exogenous addition of HA to explanted heart tissue from these embryos was sufficient to restore wild-type levels of cardiac endothelial cell motility, functioning not only as a requisite migration substrate but also to influence transformation of the cells to a motile phenotype. The product of HAS enzymes, therefore, seems to be the essential component of these events. This is consistent with our observations that antisense HAS expression in PC3M-LN4 cells inhibits tumor growth and addition of HA to double antisense-inhibited cells restores their rate of tumor formation and vascularity to control levels. Although an essential component of growth, cells apparently do not need to make HA if it is made available to them.

Temporal and tissue-specific HA deposition has been implicated in normal growth, but also promotes pathological growth. HA overproduction by cultured cells has been shown to alleviate normal contact inhibited growth.[31] Addition of HA to explanted heart cells maintains them in an undifferentiated state, in which they retain tumor cell characteristics of motility and continued proliferation.[32] HA stimulates myeloma proliferation in

munohistological data suggest this may occur in prostate carcinoma, because the hyaluronidase isoform Hyal-1 was shown to be overexpressed during human cancer progression concurrently with elevated HA deposition.[15]

Our data are consistent with a model in which tumor cells with enhanced capacity to synthesize and retain pericellular HA are surrounded by a hydrated envelope that facilitates tumorigenicity, perhaps by altering the composition and interfering with the integrity of tissue stromal matrices or permitting the tumor cells to evade immune system detection. Short HA oligosaccharides that stimulate angiogenesis may be elevated in the environs of such tumor cells through the action of hyaluronidase enzymes. Inhibition of HAS enzyme expression within the tumor would then decrease vascularization by eliminating production of this angiogenic stimulus and thereby suppress tumor growth. HA oligos may also facilitate motility and inappropriate proliferation in autocrine manner by signal transduction through tumor cell HA receptors such as CD44 and RHAMM.[46]

Acknowledgments

We thank Dr. Sundaram Ramakrishnan for expert advice and assistance with angiogenesis quantification, Dr. Ted Oegema and Dr. Joseph Barycki for many thoughtful discussions, and Dr. Leo Furcht for ongoing supportive input.

References

1. Landis SH, Murray T, Bolden S, Wingo PA: Cancer statistics, 1999. CA Cancer J Clin 1999, 49:8–31
2. Fraser JR, Laurent TC, Laurent UB: Hyaluronan: its nature, distribution, functions and turnover. J Intern Med 1997, 242:27–33
3. Evanko SP, Angello JC, Wight TN: Formation of hyaluronan- and versican-rich pericellular matrix is required for proliferation and migration of vascular smooth muscle cells. Arterioscler Thromb Vasc Biol 1999, 19:1004–1013
4. Camenisch TD, Spicer AP, Brehm-Gibson T, Biesterfeldt J, Augustine ML, Calabro Jr A, Kubalak S, Klewer SE, McDonald JA: Disruption of hyaluronan synthase-2 abrogates normal cardiac morphogenesis and hyaluronan-mediated transformation of epithelium to mesenchyme. J Clin Invest 2000, 106:349–360
5. Gakunga P, Frost G, Shuster S, Cunha G, Formby B, Stern R: Hyaluronan is a prerequisite for ductal branching morphogenesis. Development 1997, 124:3987–3997
6. Yung S, Thomas GJ, Davies M: Induction of hyaluronan metabolism after mechanical injury of human peritoneal mesothelial cells in vitro. Kidney Int 2000, 58:1953–1962
7. Auvinen P, Tammi R, Parkkinen J, Tammi M, Agren U, Johansson R, Hirvikoski P, Eskelinen M, Kosma VM: Hyaluronan in peritumoral stroma and malignant cells associates with breast cancer spreading and predicts survival. Am J Pathol 2000, 156:529–536
8. Bohm J, Niskanen L, Tammi R, Tammi M, Eskelinen M, Pirinen R, Hollmen S, Alhava E, Kosma VM: Hyaluronan expression in differentiated thyroid carcinoma. J Pathol 2002, 196:180–185
9. Anttila MA, Tammi RH, Tammi MI, Syrjanen KJ, Saarikoski SV, Kosma VM: High levels of stromal hyaluronan predict poor disease outcome in epithelial ovarian cancer. Cancer Res 2000, 60:150–155
10. Ropponen K, Tammi M, Parkkinen J, Eskelinen M, Tammi R, Lipponen P, Agren U, Alhava E, Kosma VM: Tumor cell-associated hyaluronan as an unfavorable prognostic factor in colorectal cancer. Cancer Res 1998, 58:342–347
11. Lokeshwar VB, Obek C, Soloway MS, Block NL: Tumor-associated hyaluronic acid: a new sensitive and specific urine marker for bladder cancer [published erratum appears in Cancer Res 1998, 58:3191]. Cancer Res 1997, 57:773–777
12. De Klerk DP: The glycosaminoglycans of normal and hyperplastic prostate. Prostate 1983, 4:73–81
13. De Klerk DP, Lee DV, Human HJ: Glycosaminoglycans of human prostatic cancer. J Urol 1984, 131:1008–1012
14. Lipponen P, Aaltomaa S, Tammi R, Tammi M, Agren U, Kosma VM: High stromal hyaluronan level is associated with poor differentiation and metastasis in prostate cancer. Eur J Cancer 2001, 37:849–856
15. Lokeshwar VB, Rubinowicz D, Schroeder GL, Forgacs E, Minna JD, Block NL, Nadji M, Lokeshwar BL: Stromal and epithelial expression of tumor markers hyaluronic acid and HYAL1 hyaluronidase in prostate cancer. J Biol Chem 2001, 276:11922–11932
16. Weigel PH, Hascall VC, Tammi M: Hyaluronan synthases. J Biol Chem 1997, 272:13997–14000
17. Shyjan AM, Heldin P, Butcher EC, Yoshino T, Briskin MJ: Functional cloning of the cDNA for a human hyaluronan synthase. J Biol Chem 1996, 271:23395–23399
18. Watanabe K, Yamaguchi Y: Molecular identification of a putative human hyaluronan synthase. J Biol Chem 1996, 271:22945–22948
19. Spicer AP, McDonald JA: Characterization and molecular evolution of a vertebrate hyaluronan synthase gene family. J Biol Chem 1998, 273:1923–1932
20. Brinck J, Heldin P: Expression of recombinant hyaluronan synthase (HAS) isoforms in CHO cells reduces cell migration and cell surface CD44. Exp Cell Res 1999, 252:342–351
21. Itano N, Sawai T, Yoshida M, Lenas P, Yamada Y, Imagawa M, Shinomura T, Hamaguchi M, Yoshida Y, Ohnuki Y, Miyauchi S, Spicer AP, McDonald JA, Kimata K: Three isoforms of mammalian hyaluronan synthases have distinct enzymatic properties. J Biol Chem 1999, 274:25085–25092
22. Kosaki R, Watanabe K, Yamaguchi Y: Overproduction of hyaluronan by expression of the hyaluronan synthase Has2 enhances anchorage-independent growth and tumorigenicity. Cancer Res 1999, 59: 1141–1145
23. Liu N, Gao F, Han Z, Xu X, Underhill CB, Zhang L: Hyaluronan synthase 3 overexpression promotes the growth of TSU prostate cancer cells. Cancer Res 2001, 61:5207–5214
24. Pettaway CA, Pathak S, Greene G, Ramirez E, Wilson MR, Killion JJ, Fidler IJ: Selection of highly metastatic variants of different human prostatic carcinomas using orthotopic implantation in nude mice. Clin Cancer Res 1996, 2:1627–1636
25. Simpson MA, Reiland J, Burger SR, Furcht LT, Spicer AP, Oegema Jr TR, McCarthy JB: Hyaluronan synthase elevation in metastatic prostate carcinoma cells correlates with hyaluronan surface retention, a prerequisite for rapid adhesion to bone marrow endothelial cells. J Biol Chem 2001, 276:17949–17957
26. Simpson MA, Wilson CM, Furcht LT, Spicer AP, Oegema Jr TR, McCarthy JB: Manipulation of hyaluronan synthase expression in prostate adenocarcinoma cells alters pericellular matrix retention and adhesion to bone marrow endothelial cells. J Biol Chem 2002, 277: 10050–10057
27. Wild R, Ramakrishnan S, Sedgewick J, Griffioen AW: Quantitative assessment of angiogenesis and tumor vessel architecture by computer-assisted digital image analysis: effects of VEGF-toxin conjugate on tumor microvessel density. Microvasc Res 2000, 59:368–376
28. West DC, Kumar S: The effect of hyaluronate and its oligosaccharides on endothelial cell proliferation and monolayer integrity. Exp Cell Res 1989, 183:179–196
29. Sato E, Miyamoto H, Koide SS: Hyaluronic acid-like substance from mouse ovaries with angiogenic activity. Z Naturforsch [C] 1990, 45: 873–880
30. Sattar A, Rooney P, Kumar S, Pye D, West DC, Scott I, Ledger P: Application of angiogenic oligosaccharides of hyaluronan increases blood vessel numbers in rat skin. J Invest Dermatol 1994, 103:576–579
31. Itano N, Atsumi F, Sawai T, Yamada Y, Miyaishi O, Senga T, Hamaguchi M, Kimata K: Abnormal accumulation of hyaluronan matrix diminishes contact inhibition of cell growth and promotes cell migration. Proc Natl Acad Sci USA 2002, 99:3609–3614
32. Iocono JA, Bisignani GJ, Krummel TM, Ehrlich HP: Inhibiting the differentiation of myocardiocytes by hyaluronic acid. J Surg Res 1998, 76:111–116

bone marrow, possibly by locally enhancing autocrine response to interleukin-6.[33] Specific relevance of HA biosynthetic enzymes to tumor growth has been demonstrated by HAS2 and HAS3 overexpression, both of which were shown to promote anchorage-independent growth,[22,34] and to enhance subcutaneous tumorigenicity in nude mice.[22,23] In some cases, HA involvement in tumorigenic behavior has been accompanied by altered motility and metastasis.[20,35–37] In the case of PC3M-LN4 subcutaneous tumors, there was no evidence of invasiveness or spontaneous metastasis either in control or in antisense HAS-inhibited tumors, suggesting altered motility is not a significant component of the tumorigenic mechanism of up-regulated HAS. It is more likely, therefore, that the observed differences in growth properties and tumor angiogenesis of the HAS antisense cells are modulating development of the tumors. As a corollary, metastasis of these cells in other models (ie, prostate orthotopic and intracardial injection[24]) may be promoted by the influence of HA in growth and vascularization at the remote site.

Interestingly, expression of antisense mRNA for HAS2 and HAS3 individually and in concert impacted tumor growth to the same extent. The most straightforward explanation for this phenomenon is that there is a requisite threshold of HA production that must be achieved or exceeded to effect control of growth or angiogenesis. In support of this, synthesis and secretion of HA were reduced differentially in all three HAS antisense transfectant cell lines, but cell surface HA was virtually unmeasurable by particle exclusion assay in any of the three lines.[26] Another possible explanation is a general disruption by antisense expression in the PC3M-LN4 cells. However, restored growth of tumors on augmentation of HA in the injection medium suggests this is not the case. It is also possible that there is nonspecific inhibition of both HAS2 and HAS3 by each respective antisense. The region selected for expression in antisense orientation, however, is the first 300 nucleotides of coding sequence, where the greatest differences in sequence alignment are manifest. Furthermore, reverse transcriptase-polymerase chain reaction amplification of HAS2 and HAS3 from the antisense-inhibited cells demonstrated specificity of message destabilization and quantification of HA synthesis indicated incomplete inhibition in the single antisense HAS cells. Collectively, these data support a threshold of HA synthesis that probably correlates to HA surface retention.

Several possible additional effects, which may be overlaid on this model, cannot be ruled out. First, there may be differential temporal regulation of the HAS isozymes necessary for cell division, which would be precluded by antisense expression. HAS2, for example, seems to be the most highly regulated isozyme, because gene regulation studies report no significant changes in the levels of HAS1 or HAS3 transcripts to various stimuli that impact HAS2.[6,38,39] In addition, although cells in culture and 21-day tumor sections failed to exhibit differences in apoptosis, absence of the requisite threshold on injection into the animals may initiate immediate cell death. This would diminish the original number of cells available to develop into a tumor, but would be undetected in our assay. HAS antisense-expressing cells could exhibit delayed initial growth rate, possibly as a result of reduced ability to stimulate angiogenesis, that would ultimately approach the rate of control cell growth. Preliminary experiments to determine the sacrifice endpoint for subcutaneous injection, in which the size of HAS antisense tumors no longer increased after 21 days (data not shown), argue against equivalent but delayed growth. Finally, the stably selected cells are a heterogeneous population that may still include a small percentage of HA-overproducing cells capable of growth. Abundance of cell surface HA has been hypothesized to envelope the cell in a semiorganized matrix that protects human gliomas[40] and also virulent strains of *Streptococcus pyogenes* bacteria[41] from cytotoxic killing mediated by natural killer cells in the bloodstream. SCID mice lack T and B cells, but retain natural killer cell activity, so antisense inhibition of surface HA may render PC3M-LN4 cells more susceptible to the vestiges of immune function in the animals. However, if this were the only mechanism of suppressed growth, the resultant tumors would be expected to be HA-rich and GFP-negative, suggesting this explanation also is incomplete.

Blood vessel densities of each antisense HAS permutation were decreased to a similar extent relative to controls, reflecting the effect observed in tumor growth kinetics. Because intrinsic differences in proliferation and apoptosis, both in cell cultures and in tumor sections, do not fully explain tumor size differential, it is likely that the postulated requisite tumor cell HA synthesis threshold directly impacts the ability of the cells to vascularize a developing tumor. Vessel density within the tumor was altered on a per-cell basis, not merely by a linear decrease with tumor size, suggesting direct impact of some factor produced by the tumor cell on endothelial recruitment. HAS3 overexpression has been correlated with increased blood vessel density in subcutaneous tumors,[23] but this is the first report of impaired HA production leading to decreased vascularization of a tumor. The role of HA, particularly of its oligosaccharides, in angiogenesis is well documented. Application of HA oligosaccharides has been shown to locally increase blood vessel density of rat skin.[30] HA oligo fractions extracted from rat ovaries were used to demonstrate the essential role of HA in ovarian neovascularization.[29] HA oligosaccharide products formed by hyaluronidase degradation of high-molecular weight HA was shown to stimulate blood vessel formation in a chick chorioallantoic membrane assay for angiogenesis.[42] Subsequently, the same group showed HA oligos specifically mediated endothelial cell proliferation and recruitment, while high-molecular weight HA was actually anti-proliferative,[28] suggested elevated HA in tumors appeared to correlate with angiogenesis,[43] and that molecular weight differences in HA were mediated by cells within the tumor.[44] Tumor cells may therefore benefit from the presence of HA polymer either by stimulating or exploiting existing hyaluronidase activity within the tissue they are invading, or by expressing it themselves. In fact, overexpression of hyaluronidase in gliomas has been correlated to angiogenesis,[45] and im-

33. Vincent T, Jourdan M, Sy MS, Klein B, Mechti N: Hyaluronic acid induces survival and proliferation of human myeloma cells through an interleukin-6-mediated pathway involving the phosphorylation of retinoblastoma protein. J Biol Chem 2001, 276:14728–14736
34. Li Y, Heldin P: Hyaluronan production increases the malignant properties of mesothelioma cells. Br J Cancer 2001, 85:600–607
35. Dube B, Luke HJ, Aumailley M, Prehm P: Hyaluronan reduces migration and proliferation in CHO cells. Biochim Biophys Acta 2001, 1538:283–289
36. Itano N, Sawai T, Miyaishi O, Kimata K: Relationship between hyaluronan production and metastatic potential of mouse mammary carcinoma cells. Cancer Res 1999, 59:2499–2504
37. Yu Q, Toole BP, Stamenkovic I: Induction of apoptosis of metastatic mammary carcinoma cells in vivo by disruption of tumor cell surface CD44 function. J Exp Med 1997, 186:1985–1996
38. Jacobson A, Brinck J, Briskin MJ, Spicer AP, Heldin P: Expression of human hyaluronan synthases in response to external stimuli. Biochem J 2000, 348:29–35
39. Zhang W, Watson CE, Liu C, Williams KJ, Werth VP: Glucocorticoids induce a near-total suppression of hyaluronan synthase mRNA in dermal fibroblasts and in osteoblasts: a molecular mechanism contributing to organ atrophy. Biochem J 2000, 349:91–97
40. Gately CL, Muul LM, Greenwood MA, Papazoglou S, Dick SJ, Kornblith PL, Smith BH, Gately MK: In vitro studies on the cell-mediated immune response to human brain tumors. II. Leukocyte-induced coats of glycosaminoglycan increase the resistance of glioma cells to cellular immune attack. J Immunol 1984, 133:3387–3395
41. Cywes C, Wessels MR: Group A Streptococcus tissue invasion by CD44-mediated cell signalling. Nature 2001, 414:648–652
42. West DC, Hampson IN, Arnold F, Kumar S: Angiogenesis induced by degradation products of hyaluronic acid. Science 1985, 228:1324–1326
43. West DC, Kumar S: Tumour-associated hyaluronan: a potential regulator of tumour angiogenesis. Int J Radiat Biol 1991, 60:55–60
44. Rooney P, Kumar S, Ponting J, Wang M: The role of hyaluronan in tumour neovascularization (review). Int J Cancer 1995, 60:632–636
45. Liu D, Pearlman E, Diaconu E, Guo K, Mori H, Haqqi T, Markowitz S, Willson J, Sy MS: Expression of hyaluronidase by tumor cells induces angiogenesis in vivo. Proc Natl Acad Sci USA 1996, 93:7832–7837
46. Turley EA, Noble PW, Bourguignon LY: Signaling properties of hyaluronan receptors. J Biol Chem 2002, 277:4589–4592